DOCTOR OF PHILOSOPHY

Absorption, Storage and Release Characteristics of Poly(1-methylpyrrol-2-ylsquaraine) Particles

Bennett, Joy

Award date:
2008

Awarding institution:
Coventry University

Absorption, Storage and Release Characteristics of Poly(1-methylpyrrol-2-ylsquaraine) Particles

Joy B. Bennett

PhD

2008

A thesis submitted in partial fulfilment of the University's requirements for the Degree of Doctor of Philosophy. The Faculty of Health and Life Science, Coventry University.
March 2008

Acknowledgements

I would like to acknowledge the financial support given by the School of Health and Life Sciences, Coventry University. I would like to thank my Director of Studies Dr. D.E. Lynch for his guidance and support during this project and my supervisors Dr. M. Bateman and Mr. A. Newman for their education in using the spectroscopy equipment. I would also like to thank Mrs Karen Smith for her tutorials on statistical analysis. I shall be eternally grateful to my good friends the excellent HLS laboratory technicians Mrs. A. Nuttall and Mr. D. Dugdale for being so kind, helpful and patient whilst working in their laboratory and for taking the time and trouble to keep in touch when times were difficult. Thank you Anne and Danny, your constant support kept me going. I would also like to thank my boss Tim Lowe for his constant nagging to hurry up and finish the project.

I would also like to thank my family and friends for putting up with me throughout all of my time at university, particularly during the last year when my daughter Dawn became ill. I would like to give a big thank you to my partner John for keeping the computer working and to my mom Beryl for looking after my children during all of the time I was at University. Without their support none of this research would have been possible.

Contents

Figures

Chapter One - Introduction to Porous Adsorbent Materials

Chapter Two - Introduction to Squaraines

Chapter Three – Analytical Instumentation

Chapter Four – Adsorption Studies

Chapter Five – Release Profile Studies

Chapter Six – Over-coating Studies

Chapter Seven – Conclusions and Further Work

Tables

Chapter One - Introduction to Porous Adsorbent Materials

Chapter Two - Introduction to Squaraines

Chapter four – Adsorption Studies

Abstract

Poly(1-methylpyrrol-2-ylsquaraine) (PMPS) particles are a fine blue-black insoluble powder. Scanning electron microscopy (SEM) pictures reveal that the PMPS particles are microspheres with diameters ranging from 1.3 - 4 micrometers (distribution peaking at 1.9 micrometers). The absorption capacity values of PMPS particles were studied for a large majority of the elements in the periodic table in order to establish a pattern or trend in absorption. The elements specifically targeted at the beginning of the research were the biological elements vital to sustain life and the heavy metals that pose a threat to the environment via pollution and poisoning.

Fifty-four elements were investigated in total and all absorbed in varying amounts ranging from 0.01 mmol/g for caesium up to 5.66 mmol/g for phosphorous. It was found that varying the initial elemental compound, temperature and solvent concentrations vastly altered the amount of element absorbed. The majority of elements absorbed best when dissolved in hot concentrated hydrochloric acid at 50^{o}C, some preferred cold conditions (4^{o}C) and/or a neutral solvent (water). The freshness of the elemental compound had a huge impact on the absorption capacities, i.e. new compounds absorbed much better than old stock. A comparison between chloride salts and the hydroxides of Group 1 alkali metals revealed that the hydroxides absorbed much better than the salts, sometimes with more than a ten-fold increase.

Release profiles were studied for PMPS particles containing eleven different elements when subjected to an aqueous medium. The study focused on some of the elements that are commonly utilised in industry and also the soft acids and bases primarily because they had some of the highest sorption values and the fact that the majority are known to be particularly toxic to man. The amount of ions released varied enormously ranging from 0% release for selenium up to 83% for arsenic. It was interesting to observe

that arsenic had the highest percentage release despite having the lowest sorption uptake and selenium had the lowest (zero) percentage release despite having one of the highest sorption uptakes. Analysis of the release data revealed that there appears to be two types of profile emerging. In the first type of profile the metallic ions leached out of the PMPS particles slowly over a period of time until equilibrium was reached whereupon no more ions were released. This happened for the arsenic, copper, lead, mercury, cadmium, silver and gold ions. In the second type of profile all of the free ions were released as soon as water was added, in the first 2 mL aliquot. This happened for the manganese, sodium and caesium ions. It would appear that the ions that have the gradual release profile are the heavier ions on the right hand side of the periodic table, which also means that they are soft acids or bases. The ions that have the second type of profile, where release was achieved in the first aliquot are situated on the left hand side of the periodic table and were all found to be hard acids.

Over-coating studies using PMPS particles containing copper and sodium were separately investigated. The results revealed that PMPS-Cu particles when overcoated with a polymer do appear to have a slow release profile.

Chapter One

Introduction

to

Porous Absorbent

Materials

1.1 Aim

The study of a novel porous polymer material called poly(1-methylpyrrole-2-ylsquaraine) (PMPS) particles was undertaken to assess its sorption, storage and release properties for possible use in a variety of commercial products, such as elemental absorbents, anti-bacterial materials, trace radioactive materials, chromatography materials, slow release fertilizers and micro-organism feed stocks. Scanning electron microscope (SEM) pictures reveal that the fine blue/black PMPS powder comprises of spherical particles with diameters ranging from 1.3 - 4 micrometers (distribution peaking at 1.9 micrometers) (Fig. 1.1). The PMPS particles can be easily incorporated into any commercially available polymer materials. The use of these commercial polymer materials had the advantage that the overall shape of the final product can be anything from powders, fibres or cloth to solid blocks that can be used to produce any engineered part.

Fig 1.1 has been removed due to third party copyright. The unabridged version of the thesis can be viewed at the Lanchester Library, Coventry University

Figure 1.1 (a) Scanning electron microscope picture of PMPS particles and (b) its chemical structure.

The project initially concentrated on the study of two main groups of elements nominally the elements essential in making fertilizers and inhibitors. Research for the fertilizers involved testing various elements such as magnesium, potassium and phosphorus, the latter half of the first row of the d-transition series and molybdenum. The inhibitors primarily involve silver, as an anti-bacterial, and copper, as an anti-algal. Once these initial studies were completed a more in depth study of the periodic

table was undertaken to be able to establish a pattern of sorption for the beads. Particular attention was given to the biological elements vital to sustain life and the heavy metals that pose a threat to the environment via pollution and poisoning. In total fifty-four elements were investigated and all were sorbed into the PMPS, however the amount ranged from 0.01 mmol/g for caesium up to 5.66 mmol/g for phosphorous. It was found that varying the initial elemental compound, temperature, pH and solvent concentrations could vastly alter the amount of element absorbed. Release profiles were studied for eleven elements, of which the most interesting was selenium. This is because selenium did not release from the PMPS at all despite being one of the highest absorbing elements. An investigation into formulating methods of slow release of sodium and copper PMPS particles was carried out.

1.2 Introduction to porous adsorbent materials

Considerable interest has been shown in finding breakthroughs into the design and processing of novel porous materials for many years. This is because porous materials are used extensively in a large number of applications in many technological fields such as catalysis, separation, purification, immobilization of biological molecules, drug delivery, medical diagnosis, gas storage, nano-technology, photonics adsorption and mostly environmental science (Zhao, 2006). Environmental contamination from heavy metals represents a huge potential threat to humans, plants and animals. The last decades have shown a remarkable increase in heavy metal contamination volumes. They are released into the environment in a number of different ways; coal combustion, sewage waste-waters, automobile emissions, battery industry, mining activities, tanneries, alloy industries and the utilization of fossil fuels are just a few examples. At least twenty metals are classified as toxic and half of

these, including cadmium, arsenic, mercury, chromium, copper, lead, nickel, selenium, silver and zinc are emitted into the environment in quantities that pose a risk to human health (Genc *et al*., 2002). Much research is being done to develop methods to remove heavy metal ions from environmental components and subsequently reuse them. Processes used in the removal of such contaminants from water include filtration, flocculation, ion-exchange resins, adsorption, reverse osmosis and precipitation. Many of these processes involve high costs and the production of toxic derivatives. The need to find a cost effective way of cleaning the environment is being researched extensively.

The favoured characteristics of porous materials are high surface area, large pore volume, and uniformity in pore size. They must also have high abrasion resistance, high thermal stability and small micropore diameter, which results in higher exposed surface area and hence a high capacity of adsorption. The adsorbents must also have a distinct macropore structure which enables fast transport of the gaseous vapours. There are a huge variety of compounds available that can store multiple elements, although it is much more beneficial for a compound to be specific to a certain type of element depending on size and coordination of the atoms. Adsorbents are usually formed into spherical pellets, rods, mouldings or monoliths (Zhao, 2006).

1.3 Adsorption and absorption of ions

Adsorption is the process that occurs when a gas or liquid solute accumulates on the surface of a solid (adsorbent), forming a molecular or atomic film (the adsorbate). It is different from absorption, in which a substance diffuses to fill the pores of a solid, or to dissolve in a liquid to form a solution. Desorption is the reverse

process. Adsorption and absorption occur in most natural physical, biological, and chemical systems, and are widely used in industrial applications such as catalysis, separation and purification etc. Adsorption ion exchange and chromatography are sorption processes in which certain adsorptives are selectively transferred from the fluid phase to the surface of insoluble, rigid particles suspended in a vessel or packed in a column. Similar to surface tension, adsorption is a consequence of surface energy. In a bulk material, all the bonding requirements (be they ionic, covalent or metallic) of the constituent atoms of the material are filled. But atoms on the (clean) surface experience a bond deficiency, because they are not wholly surrounded by other atoms. Thus it is energetically favourable for them to bond with whatever happens to be available. The exact nature of the bonding depends on the details of the species involved, but the adsorbed material is generally classified as exhibiting physisorption or chemisorption (Atkins, 1998).

The same facts can apply to absorption, the only difference being that the absorpate is a porous material which enables molecules to pass inside, although some absorption occurs without any bond interaction, i.e. purely acting as a container. Physisorption (physical sorption) is caused by van der Walls interaction between the sorbate and the substrate. Van der Walls interactions have a long range but are weak, and the energy released (enthalpy) when a particle is physisorbed is very small. Such small energies can be absorbed as vibrations of the lattice and dissipated as thermal motion, and a molecule bouncing across the surface will gradually lose its energy and finally adsorb to it in the process called accommodation. The small enthalpy change is insufficient to lead to bond breaking so a physisorbed molecule retains its identity. In chemiosorption (chemical sorption) the molecules (or atoms) stick to the sorbate by forming a chemical bond (usually covalent) and will tend to find sites that maximise

their co-ordination number. The enthalpy of chemisorption is very much greater than that for physisorption. Typical values are in the region of 200 kJ/mol compared to an average of only 20 kJ/mol for physisorption. This may result in the molecule being torn apart at the demand of the unsatisfied valencies of the surface atoms, resulting in the existence of molecular fragments on the surface. This is one reason why solid surfaces catalyse reactions. Chemisorption is almost always exothermic. The enthalpy of adsorption depends on the extent of surface coverage, mainly because the adsorped particles interact. If the particles repel each other the adsorption becomes less exothermic as coverage increases. Low-energy electron diffraction (LEED) studies show that such species settle on the surface in a disordered way until packing requirements demand order. If the adsorbing particles attract one another, then they tend to cluster together in islands, and growth occurs at the borders. These adsorbents also show order-disorder transitions when they are heated enough for the thermal motion to overcome the particle-particle interactions, but not so much that they are desorbed.

Adsorption is usually described through isotherms, that is functions which connect the amount of adsorbate on the adsorbent, with its pressure (when a gas) or concentration (when a liquid). The first isotherm is due to Freundlich and Küster (1894) and is a purely empirical formula valid for gaseous adsorbates: $x / m = k P^{1/n}$, where x is the adsorbed quantity, m is the mass of adsorbent, P is the pressure of adsorbate and k and n are empirical constants for each adsorbent-adsorbate pair at each temperature. The function has an asymtotic maximum. As the temperature increases, the adsorbed quantity rises more slowly and more pressure is required to achieve the maximum.

In 1916, Irving Langmuir published a new isotherm for gases adsorbed on solids, which retained his name. It is an empirical isotherm derived from a proposed kinetic mechanism. It is based on four hypotheses:

- The surface of the adsorbent is uniform, i.e. all the adsorption sites are equal.
- Adsorbed molecules do not interact.
- All adsorption occurs through the same mechanism.
- Adsorption cannot proceed beyond monolayer coverage.

These four points are seldom true: there are always imperfections on the surface, adsorbed molecules are not necessarily inert, the mechanism is clearly not the same for the very first molecules as for the last to adsorb. The fourth condition is the most troublesome, as often more molecules can adsorb on the monolayer. The dynamic equilibrium being: $A_{(g)} + M_{(surface)} \rightleftharpoons A_{(g)}M_{(surface)}$

Molecules do frequently form multilayers as some are adsorbed onto already adsorbed molecules and so making the Langmuir isotherm invalid. In 1938 Stephan Brunauer, Paul Emmett and Edward Teller developed an isotherm that takes into account that possibility. The proposed mechanism, more commonly known at the BET isotherm, would more realistically have an equilibrium such as:

$$A_{(g)} + M_{(surface)} \rightleftharpoons A_{(g)}M_{(surface)}$$

$$A_{(g)} + A_{(g)}M_{(surface)} \rightleftharpoons A_{(g)2}M_{(surface)}$$

$$A_{(g)} + A_{(g)2}M_{(surface)} \rightleftharpoons A_{(g)3}M_{(surface)} \text{ and so on}$$

A BET isotherm is not accurate at all pressures, but it is widely used in industry to determine the surface areas of solids. Langmuir isotherms work better for chemisorption and BET isotherms works better for physisorption (Atkins, 1998).

The term sorption is a more general term which covers adsorption, absorption, and also ion exchange; since if a material is porous it will probably have both adsorpton and absorption taking place.

1.4 Hard and soft acids and bases

One of the most widely used theories to predict and to explain chemical reactions in science is the hard or soft acid or base (HSAB) concept. The principle of the HSAB theory is used to gain a qualitative understanding of the predominant factors which drive chemical reactions particulary in transition metal chemistry (Rayner-Canham, 1999). This theory has been quoted in literature to explain the sorption properties of some materials (Goel *et al*., 2005, Merrifield *et al.*, 2004). Ralph Pearson devised the Hard Soft Acid Base (HSAB) principle in the early 1960's as a qualitative theory for the prediction of reactions. He proposed that Lewis acids and bases could be grouped as either "hard" or "soft" and predicted that reactions favour the pairing of harder acids with harder bases and softer acids with softer bases (Pearson, 1963). The hard acids consist of most of the metal ions in the periodic table. They are characterised by low electronegativities and often, high charge densities and are non-polarisable. They can generally be defined as being any cation with a large positive charge or whose *d* electrons are generally unavailable for π bonding, such as the alkali earth ions and Al^{3+}. A group of hard acids, however, that do not fit this descripton are Cr^{3+}, Mn^{2+} and Co^{3+}.

Soft acids are generally the lower right hand section of the metallic elements in the periodic table. They have low charge densities and can be easily polarized, thus having a tendancy to form covalent bonds. Gold (Au^{+}) is reported to be the softest of all acids. There are also elements that are borderline between hard and soft acids.

The oxidation number of the element seems to be the determining factor between hard, soft or borderline (Rayner-Canham, 1999, Miessler, 2004). Table 1.1 lists acids into hard, borderline or soft categories.

Table 1.1 Hard and soft acids as defined by Miessler (2004).

Hard Acids	Borderline Acids	Soft Acids
H^+, Li^+, Na^+, K^+ Be^{2+}, Mg^{2+}, Ca^{2+}, Sr^{2+}, Sn^{2+} BF_3, BCl_3, $B(OR)_3$ Al^{3+}, $Al(CH_3)_3$, $AlCl_3$, AlH_3 Cr^{3+}, Mn^{2+}, Co^{3+}	$B(CH_3)_3$ Rh^{3+}, Co^{2+}, Ni^{2+}, Cu^{2+}, Zn^{2+} Rh^{3+}, Ir^{3+}, Ru^{3+}, Os^{2+}	BH_3, Tl^+, $Tl(CH_3)_3$ Cu^+, Ag^+, Au^+, Cd^{2+}, Hg^+, Hg^{2+}, CH_3Hg^+, $[Co(CN)_5]^{3-}$, Pd^{2+}, Pt^{2+}, Pt^{4+}, Br_2, I_2
Ions with oxidation states of 4 or higher		
HX (hydrogen-bonding molecules)		Metals with zero oxidation state π acceptors: e.g. trinitrobenzene, quinones, tetracyanoethylene

Bases are also classified as being hard or soft. The hard bases, like the hard acids also have low electronegativities and high charge densities and are non-polarizable. They are mainly found to be fluorine and oxygen bonded compounds including oxide, hydroxide, nitrate, phosphate, carbonate, sulfate and perchlorate. Chloride is considered borderline hard. The soft bases, as the soft acids, are the less electronegative, easily polarizable non-metals which include carbon, sulfur, phosphorous and iodides (I^-). They tend to favor covalent bonding. Borderline bases are able to switch depending on how they bond, especially if they have more than one atom available for bonding, as in the case of ambidentate ligands. A common example of this is the thiocyanate ion, NCS^-. This ion can bond through the nitrogen atom (-NCS) which classes it as a borderline base or alternatively it can bond through the sulfur atom (-SCN) changing it to a soft base. Table 1.2 lists bases into their hard, borderline or soft categories. It is interesting to note that elements that are considered

toxic in very low concentrations are nearly always found to be soft acids or bases. The environmentally toxic non-metals and semi-metals, arsenic, selenium and tellurium are classed as very soft bases (Rayner-Canham, 1999).

Table 1.2 Hard and soft bases as defined by Miessler (2004).

Hard Bases	Borderline Bases	Soft Bases
		H^-
F^-,Cl^-	Br^-	I^-
H_2O, OH^-, O^{2-}		H_2S, HS^-, S^{2-}
ROH, RO^-, R_2O, CH_3COO^-		RSH, RS^-, R_2s
NO_3^-, CLO_4^-	NO_2^-, N_3^-	SCN^-, CN^-, RNC, CO
CO_3^{2-}, SO_4^{2-}, PO_4^{3-}	SO_3^{2-}	$S_2O_3^{2-}$
NH_3, RNH_2, N_2H_4	$C_6H_5NH_2$, C_5H_5N, N_2	R_3P, $(RO)_3P$, $R_3AsC_2H_4$, C_6H_6

A variation of the classification of which elements are hard and soft differs depending on the literature read. A more visual placement of the elements that make up hard, soft and borderline acids can be found in the periodic table below, which differes slightly to Table 1.1 above.

Table 1.3 The classification of the HSAB acid ions as defined by Rayner-Canham (1999).

H																He
Li	Be											**B**	C	N	O	F	Ne
Na	**Mg**											**Al**	Si	**P**	**S**	Cl	Ar
K	**Ca**	**Sc**	**Ti**	**V**	**Cr**	**Mn**	**Fe**	**Co**	**Ni**	**Cu**	**Zn**	**Ga**	**Ge**	**As**	**Se**	Br	Kr
Rb	**Sr**	**Y**	**Zr**	**Nb**	**Mo**	Tc	**Ru**	**Rh**	**Pd**	**Ag**	**Cd**	**In**	**Sn**	**Sb**	Te	I	Xe
Cs	**Ba**	*	**Hf**	**Ta**	**W**	**Re**	Os	**Ir**	**Pt**	**Au**	**Hg**	**Tl**	**Pb**	**Bi**	Po	At	Rn
Fr	Ra	**	Rf	Db	Sg	Bh	Hs	Mt	Ds	Rg	Uub	Uut	Uuq	Uup	Uuh	Uus	Uuo

*	**La**	**Ce**	Pr	Nd	Pm	Sm	**Eu**	Gd	Tb	Dy	Ho	Er	Tm	**Yb**	Lu
**	Ac	Th	Pa	U	Np	Pu	Am	Cm	Bk	Cf	Es	Fm	Md	No	Lr

Key **Hard** **Borderline** **Soft**

1.5 A Review of sorbents for heavy metals

There are a huge number of materials both natural and synthetic that are able to absorb or adsorb heavy metals with varying degrees of success. A comparison of the reported results is very difficult due to huge inconsistences in the data presented such as specific test conditions not being reported and results being recorded using different units of sorption primarily mg/g, mmol/g and mmol/L. In some instances the results were converted in an attempt to compare different materials. Some literature is not clear as to whether the material actually absorbs, adsorbs or does a combination of both. It can, however, be deduced from the published literature that sorption, in whatever form, appears to depend heavily on a number of experimental conditions such as pH, metal concentration, ligand concentration, competing ions, and particle size. Cost information is seldom reported but the expense of individual sorbents would generally depend on the degree of processing required and local availability. It has been reported that a sorbent can be assumed as low cost if it requires little processing, is abundant in nature, or is a by-product or waste material from another industry (Bailey *et al*., 1999). To review every single product that is claimed to absorb would take a life time, below is a comprehensive review of some commonly used products.

1.6 Carbon

Activated carbons are highly porous, amorphous solids consisting of micro-crystallites with a graphite lattice. The first reported uses of carbon go so far back into history that it is impossible to document accurately. It is reported that charcoal was used for the filtration of drinking water by ancient Hindus in India, and carbonized wood was used as a medical adsorbent and purifying agent by the

Egyptians as early as 1500 B.C. (Mohan and Pittman, 2006). Activated carbon can be manufactured from any carbonaceous material such as peat, human hair, wool, silk, water hyacinth, tree bark, fly ash, sawdust, cow dung, peanut hull, nut shell, bone char, tea leaves, wood charcoal, coal, coconut shell, rice hulls and rice bran, and agricultural waste. The general procedure for the manufacture of activated carbon can be seen in Figure 1.2.

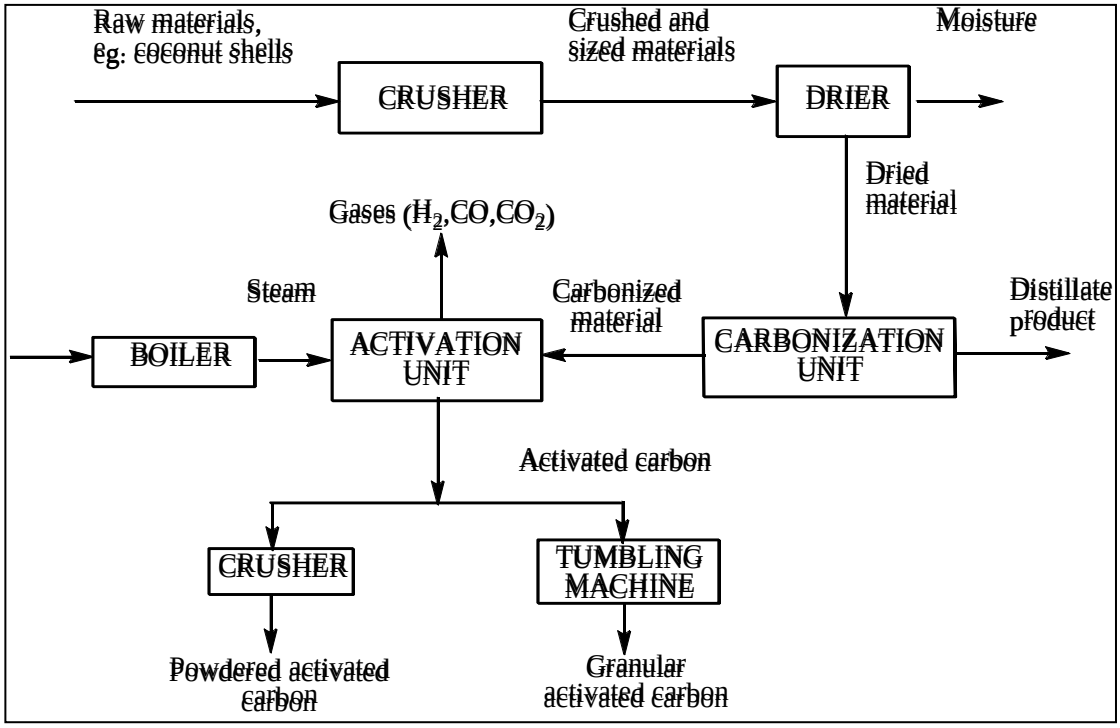

Figure 1.2 Flow diagram for the production of activated carbon.

The manufacturing process consists of two phases, carbonization and activation. The carbonization process includes drying and then heating to separate by-products, including tars and other hydrocarbons, from the raw material, as well as to drive off any gases generated. The carbonization process is completed by heating the material at 400–600°C in an oxygen-deficient atmosphere that cannot support combustion. The carbonized particles are “activated” by exposing them to an activating agent such as steam at high temperature. The steam burns off the decomposition products from the carbonization phase developing a porous, three-

dimensional graphite lattice structure. The size of the pores developed during activation is a function of the time that they are exposed to the steam. Longer exposure times result in larger pore sizes. The most popular aqueous phase carbons are bituminous based because of their hardness, abrasion resistance, pore size distribution, and low cost. Activated carbon is the most widely used adsorbent being employed for adsorption of organic substances and non-polar adsorptives and it is also usually used for waste gas (and waste water) treatment. Its usefulness derives mainly from its large micro-pore and meso-pore volumes and the resulting high surface area (Valix *et al*., 2004). Photographs of the two forms of activated carbon (powdered and granular) can be seen below in Figure 1.3. One of the main disadvantages of using carbon is that it is combustible (Meena *et al*., 2005).

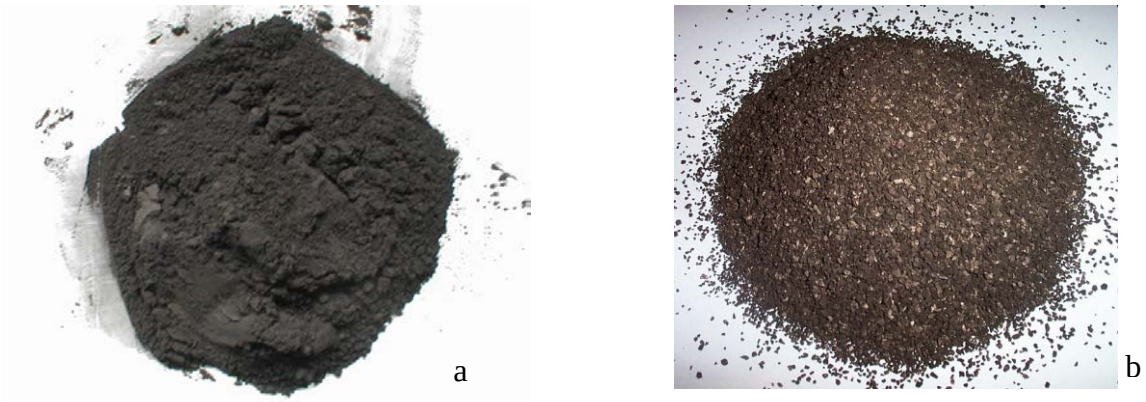

Figure 1.3 (a) Powdered activated carbon and (b) granular activated carbon.

Ramos *et al.* (2002) studied zinc adsorption from aqueous solutions onto different commercially available activated carbons and observed the effects of solution pH and temperature. The carbons tested were C, Centaur HSL, F-300 and F-400. The C carbon is prepared from sawdust and calcined at high temperature using phosphoric acid as a catalyst. Centaur HSL carbon is produced from bituminous carbon according to a patented process by Calgon Carbon Corporation. F-300 and F-400 carbons are also manufactured by Calgon Carbon Corporation using bituminous

carbon. Results showed that an average of three times more zinc adsorbed onto the C carbon compared to the other three carbons tested. A comparison of the total surface areas of the different carbons was calculated and it was found that the C carbon actually had the smallest surface area, indicating that zinc absorption is specific and dependent on the concentration of specific active sites on the activated carbon surface rather than the total surface area available. The maximum uptake was found to be 19.9 mg/g although the initial starting concentration of the zinc solution is not given in the report. Further experiments revealed that solution pH plays a very important role in zinc absorption onto activated carbon, with pH<2 no absorption occurred whereas maximum absorption was achieved at pH 7. Temperature studies also varied depending upon which carbon was being tested although the favourable C carbon was found to be temperature independent.

Goel *et al*. (2005) have been looking for ways of removing lead in wastewaters by using a modified activated carbon. They report that the current remediation procedures for lead removal are pH adjustment with lime or alkali hydroxides, coagulation-sedimentation, and ion exchange. Their research focused on adsorption techniques using commercial activated carbon and an alkali sulfide treated activated carbon. Their theory was that heavy metals have more affinity for sulfides than other anions as naturally occurring metals are often found as sulfides. They state that the chemical affinity of lead towards sulfur groups is higher in accordance with research reported by Pearson (1963) and (Gomez-Serrano *et al*., 1998) who both state that molecules where the donor atom is fluorine, oxygen or nitrogen are all very hard whereas for similar molecules where the donor atom is chlorine, sulfur or phosphorous there is always a large drop in absolute hardness. The theory of hard and soft acids and bases has been discussed previously in section 1.4.

The activated carbon material used was made from coconut shell and was modified to contain sulfur using sodium sulfide. Absorption studies confirmed that the sulfur containing activated carbon absorbed 35% more lead ions than activated carbon on its own having a capacity of 29.44 mg/g. Goel *et al*. (2005) compared his findings to a selection of other absorbents for lead ions and concluded that the results justified more efficient absorption studies. The adsorption material was placed into a column to ascertain the practical applicability of the adsorbent for real industrial wastewaters. It was found that the concentration of lead uptake was dependent upon the adsorbent concentration, hydraulic loading rate, feed concentration and adsorbent bed height. Repeated usage reduced the uptake down to 2.89 mg/g and not the originally reported 29.44 mg/g. The reason for the drop in absorption capacity was ascertained to be due to the potential irreversibility of the sorption process.

Jusoh *et al.* (2007) also studied the effectiveness of activated carbon made from coconut shell to remove the heavy metals cadmium and lead from a solution. Changing the flow rate of the solution altered the amount of uptake. The results concluded that a slow flow rate producing a higher contact time increased uptake. The optimum results showed that granular activated carbon (GAC) was able to remove cadmium and lead from a 20 mg/L mixed aqueous solution reducing levels down to 0.0047 mg/L for cadmium and 0.0987 mg/L for lead.

Commercially available activated carbons from coconut shell, lignite, peat etc are effective for the removal of various pollutants. However they are expensive and their regeneration costs are high. In the search for a cheaper readily available alternative Namasivayam and Sangeetha (2006) investigated the use of a waste by-product of the coir industry known as coir pith. Coir fibres are found between the husk and the outer shell of a coconut and make up about one third of the coconut pulp.

The remaining two thirds is called the pith. It is a spongy cork-like material that is biodegradable but takes up to 20 years to decompose. The extraction of 1 kg of coir fibres generates 2 kg of coir pith, and in India an estimated 500,000 million tonnes of coir pith is produced per annum. Figure 1.4 shows photographs of a coir pith storage yard and a block of pressed coir pith.

Fig 1.4 has been removed due to third party copyright. The unabridged version of the thesis can be viewed at the Lanchester Library, Coventry University

Figure 1.4 Photograph of (a) a coir pith storage and drying yard and (b) coir pith that has been pressed into a block (http://www.wonderpeat.com/process_main.html, 2008).

Research entailed boiling the coir pith in a solution of zinc chloride and then carbonizing the filtered material at 700^{o}C and subsequently washing to remove any excess zinc chloride. The removal of toxic anions, heavy metals, organic compounds and dyes from water was studied and the characteristics of zinc chloride activated coir pith carbon (ZnCPC) were compared with coir pith carbon without zinc chloride (CPC). It was generally found that the percent removal of all compounds increased with an increase in contact time and adsorbent dose. The optimum results concluded that more than 90% removal of nitrate, phosphate, vanadium, thiocyanate, molybdate, mercury, and chromium was obtained by using ZnCPC in an aqueous solution with a concentration of 20 mg/L at 35^{o}C when stirred for three hours. The percent removal of sulfate, selenite and nickel was found to be 70, 74, and 41% respectively under the same adsorption conditions. The results for the CPC without zinc added were zero for all except three elements, these being mercury 80%, chromium 18% and nickel 58%.

The ZnCPC was also tested and found to be very successful in the removal of organic compounds and dye solutions with an average uptake of over 90%.

1.7 Carbon aerogels

Carbon aerogels are a newly emerging adsorbent material composed of covalently bonded nanometre sized particles that are arranged in a three-dimensional network having high porosity and large surface areas (Pekala, 1989). They can be manufactured into a variety of forms such as solid shapes, powder or sheets. Meena *et al*. (2005) studied the effectiveness of using carbon aerogel for the removal of cadmium, zinc, manganese, mercury, nickel, copper and lead in the hope of providing a cost effective and efficient system for the purification of effluents and wastewater. They studied the effects of pH, solution concentration, contact time and adsorbent dose. It was found that the percentage removal of heavy metals increases rapidly with increase in the dose of the adsorbent, obviously due to the greater availability of the exchangeable sites and increased surface area. Contact time required to attain equilibrium is dependant on the initial concentration of the heavy metals. The optimal contact time was found to be about 48 hours. The most important parameter controlling uptake of heavy metals was found to be pH. It was found that the optimum adsorption of mercury, manganese, copper, zinc, and nickel occurred at pH 6, lead at pH 7 and cadmium pH 4. The decrease in adsorption at higher pH (above pH 6) is probably due to the formation of soluble hydroxyl complexes. The difference in adsorption behaviour of different heavy metal ions may be because of differences in their ion exchange capacity on the surface depending on their charge density, extent of hydrolysis and solubility of hydrolysed metal ions in solution under present experimental conditions. Temperature studies found that the metal ion

adsorption increased with an increase in temperature from 20 to 60^{o}C indicating an endothermic reaction. The increase in adsorption with temperature may be attributed to an increase in the number of active surface sites available for adsorption on the adsorbent. At higher temperatures it may be possible that the solute can diffuse within the pores of the adsorbate. Since diffusion is an endothermic process greater adsorption will be observed at higher temperatures. Results showed that nearly 100% removal of heavy metal ions under optimised conditions was achieved when using 10 g/L of aerogel to remove metal ions from a solution with a concentration of 3 mg/L. It appears that Meena *et al.* did not report any experiments to measure the maximum uptake of ions from a concentrated solution.

1.8 Biosorption

Biosorption is the sorption of metals onto dead biological materials or onto the materials that have been derived from living organisms. Studies have shown that a huge variety of materials can be used for this purpose. One of the main advantages of using biosorbents is that the prime biomass is naturally abundant and it has a significantly reduced cost compared to synthetic adsorbents. However more importantly they are non-toxic and can prove to be very efficient. Biomass acts as an ion exchanger of biological origin. The cell wall structure of certain algae, fungi and bacteria has been found to be responsible for this phenomenon. Ongoing pioneering research carried out over the last thirty years on biosorption of heavy metals at McGill University in Montreal has led to identification of a large number of microbial biomass types that are extremely effective in concentrating metals. These biomass types, serving as a basis for metal biosorption processes, can accumulate in excess of 25% of their dry weight in deposited heavy metals: lead, cadmium, uranium, copper,

zinc, chromium and others. A whole new family of suitably "formulated" biosorbents have been used in the process of metal removal and detoxification of industrial metal-bearing effluents. The sorption packed-column configuration is the most effective mode of application for the purpose. Recovery of the deposited metals from saturated biosorbent can be accomplished because they can often be easily released from the biosorbent in a concentrated wash solution which also regenerates the biosorbent for subsequent multiple reuse. This and the extremely low cost of biosorbents make the process highly economical and competitive particularly for environmental applications in detoxifying effluents of e.g.

- metal-plating and metal-finishing operations,
- mining and ore processing operations,
- metal processing, battery and accumulator manufacturing operations,
- thermal power generation (coal-fired plants in particular),
- nuclear power generation, (etc.)

Volesky *et al.* (2003) have attempted to get companies to invest in the production and use of biosorbents as an alternative to synthetic ion exchange or activated carbon sorption. They have published data for biosorption of anionic metal complexes such as gold cyanide, selenium, chromium and vanadate by using waste crab shells, the main constituent being chitin, which is one of the most popular materials under investigation as a biosorbate. Chitin is one of the main components found in the cell walls of fungi, the exoskeletons of insects and other arthropods, and in some other animals. A photograph of chitin made from snow crabs can be seen below (Fig. 1.5).

Fig 1.5 has been removed due to third party copyright. The unabridged version of the thesis can be viewed at the Lanchester Library, Coventry University

Figure 1.5 Photograph of chitin made from snow crabs (www3.jetro.go.jp/.../0001069000/1069870_e.html, 1995).

Chemically it is a polysaccharide constructed from units of *N*-acetylglucosamine (more completely, *N*-acetyl-D-glucos-2-amine). These are linked together in a β-1,4 fashion (in a similar manner to the glucose units which form cellulose). In effect chitin may be described as cellulose with one hydroxyl group on each monomer replaced by an acetylamine group. This allows for increased hydrogen bonding between adjacent polymers, giving the polymer increased strength. Chitin is one of the many naturally occurring polymers.

Chitosan is a high molecular weight polymer derived from chitin (Fig. 1.6). It is synthesized by the removal of the acetyl groups (CH_3-CO) from the chitin polymer chain using dilute acids. By controlling the number of acetyl groups removed along the chain (or by adding new groups to sites that once had an acetyl group), chemists can tune the properties of chitosan to make it more versatile.

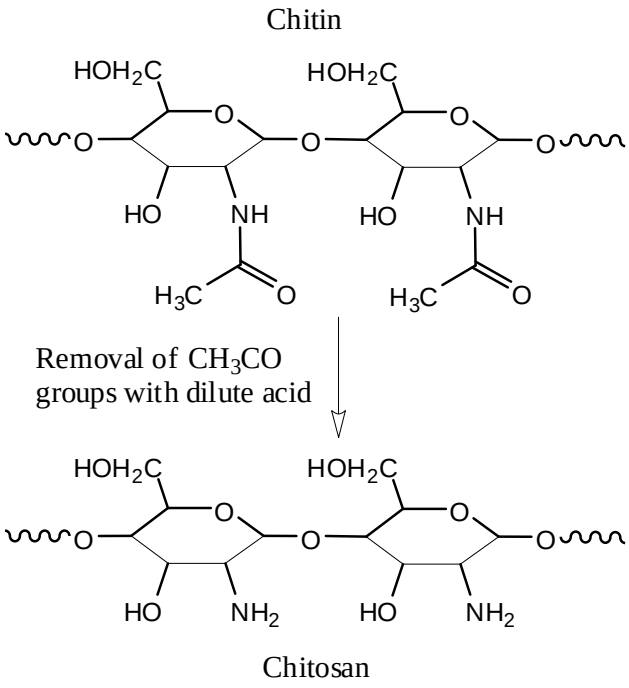

Figure 1.6 Chemical conversion of chitin to chitosan.

When chitosan comes in contact with blood it induces clotting. Using a modified form of chitosan researchers in Oregon developed a durable and flexible field dressing that sticks to and seals wounds. The result was the HemCon® Bandage, which was designed to control life threatening bleeding. The bandage claimed FDA approval in a near-record 48 hours, and was deployed on the battlefield of Iraq in 2003. Since then, the bandage has been used extensively and is credited with helping save over 100 lives with no adverse events reported (Gregory and Wiesmann, 2007). Scanning electron microscope pictures of chitosan microspheres can be seen below in Figure 1.7.

Fig 1.7 has been removed due to third party copyright. The unabridged version of the thesis can be viewed at the Lanchester Library, Coventry University

Figure 1.7 Scanning electron microscope pictures of chitosan microspheres obtained by spray drying from aqueous solutions with (a) 0.5%w/w chitosan and (b) 2.5%w/w chitosan (Oliveiral et al., 2005).

Chitosan is commonly used in water processing engineering as part of a filtration process where it causes fine sediment particles to bind together, which are then subsequently removed with the sediment during sand filtration. Sand filtration apparently can remove up to 50% of the turbidity alone while the Chitosan with sand filtration removes up to 99% turbidity. Chitosan is useful in other filtration situations where removal of suspended particles from a liquid is needed. Chitosan, in combination with bentonite, gelatin, silica gel, isinglass, or other fining agents is used to clarify wine, mead, and beer. It is also known to remove phosphorus, heavy minerals, and oils from water. It can also be used as a protective coating on food and seeds and serve as a time-release structure for medicines (Nicol, 1991).

Many researchers have investigated chitin and chitosan for heavy metal removal. The fact that it can be engineered into many desired shapes such as beads, membranes and ground particles makes it particularly resourceful along with the high nitrogen content and porosity contributing to relatively high sorption capacities. The removal of arsenic, cadmium, copper, lead, mercury, molybdenum, nickel, vanadium, uranium and zinc have been investigated across the world by various researchers. The only drawback being the lack of specificity towards several highly toxic heavy metals limits the use of chitosan as an effective sorbent.

Merrifield *et al.* (2004) attempted to enhance the adsorption capacity of chitosan beads by graft polymerization of a thiol-containing compound. They were working on the principle that the ability of a material to capture metals is controlled in part by the number of available functional groups used for binding metals. Functional groups with a known affinity for specific metals can be attached to other substances in order to create an effective adsorbent. The thiol (-SH) group is known to form stable complexes with soft heavy metals of high polarizability such as mercury, silver and gold and to a lesser extent cadmium and zinc, while failing to co-ordinate well with the more abundant smaller, lighter, hard metals such as calcium, sodium and magnesium. They studied the uptake of mercury using the thiol-grafted chitosan gel beads. Mercury is characterized as a soft Lewis acid due to its high polarizability. It forms strong covalent bonds with soft Lewis bases, notably reduced sulfur in the thiol group and also the amine functional groups. The molar absorption capacity of the thiol-grafted chitosan gel beads for mercury removal was found to be approximately 8 mmol/g-dry beads at pH7. They report their results to be favourable with several other sorbents for the removal of mercury.

Hacettepe University, Turkey, synthesized novel metal chelating membrane disks called Procion Brown MX 5BR immobilized poly(hydroxyethyl methacrylate/chitosan) composite membranes, (also called interpenetrating net-work, IPN, membranes) for the removal of three toxic heavy metal ions cadmium, lead and mercury from aqueous solutions. The IPN membrane was synthesized by mixing a solution of chitosan with the monomer 2-hydroxyethylmethacrylate (2-HEMA) with azobisisobutyronitrile (AIBN) as the initiator and cut into 0.75 cm disks after polymerization was complete.

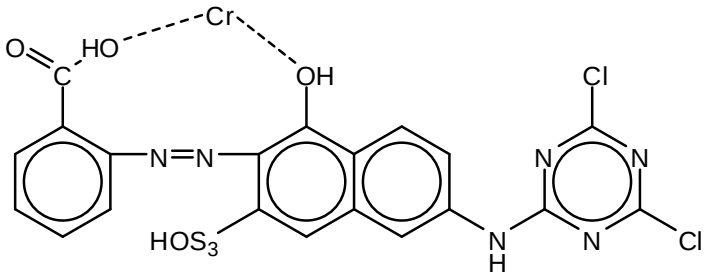

Figure 1.8 Chemical structure of Procion Brown MX 5BR.

The Procion Brown MX 5BR (Fig. 1.8) was covalently bonded onto the IPN membrane via a nucleophilic reaction between the chloride of its triazine ring and the amide and the hydroxyl groups of the IPN under alkaline conditions. The maximum absorption capacities (Table 1.4) were reported using a concentration of 100 mg/L for each solution at pH 5.0 and temperature of 20^{o}C.

Table 1.4 Results for Procion Brown MX 5BR uptake of metal ions.

	Cadmium		Lead		Mercury	
	mg/g	mmol/g	mg/g	mmol/g	mg/g	mmol/g
Single solutions	18.5	0.17	22.7	0.11	68.28	0.34
Mixed solution	1.8	0.02	2.2	0.01	52.60	0.26

These results show that Procion Brown MX 5BR immobilized poly(hydroxyethyl methacrylate/chitosan) has a much higher preference for mercury ions than cadmium and lead (Genc *et al*., 2002).

Genc *et al*. (2003) then attached Procion Green H-4G (Fig 1.9) to IPN membranes and again studied the removal of cadmium, lead and mercury. Procion Green H-4G is an aromatic polysulfonated dye containing a ratio of seven acidic sulfonate groups to three basic secondary amino groups as can be seen below in Table 1.5.

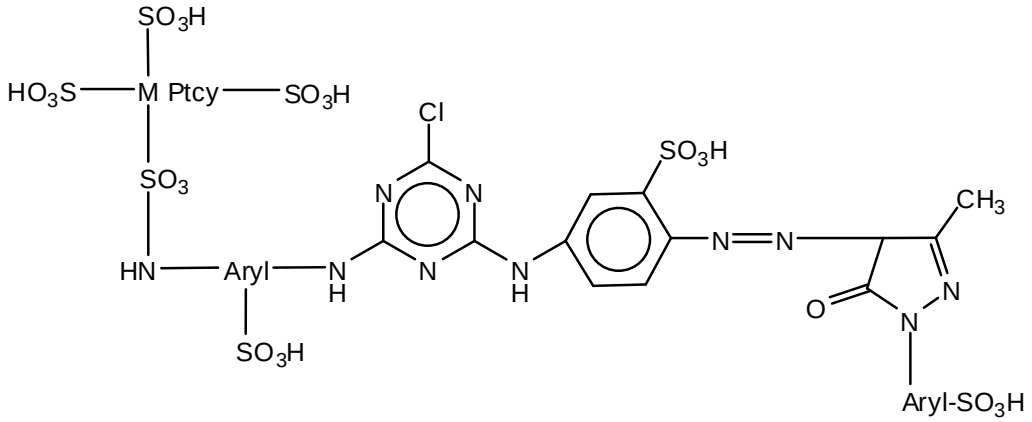

Figure 1.9 Chemical structure of Procion Green H-4G.

Table 1.5 Results for Procion Green H-4G uptake of metal ions.

	Cadmium		Lead		Mercury	
	mg/g	mmol/g	mg/g	mmol/g	mg/g	mmol/g
Single solutions	43.60	0.39	68.81	0.33	48.22	0.24
Mixed solution	12.74	0.11	28.80	0.14	18.41	0.09

The results recorded in Table 1.5 show that Procion Green H-4G appears to be more effective at removing heavy metal ions cadmium and lead than the Procion Brown MX 5BR (Table 1.4) in single solutions but does not show any selective affinity for a particular ion in the mixed solutions therefore would not be as effective as the Procion Brown MX 5BR.

At the same time another Turkish university was also researching IPN membranes synthesized from 2-hydroxyethyl methacrylate (HEMA) and chitosan (pHEMA/chitosan) with Procion Brown MX-5BR (PB MX-5BR) covalently attached onto IPNs membrane as a metal chelating dye-ligand. Bayramoglu *et al*. (2002), from Kirikkale University, attached two different Lewis metal ions iron and copper onto the dye-ligand for utilization in immobilized metal affinity chromatography (IMAC). The binding characteristics of a model protein (lysozyme) to IMAC adsorbents and selectivity of immobilized metal ions (Fe^{3+} and Cu^{2+}) to the lysozyme were investigated from aqueous solution using the dye-ligand-attached IPN membrane as a control system. The lysozyme adsorption capacities of the dye-

ligand, dye-ligand-Fe^{3+} and dye-ligand-Cu^{2+} immobilized IPN membranes were 79.1, 147.4, and 128.2 mg/ml, respectively. The IPN metal-chelate affinity membranes were reusable without significant reduction in the protein adsorption capacities. These features make the dye-ligand and metal chelate affinity membranes very good candidates for use in metal-affinity chelate separation of proteins and would be effective in processing large volumes of biological fluid containing a target protein.

Another polysaccharide similar to chitosan is alginate (Fig. 1.10), which is a viscous gum that is abundant in the cell walls of brown algae. It has a structure similar to chitosan having the same ß linkage between carbons one and four. Karagunduz *et al.* (2006) researched alginate and reported it to have a great affinity to divalent cations. Karagunduz's main objective was to investigate the removal of copper from solution by alginate and surfactant entrapped dried alginate beads. Equilibrium and kinetic experiments were carried out and showed that the sorption of copper ions increased as the pH of the aqueous solution increased.

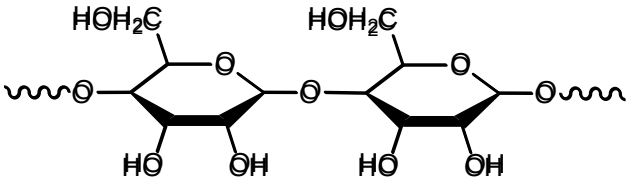

Figure 1.10 Chemical structure of alginate.

Curdlan (Fig. 1.11) is a biodegradable polysaccharide, which is also similar to chitosan, characterized by repeating glucose subunits joined by a ß linkage between carbons one and three of the glucose ring. While the primary structure is a long chain, curdlan forms more complex tertiary structures due to intramolecular and intermolecular hydrogen bonding. It is insoluble in water but soluble in alkali

solutions. When suspended in water and heated to over 80^{o}C an irreversible gel was formed (Cheeseman and Brown, 1995).

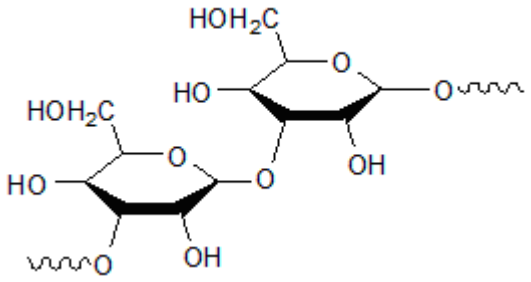

Figure 1.11 Chemical structure of curdlan.

Moon and Lee (2005) carried out research on an adsorption filter made from a combination of curdlan and activated charcoal for the removal of heavy metals from oriental herbs. Its absorption characteristics were studied for four heavy metals, copper, manganese, lead and cadmium. The ratio of curdlan to activated carbon was changed to determine the best concentration performance. Experiments were carried by adding 0.1g of adsorbent to 20 mL of metal ion solution (1000mg/L of lead, cadmium, copper and manganese) and stirring for one hour. The solution was separated by centrifugation and the ion content determined using atomic absorption spectroscopy (AAS). Copper ion absorption was found to be the highest (161 mg/g) followed in decreasing order by manganese (75 mg/g), lead (72 mg/g), and finally cadmium (41 mg/g). The results also showed that heavy metal adsorption generally increased with increasing activated carbon content. This indicated that activated carbon was the main adsorbent and that the curdlan only acted as a binder, although the large amount of hydroxyl groups on the surface of the particles should have helped enhance the adsorption.

Gode and Pehlivan (2007) studied the removal of chromium from aqueous solutions using a new chelate-resin known as (b-DAEG-sporopollenin and CEP-sporopollenin). Sporopollenin is a natural polymer contained in the outer wall of

spores and pollen. It is highly resistant to chemical attack, has a high capacity, is stable and has a constant chemical structure that exhibits very good stability even after prolonged exposure to mineral acids and alkalis. The detailed chemical structure is as yet unknown, but its empirical formula has been found to be $C_{90}H_{144}O_{27}$. The results show that the metal uptake increased with metal ion concentration. Sporopollenin has also been filled with organic, inorganic and magnetic nanoparticles (Fig. 1.12) (Paunov *et al*., 2007).

Fig 1.12 has been removed due to third part copyright. The unabridged version of this thesis can be viewed at the Lanchester Library, Coventry University

Figure 1.12 Scanning electron microscope pictures of sporopollenin microcapsules loaded with a range of inorganic and organic nanomaterials (Paunov *et al*., 2007).

Satiroglu et al. (2002) studied the adsorption characteristics of fungi. Three different forms of one fungus called polyporus versicolor (active, alkali-pretreated and heat-inactivated) were used for the removal of zinc, cadmium and mercury by the process of biosorption. The theory of the research was that cell surfaces are anionic due to the presence of ionised groups such as carboxylate, hydroxyl and phosphate in various cell wall polymers. Uncharged groups such as peptide *N* atoms may also function as ligands to complete the co-ordination number requirements of the metal ion. Organisms will have various distributions of charge and geometry for these binding groups, and so may well selectively bind certain metal ions. The extent of

uptake of metal may vary with pH, due to the protonation of these anionic groups. The uptake of heavy metal ions by microorganisms has often been observed to occur in two stages; an initial rapid uptake due to surface adsorption on the cell walls and a subsequent slow uptake due to membrane transport of the metal ions to the cytoplasm of the cells. Surface adsorption is a physiochemical phenomenon. The cell walls of many micro-organisms consist of polysaccharides, proteins and lipids collectively offering a whole host of functional groups capable of binding to heavy metals. These functional groups, such as amino, carboxylic, phosphate and thiol groups differ in their affinity and specificity for metal binding. The maximum amount of metal ion adsorbed by each type of biosorbent (Table 1.6) was studied using initial metal ion concentrations of 200 mg/L, pH 6 and temperature of 20^{o}C.

Table 1.6 Biosorption capacities of Polyporus versicolor.

	Zinc	Cadmium	Mercury
NaOH treated	139.3	232.2	290.3
Heat-inactivated	70.8	118.2	168.9
Activated	54.1	90.0	131.4

Equilibrium bead loading (mg/g adsorbent)

The results conclude that different forms of polyporus versicolor can be successfully used as biosorbing agents for the removal of zinc, cadmium and mercury ions from aqueous medium. The absorption of metal ions onto the biosorbents depends on the experimental conditions, particularly the medium pH and the initial concentration of the metal ions. The order of affinity of the different forms of biosorbents for the three metal ions studied was found as, NaOH treated>heat-inactivated>activated. The NaOH treated fungus can be applied easily using existing treatment technologies.

Hardin and Admassu (2005) studied the ability of four common plant sources; wood, grass, compost and peat moss to remove cadmium, chromium and lead from dilute aqueous solutions. The dried, ground vegetation was immobilized in

polysulfone and poly(bisphenyl A) carbonate to form spherical beads through a phase inversion process. Tests were carried out using single and multiple ion solutions with a concentration of 200 mg/L for each ion.

Table 1.7 Biosorption capacities of polysulfone beads.

	Cadmium		Chromium		Lead	
	Single-species	Multiple-species	Single-species	Multiple-species	Single-species	Multiple-species
Wood	2.73	2.57	3.96	3.76	2.13	3.73
Grass	1.92	3.44	3.98	3.95	3.15	3.95
Compost	2.59	3.97	4.00	4.00	3.17	3.94
Peat	3.00	3.99	3.96	4.00	3.93	3.89
None	0.87	0.28	0.03	0.30	1.37	0.29

Bead loading of 4 mg/g corresponds to complete removal of the ion from solution.
Equilibrium bead loading (mg/g adsorbent) for polysulfone beads

Table 1.8 Biosorption capacities of polycarbonate beads.

	Cadmium		Chromium		Lead	
	Single-species	Multiple-species	Single-species	Multiple-species	Single-species	Multiple-species
Wood	3.41	2.64	3.98	3.98	1.50	3.94
Grass	3.60	2.82	3.53	3.87	3.64	3.96
Compost	3.90	3.50	3.99	3.98	3.96	3.97
Peat	2.92	3.98	3.99	4.00	1.72	3.97
None	1.33	0.28	1.01	0.31	1.24	0.33

Bead loading of 4 mg/g corresponds to complete removal of the ion from solution.
Equilibrium bead loading (mg/g adsorbent) for polycarbonate beads

The results reported in the journal state that in general polysulfone produces more efficient beads. Hardin hypothesised that the polysulfone forms a more porous matrix that results in a larger overall surface area per unit volume. The beads showed a high affinity for cadmium, chromium and lead, efficiently removing the ions from both single-ion and multiple-ion solutions and in some cases increasing the equilibrium loading of the bead.

If a direct comparison is made of the Tables 1.7 and 1.8 it can be seen that there is actually not a great deal of difference between the two sets of data. When the Hardin data is compared to the Satiroglu *et al*. data for the polyporus versicolor

(Table 1.6) there is a huge difference in numbers suggesting that the polyporus versicolor is far more efficient than either the polysulfone and polycarbonate beads, or it could be hypothesised that there is a mistake in the calculations. If Hardins data units were mmol/g and not the mg/g as reported then their claims for a successful product would make much more sense.

ClearEarth is a natural material that is claimed by its manufacturers to be effective in treating a broad range of contaminants such as heavy metals, complex hydrocarbons, pesticides and radioactivity. The material naturally contains a mix of elements including sodium, potassium, magnesium and calcium bound around a complex organic fibre structure. It is extracted under licence from freshwater lakes where the material has been immersed in an anaerobic environment for the last 12,000 years. The material is constantly being regenerated. Extraction can only be done under licence and the known reserves are expected to last for many hundreds of years. The material has a very large surface area where larger contaminant molecules can be caught. The organic fraction of the material is attracted to cations such as lead, zinc, cadmium, copper, nickel mercury, thallium and hydrocarbons (crude oil). ClearEarth is reported to eradicate metal contamination by the process of ion exchange.

When tested on a different effluent for the rate of uptake the material demonstrated that within 15 minutes of agitation constant levels were achieved at a ratio of 1 part ClearEarth to 20 parts effluent.

Table 1.9 Results for ClearEarth uptake.

	Zinc	Lead	Cadmium
Initial concentration	10.0	0.44	1.8
Final concentration	0.77	0.09	0.13
Percentage uptake	92%	80%	93%

Equilibrium bead loading (mg/g adsorbent)

The metal ions zinc, lead and cadmium (Table 1.9) were found to have an uptake level in excess of 80%. It was reported that the ions would not leach from the medium within a wide range of pH. In the case of hydrocarbons, the material acts as an absorbent of long chain and complex molecules, stopping their migration and promoting biological degradation. It is proposed that ClearEarth could be used as part of a filter system where the contaminant is either dissolved or mixed as an emulsion, or by incorporating it directly into the ClearEarth (ClearEarth, 2006).

Humin is a fraction of humic substances, which are components of the natural organic matter present in soils, peat, sediments and water. They consist of a complex mixture of molecules whose molecular weight varies vastly but is insoluble. The material is extremely porous and has a very large surface area making it extremely useful as an adsorbent. In addition it also contains various potential binding sites for heavy metal ions. Batch studies have shown that humin can efficiently adsorb different heavy metal ions from aqueous solutions having a pH of 5. De la Rosa *et al*. (2003) performed column experiments using silica-immobilized humin in order to evaluate the removal and recovery of metal ions under flow conditions. Various absorption studies were undertaken using copper and lead individually and competitive adsorption using cadmium, copper, lead, nickel and chromium. The concentration of the metal ions in solution was 0.1mM. Maximum absorption capacities for single cations and mixed cations are shown below in Tables 1.20 and 1.21.

Table 1.20 Results for single cation absorption in humin.

	initial conc (mg/L)	uptake (μmol/g)
Copper	6.5	175.6
Lead	21	150.6

Table 1.21 Results for mixed cation absorption in humin.

	initial conc (mg/L)	uptake (μmol/g)
Cadmium	11	5.3
Copper	6.5	63
Lead	21	100
Nickel	6	4.5
Chromium	5	131.5

The selectivity of the humin compound was found to be in favour of $Cr^{3+}>Pb^{2+}>Cu^{2+}>Cd^{2+}>Ni^{2+}$. Desorbtion studies found that copper, lead and nickel were recovered between 82% and 100%, cadmium between 72% and 80% while chromium was recovered between 45% and 70% when washed and recycled three times. The results concluded that silica-immobilized humin is a suitable material for the removal of copper; lead and chromium ions from aqueous solutions under flow conditions and have a high potential for the treatment of metal-contaminated waste-waters.

Fly ash is the finely divided mineral residue resulting from the combustion of coal in power stations. It consists of inorganic, incombustible matter present in the coal that has been fused during combustion into a glassy, amorphous structure. Fly ash material is solidified while suspended in the exhaust gases and is collected by electrostatic precipitators or filter bags. Since the particles solidify while suspended in the exhaust gases, fly ash particles are spherical in shape (Fig. 1.13) and are generally less than 250 micrometers in size with a melting point of 1000^{o}C. The fly ash particles possess very high mechanical strength and are chemically inert (Royal *et al.*, 2008). They consist mostly of silicon dioxide (SiO_2), aluminium oxide (Al_2O_3) and iron oxide (Fe_2O_3).

Figure 1.13 Scanning electron microscope picture of fly ash particles (Hoffman, 2000).

The elemental composition of fly ash is highly variable and directly related to compositional variations in the parent coal, and to the operational characteristics of the individual power plants. It already contains traces of a large number of elements, many of which are toxic. Fly ash collected by means of an electrostatic precipitator from the coal-fired thermal power plant of the National Thermal Power Corporation located at Talcher in India was characterized using particle-induced x-ray emission (PIXE) and energy-dispersive x-ray fluorescence (EDXRF) techniques. It was found to contain sixteen elements, namely potassium, calcium, titanium, vanadium, chromium, manganese, iron, nickel, copper, zinc, gallium, arsenic, rhubidium, strontium, yttrium and lead (Vijayan *et al*., 1997). The Environmental Protection Agency however confirms that coal fly ash need not be regulated as a hazardous waste (Browner, 2000).

The majority of fly ash is used in the manufacture of cement but there is a large amount of fly ash with high-unburned carbon content that cannot be used as a cement additive because of the adverse effects it has on the quality of the concrete thus creating a research need to develop an alternative technology that can further exploit fly ash. Cho *et al*. (2005) investigated the possibility of utilizing it as a low-cost adsorbent in the treatment of wastewater containing the heavy metals zinc, lead cadmium and copper. They report fly ash to be a strong alkali material exhibiting a

pH of 10-13 when added to water with its surface being negatively charged. Tests were carried out under various conditions such as pH, heavy metal concentration and fly ash dosages through kinetic and isotherm studies and reported the optimum removal conditions for each metal ion. A series of tests investigated how the presence of other metal ions affected the removal of one metal ion. The conclusion was that the percent removal of heavy metal ions increased as the pH increased and that most of the metal ions had a 95% removal when the pH was above 8. The report does not state the concentration of metal ions per mass of fly ash in mg/g so the comparison with other methods is difficult. However, it is reported that when separating a mixed solution the concentration of the ions in solution influenced the efficiency of the fly ash sometimes enhancing efficiency but also sometimes reducing efficiency.

Naturally occurring clay may serve as cost-effective sorbents for the removal of heavy metals. Although sorption capacity is usually less than those of synthetic sorbents, these materials could provide an inexpensive substitute for the treatment of heavy metal wastewaters. To enhance the sorption capacity the clays are modified in a variety of ways such as treatment by inorganic and organic compounds and acids or bases. Clay is a group of crystalline minerals, mainly hydrous silicates. Smectite is a kind of clay produced when water eats away at sedimentary rocks. It is a special kind of clay that absorbs water and swells substantially. Each crystal of the mineral is made up of a system of sheets of alternating aluminium-oxygen and silicon-oxygen molecules. Between the sheets the air is charged with an electrostatic force that sucks in water so that the crystal swells up to eight times its original size. Most of it is formed when ash from volcanic action meets sea or rainwater and is changed by chemical interaction (Say *et al*. 2006).

Organoclays have recently attracted much attention in a number of applications such as polymer-clay nano-composites, absorbents of organic pollution in ground water, coating and paints. Composites have been prepared through in-situ polymerization of monomers within modified clays. It has been reported that several of these composites exhibited improved mechanical and barrier properties in comparison with the matrix polymer. Say *et al*. (2006) researched the effectiveness of dithiocarbamate-anchored polymer organosmectite composites for the removal of heavy metal ions from aqueous solutions. To do this they first modified naturally occurring smectite minerals with quartamin, styrene and chloromethylstyrene then reacted them with carbon disulfide, in order to incorporate dithiocabamate functional groups into the subsurfaces of the organoclay. Heavy metal adsorption-desorption studies were carried out for lead, cadmium and chromium ions. The maximum absorption capacities of organoclay in single and mixed metal ion solution can be seen in Tables 1.22 and 1.23:

Table 1.22 Absorption capacities of organoclay using single metal solutions.

Lead	170 mg/g	824 μmol/g
Cadmium	82 mg/g	731 μmol/g
Chromium	71 mg/g	1367 μmol/g

Table 1.23 Absorption capacities of organoclay using mixed metal solutions.

	50mg/L solution		100mg/L solution	
Lead	44 mg/g	210 μmol/g	70 mg/g	340 μmol/g
Cadmium	21 mg/g	184 μmol/g	32 mg/g	283 μmol/g
Chromium	11 mg/g	212 μmol/g	20 mg/g	390 μmol/g

The molar absorbtivity gives the same metal ion affinity sequence under non-competitive and competitive conditions as $Cr^{3+}>Pb^{2+}>Cd^{2+}$. Washing in 0.5 molar sodium chloride successfully desorbed the metal ions from the product enabling it to

be reused producing a cheap and highly selective method for the removal of heavy metal ions.

1.9 Chemically synthesized micro-porous products

The Chemistry Department at Hacettepe University, Turkey, have spent over twenty years developing micro porous products. One of the first reported papers, published in 1988 by Adil Denizli *et al*., was for the design of a new polymer-drug composite system for use in local chemotherapy to act as carriers for anticancer drugs. This was achieved by synthesizing a micro porous polymer gel called Poly(hydroxyethylmethacrylate-bisglycolacrylate) (poly(HEMA-BGA) by a low temperature radiation polymerization technique. By changing the relative amounts and the types of ingredients, drug loading and radiation dosage polymer-drug composites with different structural properties were obtained. PHEMA was reported to be a cross-linked hydrogel, being a form of matter intermediate between a solid and a liquid that does not dissolve in aqueous media but does take up water depending on the degree of cross-linking and the hydrophilicity of the polymer matrix. The PHEMA has a swelling capacity of between 30 and 35% (Denizli *et al*., 1988).

Research has shown that PHEMA can be used for numerous applications. Many subsequent papers published by Hacettepe University detailing the synthesis of various micro porous substances using this inexpensive polymer system have been reported. Tests have been carried out on the PHEMA products and prove them to be reusable in all cases at least three to five times and possibly longer. The PHEMA is synthesized by suspension polymerization of 2-hydroxyethyl methacrylate (HEMA) and ethylene glycol dimethacrylate (EGDMA) monomers in the presence of an initiator (azobisisobutyronitrile, AIBN) as seen in Figure 1.14 below. Figure 1.15

shows scanning electron microscope pictures of a PHEMA membrane. Depending on the chosen method method of reaction the PHEMA can also be made into micro spheres (Fig. 1.17 page 40).

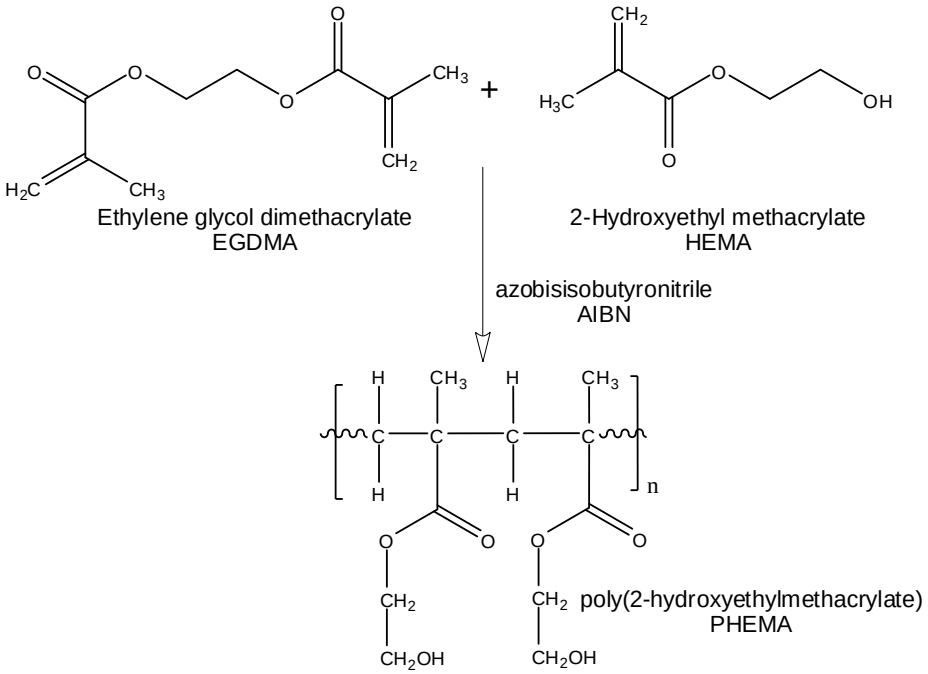

Figure 1.14 Chemical synthesis of PHEMA**.**

Fig 1.15 has been removed due to third party copyright. The unabridged version of the thesis can be viewed at the Lanchester Library, Coventry University

Figure 1.15 Scanning electon microscope pictures of a PHEMA membrane (a) cross section, magnification X120 and (b) surface, magnification X280 (Denizli *et al*., 2000b).

In 1997 Denizli *et al*. began researching effective ways of removing heavy metal pollutants from wastewater streams using (PHEMA) membranes attached to affinity dyes. The PHEMA was synthesized, as reported above, then an affinity dye called Cibacron Blue F3GA was attached covalently as a metal-chelating ligand for heavy metal adsorption, as seen below in Figure 1.16.

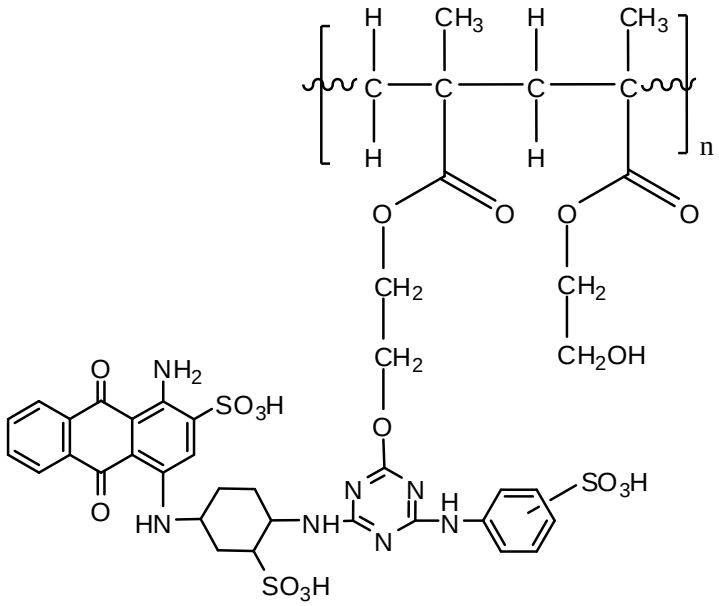

Figure 1.16 Coupling of Cibacron Blue F3GA to the PHEMA membrane.

The adsorption/desorption of heavy metal ions, arsenic, cadmium and lead from aqueous solutions was studied. Very high adsorption rates were observed and adsorption equilibriums were reached in about thirty minutes. The results for the PHEMA membranes are all reported in mmol/m^2 and not mg/g so a comparison with other materials is not possible. The maximum adsorptions of heavy metal ions onto the dye-incorporated affinity membranes from their single solutions were reported in Table 1.24.

Table 1.24 Results for PHEMA/Cibacron Blue F3 GA membrane uptake of metal ions.

	Arsenic	Cadmium	Lead
Single solutions	13	61	79
Mixed solution	11	14	10

Equilibrium bead loading (mmol/m^2 adsorbent)

It can be seen from Table 1.24 that when the heavy metal ions competed in the mixed solutions the amount of adsorption for arsenic, cadmium and lead were very similar. Desorption of heavy metal ions was carried out by using 0.1 molar nitric acid (pH 1.0). Up to 95% of the adsorbed heavy metal ions were desorbed in 60 minutes.

Repeated adsorption/desorption cycles showed the feasibility of this novel affinity membrane for heavy metal removal (Denizli *et al*., 1997).

In 2000 Denizli *et al*. synthesized PHEMA membranes carrying ethylene diamine (EDA) and Cibacron Blue F3GA for the removal of heavy metal ions copper, mercury, lead and cadmium from aqueous solutions containing different concentrations of ions (5-700 μg/L) and at different pH values (2.0-8.0). The results can be seen below in Table 1.25. It can be seen from the table that the non-specific adsorption of heavy metal ions on the unmodified PHEMA membranes was very low.

Table 1.25 Results for EDA PHEMA membrane uptake of metal ions.

EDA products	Mercury	Copper	Lead	Cadmium
PHEMA single solution ions	3.3	0.5	1.2	1.1
PHEMA Cibacron Blue F3GA single solution ions	16.3	19.9	23.4	38.4
PHEMA Cibacron Blue F3GA mixed solution ions	7.1	17.9	6.2	9.1

Equilibrium bead loading (mmol/m^2 adsorbent)

Cibacron Blue F3GA attachment significantly increased the heavy metal adsorption. When the heavy metal ions competed (in the case of the adsorption from a mixture) the results were considerably less for mercury, lead and cadmium. The observed order of adsorption was found to be $Cd^{2+}>Pb^{2+}>Cu^{2+}>Hg^{2+}$ for non-competitive single ion conditions, it then changed to $Cu^{2+}>Cd^{2+}>Hg^{2+}>Pb^{2+}$. The adsorption of heavy metal ions increased with increasing pH and reached a plateau value at around pH 5.0 (Denizli *et al*., 2000a).

In 2001 Denizli *et al*. began researching polymer micro spheres instead of membranes. The same basic chemicals were used as for previous studies with a modification to the synthesis. PHEMA micro beads were prepared by a suspension polymerization technique. Polymerization was carried out in an aqueous dispersion

medium containing magnesium oxide that was used to decrease the solubility of the monomer in the medium. The monomer phase was added to the dispersion medium and mechanically stirred with a blade type stirrer, when filtered and washed the resulting polymer formed microbeads of approximately 200 μm (Fig. 1.17).

Fig 1.17 has been removed due to third party copyright. The unabridged version of the thesis is available at the Lanchester Library, Coventry University

external part detail internal part detail

Figure 1.17 Scanning electron microscope pictures of poly(HEMA-MAGA) beads (Denizli *et al*., 2005).

PHEMA microbeads carrying Cibacron Blue F3GA (22.3 μmol g^{-1}) were prepared for the removal of Pb^{2+}, Cd^{2+}, Cu^{2+} and Zn^{2+} ions from aqueous solutions containing different amount of these ions (10–400 mg l^{-1}) and at different pH values (2.0–6.0). Adsorption rates were high and adsorption equilibrium was reached within 10 minutes. Adsorption of these metal ions onto the Cibacron Blue F3GA-immobilised micro beads from single solutions of 80 mg/L concentration at pH 5 and 20^{o}C can be seen in Table 1.26 below.

Table 1.26 Results for PHEMA/Cibacron Blue F3 GA microbead uptake of metal ions.

	Lead	Cadmium	Copper	Zinc
Single solutions	16.96	8.50	4.44	6.70
Mixed solution	2.00	-	5.88	-

Equilibrium bead loading (mg/g adsorbent)

When the heavy metal ions competed in the mixed solutions the amount of adsorption was 2.00 and 5.88 mg/g for copper and lead, respectively. Under competitive conditions the affinity of cadmium and zinc was negligible (Arpa *et al*., 2001).

The same beads (with 16.5 micromoles of Cibacron Blue attached) were reported to remove phenol, *m*-chlorophenol, *p*-chlorophenol and 2,4,6-trichlorophenol from aqueous solutions (Table 1.27). Wastewaters containing phenol compounds present a serious pollution problem because phenol-containing wastewater cannot be mixed into open water without treatment because phenol is extremely toxic with many known to be, or suspected, carcinogens. The adsorption rate of the chlorophenols was reported to be very high and achieved equilibrium in about 20 minutes.

Table 1.27 Results for the removal of phenol containing compounds using PHEMA/Cibacron Blue F3 GA microbead.

Phenol	2, 4, 6-trichlorophenol	*p*-chlorophenol	*m*-chlorophenol
88.8	94.6	97.6	109.1

Equilibrium bead loading (μmol/g adsorbent)

The micro beads were again found to be reusable for more than five cycles showing that Cibacron Blue F3GA-carrying micro beads have a very good feasibility for chlorophenol removal as well as heavy metal ion removal from aqueous solutions (Denizli *et al*., 2001).

In 2001 Denizli *et al*. synthesized PHEMA beads carrying thiazolidine for the removal of lead and cadmium ions from aqueous solutions. The size range of the beads was reported as being 150-200 micrometers. The highly cross-linked composition gives the beads a quite rigid strong structure making them suitable for fixed bed or fluidised bed continuous column applications for heavy metal removal from aqueous solutions or wastewaters. The absorption rates were reported to be high (Table 1.28) and adsorption equilibria were reached within 10 minutes. The initial concentrations of the solutions were 500 mg/L for cadmium and 250 mg/L for lead, with a pH of 5.5 at temperature of 20^{o}C.

Table 1.28 Results for PHEMA/thiazolidine bead uptake of metal ions.

	Lead	Cadmium
Single solutions	0.32	0.40
Mixed solution	0.32	0.04

Equilibrium bead loading (mmol/g adsorbent)

Converting the results back into mg/g for comparison with previous results can be seen in Table 1.29:

Table 1.29 Conversion of units for comparison of results from table 1.28.

	Lead	Cadmium
Single solutions	69.6	44.6
Mixed solution	67.5	4.00

Equilibrium bead loading (mg/g adsorbent)

The results of the mixed solution indicate that this novel metal chelating system is selective for lead ions and was much more efficient than the PHEMA beads with Cibacron Blue F3GA attached (Saglam *et al*., 2001).

Denizli *et al*. (2003) investigated the attachment of poly(ethyleneimine) (PEI) to PHEMA beads for the removal of mercury ions. Results show that the adsorption of mercury was quite fast especially when the concentration of the solution was 500 mg/L, reaching equilibrium within the first 10 minutes. This was due to the high complexation rate between the mercury ions and the amine functional groups on the PEI molecules on the surface of the PHEMA beads. The maximum mercury adsorption capacity was reported to be 1.67 mmol/g polymer, which equates to 334.9 mg/g. The conclusion of this investigation was that PEI-attached PHEMA beads having very high adsorption rates and capacities indicating that they might effectively be used for specific removal of mercury ions from aqueous solutions including wastewater.

In 2005 Denizli *et al*. synthesized *N*-methacryloyl-(l)-glutamic acid (MAGA) using methacryloyl chloride and l-glutamic acid methyl ester for use as a metal-

complexing ligand and/or co-monomer. Spherical beads with an average diameter of 150–200 μm were obtained by suspension polymerization of MAGA and 2-hydroxyethyl methacrylate (HEMA) performed in an aqueous dispersion medium. Poly(HEMA-MAGA) beads were used in the removal studies of Pb^{2+} ions (Fig. 1.18).

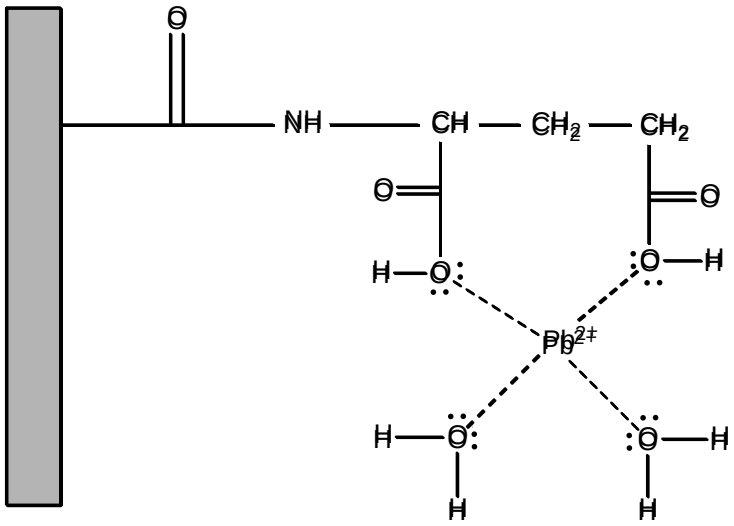

Figure 1.18 Complex formation of poly(HEMA-MAGA) bead structure.

The adsorption of Pb^{2+} ions onto just PHEMA beads was negligible (0.38 mg/g), but when the MAGA was incorporated into the polymer structure this significantly increased the lead adsorption capacity to 348 mg/g. The adsorption of Pb^{2+} ions also increased with increasing pH and reached a plateau value at around pH 5.0. Competitive adsorption of heavy metal ions from synthetic wastewater was also studied; the results can be seen in Table 1.30 below.

Table 1.30 Results for PHEMA/MAGA bead uptake.

	Lead	Mercury	Cadmium
Single solutions	42.5	26.8	17.6

Equilibrium bead loading (mg/g adsorbent)

Nickel, zinc, iron, cobalt, tin and silver were also in the synthetic wastewater solution but none of these ions adsorbed more than 1.6 mg/g. The journal reports that these beads could feasibly be used as a chelating material (Denizli *et al*., 2005).

Denizlis' research team investigated the removal of metal ions from water using poly(ethyleneglycol dimethacrylate-co-acrylamide) (polyEGDMA-co-AAm) beads. Poly(EGDMA/AAm) copolymer beads, with an average size range of 204.64 μm, were produced by suspension copolymerization of the monomers ethylene glycol dimethacrylate (EGDMA) and acrylamide (AAm), with toluene as the solvent. Poly(vinyl alcohol) and benzoyl peroxide were used as the stabilizer and the initiator. The beads were characterized by optical microscopy, infrared specroscopy (FTIR-DRS), and elemental analysis. Swell abilities in aqueous media were obtained and reported to be 14.28%. The ions under investigation were lead, mercury and cadmium. The beads were shown to have a preference for lead in both single and mixed solutions although the results for all of the mixed solution were not clearly reported in the journal (Table 1.31).

Table 1.31 Results for EGDMA/AAm bead uptake.

	Lead	Mercury	Cadmium
Single solutions	1.82	0.27	0.37
Mixed solutions			0.52

Equilibrium bead loading (mmol/g adsorbent)

The order of uptake for single ions expressed on a molar basis was reported to be $Pb^{2+}>Cd^{2+}>Hg^{2+}$. They report that the order of uptake changed when the results were expressed in terms of the amount of metal removed from the solution (mg/g) to be $Pb^{2+}>Hg^{2+}>Cd^{2+}$. It was reported that metal adsorption activity of these beads could be increased up to the level required for industrial applications (Kesenci *et al*., 2002).

In 2004 the poly(EGDMA/AAm) beads were modified by replacing the acrylamide (AAm) with *n*-vinyl imidazole (VIM) to produce Poly(ethylene glycol dimethacrylate-*n*-vinyl imidazole) [poly(EGDMA–VIM)] hydrogel (Fig. 1.19).

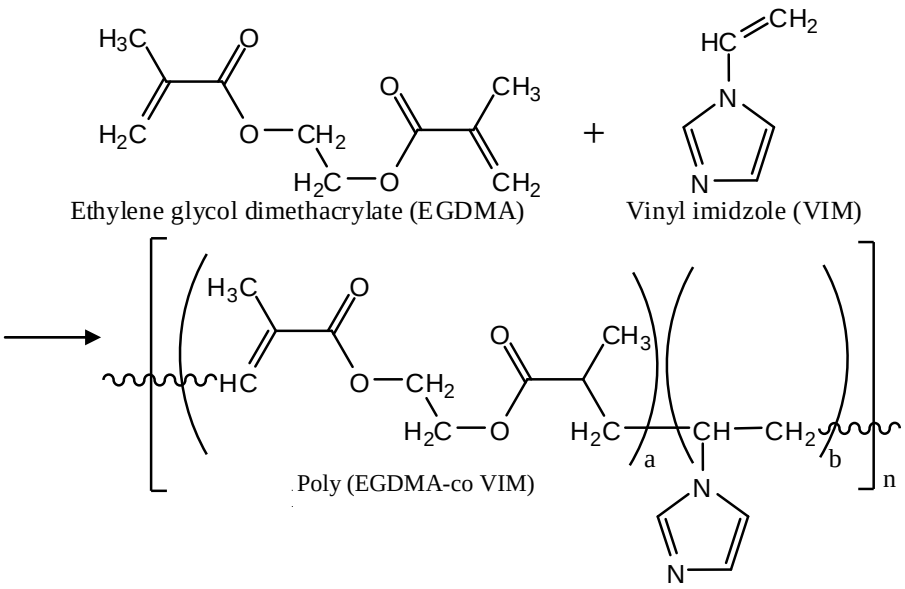

Figure 1.19 Chemical synthesis of poly(EGDMA/AAm).

The copolymer hydrogel bead composition was characterized by elemental analysis and found to contain 5 EGDMA monomer units to each VIM monomer unit, with a specific surface area of 59.8 m^2/g. They were found to have an average diameter of between 150-200 μm and a swelling ratio of 78%. The removal of heavy metal ions cadmium, mercury and lead from aqueous solutions was studied. The affinity order on a molar basis was observed as follows: Hg^{2+}>Cd^{2+}>Pb^{2+} which differs from the order in Table 1.31 below when reporting results in mg/g. Removal of heavy metal ions from synthetic wastewater was also studied (i.e. a mixed solution) with a 0.5 mmol/L initial metal concentration.

Table 1.32 Results for EGDMA/VIM bead uptake.

	Lead	Mercury	Cadmium
Single solutions	114.8	163.5	69.4
Mixed solutions	95.2	74.2	45.6

Equilibrium bead loading (mg/g adsorbent)

These results report poly(EGDMA–VIM) beads to be a potential candidate adsorbent for heavy metal removal (Kara *et al*., 2004).

The same year *N*-methacryloly-(*L*)-histidine methyl ester (MAH) was attached onto EGDMA beads for the use in immobilized metal ion affinity chromatography (IMAC). The product was called Mag-poly(EGDMA–MAH) beads. MAH was synthesized by using methacryloyl chloride and $_{L}$-histidine methyl ester dihydrochloride. The beads were produced by suspension polymerization of MAH and ethylene glycol dimethacrylate (EGDMA) in the presence of magnetite. The beads were found to have an average diameter of between 150-250 μm. Fe^{3+} ions were chelated on these magnetic beads and bovine liver catalase (an enzyme found in the blood and in most living cells that catalyses the decomposition of hydrogen peroxide into water and oxygen) was adsorbed on the metal-chelating beads from aqueous solutions containing different amounts of catalase at various pH. Desorption of catalase and reusability of these metal-chelate affinity adsorbents was also tested. The maximum catalase adsorption capacity of the mag-poly(EGDMA–MAH)–Fe^{3+} beads was observed as 83.2 mg/g at pH 7.0 (Akgol and Denizli, 2004).

Metal ion-imprinted adsorbents are a new type of carrier that can considerably enhance the adsorption capacity and the selectivity of metal ions. The ion-imprinting method is a useful technique for the preparation of adsorbents for the separation of metal ions from aqueous solutions. Denizli reports on a variety of novel molecular imprinted adsorbents to remove heavy metal ions with high selectivity. In 2002 poly(p-chloromethylstyrene-ethylene glycol dimethacrylate) (poly(p-CMS-EGDMA)) micro beads were synthesized for selective gold uptake (Kavakli *et al*., 2002). In 2003 a material specific to copper ions called Cu^{2+}-imprinted poly(ethylene glycol dimethacrylate–methacryloylamidohistidine/Cu^{2+}) (poly(EGDMA–MAH/Cu^{2+}) was synthesized. This material was in the form of micro beads with an average size of 150–200 μm. It was prepared by dispersion polymerization of EGDMA and

MAH/Cu^{2+}). The imprinted micro beads, thus obtained, adsorbed the corresponding guest Cu^{2+} ions more effectively than did the non-imprinted micro beads. The selectivity of Cu^{2+} imprinted micro beads was good even in the presence of Zn^{2+}, Ni^{2+} and Co^{2+} ions. This shows that the polymer has been templated for a specific element (Cu^{2+} ion).

Table 1.33 Competitive adsorption of copper and metal ions on the Cu^{2+} imprinted and non-imprinted micro beads (mg/g).

	Copper	Zinc	Nickel	Cobalt
Imprinted micro beads	41.2	18.3	11.7	8.2
Non-imprinted micro beads	16.8	14.4	10.8	9.3

The maximum adsorption of Cu^{2+} ions onto imprinted micro beads was ~48 mg/g when tested in a single solution. The pH significantly affected the adsorption capacity of imprinted micro beads. The observed adsorption order under competitive conditions when in mg/g was $Cu^{2+} > Zn^{2+} > Ni^{2+} > Co^{2+}$. The imprinted micro beads showed excellent selectivity for the target molecule (i.e. Cu^{2+} ions due to molecular geometry). These features make imprinted micro beads a very good candidate for selective removal of Cu^{2+} ions at high adsorption capacity (Say *et al*., 2003). In 2005 Denizli prepared Th^{4+} ion-imprinted polymer micro beads, for the selective removal of thorium ions from aqueous solutions. Thorium ions are typically known to be a hard acid and can form stable complexes with catechol, carboxylic acids and aminopolycarboxylic acids. Strong complex formations occur between the carboxylic groups of the glutamic acid and the thorium ions. The thorium ions were removed from the micro beads using 8.0 molar nitric acid solutions leaving empty templated micro beads, which were then packed into a column and used for solid phase extraction of thorium. The adsorption was found to be relatively fast (Buyuktiryaki *et al*., 2005).

1.10 Ion exchange materials

Ion exchange is defined as an exchange of ions between two electrolytes but the term is more conventionally used to denote processes of purification, separation, and decontamination of aqueous and other ion-containing solutions with the use of solid ion exchangers. In ion exchange processes ions are exchanged between a solution and an ion exchanger, a non-aqueous solid or gel. Ion exchangers are either cation exchangers for positively charged cations or anion exchangers for negatively charged anions. There are also amphoteric exchangers that are able to exchange both cations and anions simultaneously. However, the simultaneous exchange of cations and anions is more efficiently performed in ion exchange reactors called mixed beds which, as the name suggests, contain mixed anion and cation exchange resins. Ion exchange is a reversible process and the ion exchanger can be regenerated with desirable ions by washing with an excess of these ions.

The most well known ion exchange method is the process of water purifications to produce soft water in households and industries. This is accomplished by exchanging calcium and magnesium cations against sodium or hydrogen cations. However, the field where ion exchange is the most economically efficient is ionic separations where a product of highest purity must be obtained, an ion contained in a low concentration must be extracted, or streams of varying compositions must be treated. Thus a typical example of application is preparation of high purity water for electronic and nuclear industries. Ion exchange chromatography is a chromatographical method that is widely used for chemical analysis and separation of ions. For example, in biochemistry it is widely used to separate charged molecules such as proteins. Ion exchange is also widely used in industries such as food and beverage, hydrometallurgical, metals finishing, chemical and petrochemical,

pharmaceutical, sugar and sweeteners, ground and potable water, nuclear, softening and industrial water, semiconductor, power, and a host of other industries (DeSilva, 1999).

Over the decades many researchers have searched for new selective ion exchangers resulting in the emergence of a very wide variety of synthetic inorganic compounds exhibiting specific ion exchange propertes. Pan *et al*. (2006) studied the ion exchange properties of $Zr(HPO_4)_2$ (zirconium phosphate), denoted as ZrP, and its ability to remove lead ions from solution. ZrP is known to form either structurally well-defined layered crystals or an amorphous state. It has previouly been reported to be a successful ion exchanger for alkali metals but less information was known about its sorption of heavy metals. Results showed that ZrP once again appeared to be pH dependant. Favourable absorption towards lead even when in a mixed solution proved ZrP to be a viable ion exchange material.

1.10.1 Zeolites

Zeolites are defined as being micro porous crystalline solids having well-defined structures. Many occur naturally as minerals, and are extensively mined in many parts of the world. Two of the most common naturally existing zeolites are hydrated sodium aluminum silicate, its mineral name being natrolite, and hydrated sodium calcium aluminum silicate, stilbite (Fig. 1.20). Others are synthetic, and are made commercially for specific uses, or produced by research scientists (Bell, 2001). They are generally crystalline hydrated aluminosilicates of Group I and Group II elements in the periodic table, usually expressing a preference for sodium, potassium, magnesium, calcium, strontium and barium. The structure of a zeolite is based on a three-dimensional infinitely extending network of AlO_4 and SiO_4 tetrahedral units

linked between adjacent apical oxygen atoms (Breck, 1974). In addition to having silicon or aluminium as the tetrahedral atom, other compositions have also been synthesized, including the growing category of micro porous aluminophosphates, known as ALPOs. Well over 130 different zeolite framework structures are now known (Bell, 2001), the most common are zeolites A, X, Y, and ZMS-5.

Fig 1.20 has been removed due to third party copyright. The unabridged version of the thesis can be viewed at the Lanchester Library, Coventry University

Figure 1.20 Naturally occurring zeolites Natrolite and Stilbite (Amethyst, 2006).

The first reported use of molecular sieves could be traced back to 1756, when a Swedish mineralogist by the name of Cronstedt first discovered intriguing crystals in nature that seemed to froth or boil when heated in a blowpipe flame. Cronstedt called this new mineral a "zeolite," derived from the Greek words, "zeo" meaning "to boil" and "lithos" meaning "a stone" (Flanigen, 2005). Around the 1890's two English agricultural chemists, H. S. Thompson and J. Thomas Way, noted that certain soils had a greater ability than others to absorb ammonia from fertilizers. They found that complex silicates in the soil performed an ion exchange function. They were able to prepare materials of this type in the laboratory from solutions of sodium aluminate and sodium silicate. In 1906, German scientist Robert Gans used materials of this type for softening water. He sold the theory to an American company called Permutit, who patented the technology in 1913. These early materials used were found to be slow in regenerating and lacked physical stability (Nalco, 1998).

Zeolite science and technology has traditionally been very strong in the UK. This has been mainly due to the scientific legacy of the late Professor Richard Barrer, the "father of zeolite science" who, during a career spanning over 50 years, in various British universities laid the foundations for the study of zeolites and discovered many of their important properties (Bell, 2001). He began studying zeolite characteristics in 1937 and continued his research work on natural and synthetic material until his death in September 1996.

Union Carbide Corporation synthesized and manufactured the first synthetic zeolites in 1948. Synthetic zeolites, which are polar by nature, are manufactured by hydrothermal synthesis of sodium aluminosilicate in an autoclave followed by ion exchange with certain cations (Na^+, Li^+, Ca^{2+}, K^+). The channel diameter of zeolite cages usually ranges from 200 to 900 pm. This process is followed by drying of the microcrystals, which are palletized with a binder, to form macropores and thermally activated at a temperature of 650°C. Non-polar zeolites are synthesized by dealumination of polar zeolites. This is done by treating the zeolite with steam at elevated temperatures, greater than 500°C. This high temperature heat treatment breaks the aluminum-oxygen bonds and the aluminum atom is expelled from the zeolite framework. Non-polar zeolites are used in non-polar organic removal (Breck, 1974). These materials, also known as molecular sieves in the laboratory, have cavities of diverse sizes and shape that selectively trap ions and molecules as a function of their specific dimensions (Fig. 1.21).

Fig 1.21 has been removed due to third party copyright. The unabridged version of the thesis can be viewed at the Lanchester Library, Coventry University

Figure 1.21 Structure of "zeolite A" (Bell, 2001).

Zeolites have many uses in industry including separation and recovery of paraffin hydrocarbons, catalysis of hydrocarbon reactions, drying refrigerants, separation of air components, carrying catalysts in the curing of plastics and rubber, recovering radioactive ions from radioactive waste solutions, sampling air at high altitudes and removal of atmospheric pollutants such as sulfur dioxide are just a few examples. The most commonly known and widely used applications were as ion exchangers in the removal of ammonium ions from wastewater and for water softening by removing calcium and magnesium ions from "hard water" to improve the quality of drinking water and the effectiveness of detergents in washing powder (Breck, 1974). The true sodium aluminosilicate materials are now rarely used today for water softening, having been replaced with polystyrene ion exchange resins. They do however still have very large commercial markets for a variety of things such as cat litter and oil absorbers (Miessler, 2004).

Zeolites are also commonly used as ion exchangers for water removal from gases, air and liquid circuits such as in the removal of water in between double glazed sealed units and in refrigeration coolants (Buchner *et al*., 1989). The pores in a zeolite can be made to selectively hold small covalent molecules depending on their

size and shape making them excellent drying agents. Changing the pore size makes them selective for different molecules (Rayner-Canham, 1999). As much as fifty percent of a zeolite structure may be composed of pores. Essentially all of the atoms that make up its outer structure are accessible to any molecule that is small enough to enter the pore giving access to the internal network of channels (Thomas, 1992).

Pitcher *et al*. (2004) investigated the possibility of using zeolites to reduce the levels of heavy metals in motorway storm-water. They proposed that an ion exchange material could treat the water by replacing any toxic heavy metal cations in the runoff with cations released from the zeolites that have a large cation exchange capacity and an affinity for heavy metals. In their research a study of natural and synthetic zeolites was carried out for the removal of lead, copper, zinc and cadmium from motorway storm-water and a synthetic solution containing known concentrations. Results showed the synthetic zeolite known as MAP removed higher amounts of heavy metals from solution when compared with the natural zeolite called modenite. This was probably because the synthetic zeolite would have been purer than the naturally occurring one that could contain mineral impurities. The disadvantage of using zeolites is that the zeolite could escape and be released into the environment, thus adding to the pollution. Also the occasional high concentration of sodium present in motorway storm-water has the potential to re-exchange the heavy metals within the zeolite.

Sprynskyy *et al*. (2006) studied the adsorption of lead, copper, cadmium and nickel onto clinopilolite using single and mixed solutions. They report the sorption to be an ion-exchange process consisting of three stages. The first stage is for ions to be adsorbed onto the surface of the micro crystals of the zeolite, secondly an inversion

stage and then finally moderate adsorption in the interior of the zeolite. The maximum sorption capacities are recorded in Table 1.34.

Table 1.34 Results for the uptake of metal ions onto clinopilolite.

Cadmium	4.22 mg/g
Lead	27.7 mg/g
Copper	25.76 mg/g
Nickel	13.03 mg/g

The initial concentration of the cadmium solution was 80 mg/L, the rest of the solutions were 800 mg/L. They found that the adsorption was directly proportional to the concentration of the metals in the starting solution, the pH and also how fine the zeolite crystals were ground.

The National University of Singapore have done extensive research on zeolites over a number of years, primarily using MCM-41 (Mobile Crystalline Material-41 to give its full name) and ETS-10 in a successful effort to use templating strategies to prepare porous materials with desired properties to meet specific requirements of new technological applications (Zhao *et al*., 2004, Zhao *et al*., 1996, Zhao *et al*., 2006, Lv, 2006, Lv *et al*., 2006, Lv *et al*., 2007).

1.11 Metal chelating ligands

Metal complexing agents are used in a huge variety of industries. Most analytical reagents and indicators, pharmaceuticals, dyestuffs, as well as agrochemicals, are potential ligands. Alfred Werner pioneered the theory of metal ion ligand chemistry in 1893. Classically, complexation involves a lone pair of electrons from an active agent forming a bond through multiple bonds with another species such as a metal ion. All ligands that form more than one attachment to a metal ion are called chelating ligands. The word chelate comes from the Greek word chelos and means

claw-like (Rayner-Canham, 1999). Therefore by definition a metal chelating ligand must contain at least two donor atoms that are capable of bonding to the same metal ion to form a ring structure (Albion, 1994).

There are many different ligands, a very small example of basic ligands are:

- Chloride (weak, but if present in large enough quantities it can work)
- Ammonia (NH_3)
- Monoethanolamine
- EDTA
- Citrate
- Cyanide
- Quadrol (Used in some Electroless Copper baths)

One of the first ligands used was citric acid, which has been used extensively since the past century in the printing and textile industries as an additive to prevent the formation of stains due to calcium from hard water sources. Of these ligands listed above, only EDTA, Quadrol and Citrate are "chelates" in the strict scientific sense of the word, but all of them will bind with heavy metals and carry them through waste treatment systems (Williams, 1998).

The most widely used metal chelating ligand is ethylenediaminetetraacetic acid or more commonly known as EDTA (Fig. 1.22). It is a polyprotic acid containing four carboxylic acid groups and two amine groups with lone pair electrons. It is widely used to sequester di- and tri-valent metal ions and forms specially strong complexes with Mn^{2+}, Cu^{2+}, Fe^{3+}, and Co^{3+}.

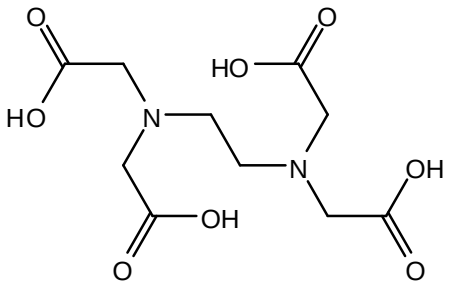

Figure 1.22 Chemical structure of EDTA.

EDTA is synthesized on an industrial scale from ethylenediamine, formaldehyde, and a source of cyanide (HCN or NaCN). On a worldwide basis over 100,000 metric tons are produced annually and it can be found in hundreds of products. Due to its strong complexing ability for most metal ions, it is used in industry as a sequestering agent. Another major use of EDTA has been in detergents especially as a replacement for phosphates, a major nutrient in wastewater. This same property also allows EDTA to be used for incidents of lead poisoning by the medical profession. However, a problem with EDTA is its inability to biodegrade in the environment. EDTA is found in many natural waters and occurs at higher levels in wastewater effluents. Western European countries have banned the use of EDTA in detergents (Sinex, 2004).

There are a huge variety of different sorts of metal chelating ligands, far too many for an in depth study in this work. Of particular interest to this project are the larger macrocyclic compounds such as crown ethers, cryptands, cavitands, calixarenes, resorcinarenes, cyclodextrines, and porphyrines. Many of them are capable of forming stable complexes with ionic organic and inorganic molecules.

1.11.1 Crown ethers

Crown ethers are heterocyclic chemical compounds that, in their simplest form, are cyclic oligomers of ethylene oxide $(-CH_2CH_2O-)_n$ in which $n \geq 4$. The crown ethers are notable for their ability to strongly solvate cations. The oxygen atoms are

ideally situated to coordinate with a cation in the interior of the ring, whereas the exterior of the ring is hydrophobic. The result is that the complexed cation is soluble in nonpolar solvents. Early reports of crown ethers concentrated on synthetic methods for their production; only later were their properties and the fundamental theoretical implications realised (Solomons and Fryhle, 2000). In 1967, Charles J. Pederson at du Pont found that cyclic polyethers could coordinate with metal ions such as potassium in non-polar solvents, thus separating them from their associated anions and rendering their salts soluble in these solvents. At the time he was trying to prepare a complexing agent for divalent cations by linking two catechols through one hydroxyl on each molecule. He hoped that this would give him a compound that could partially envelop the cations and, by ionization of the phenolic hydroxyls, neutralise the bound di-cation. A by-product that bound or complexed with potassium cations was isolated but had no ionisable hydroxyl group. He realized that the cyclic polyether by-product represented a new class of complexing agents and assigned them the trivial name "crown ethers", a simple nomenclature that is termed x-crown-y where x is the total number of atoms in the ring and y is the number of oxygen atoms. This naming has become standard format, rather than refering to their long laborious systematic names. Pederson synthesized around sixty different crowns (Pedersen, 1967).

The size of the interior of the crown ether determines the size of the cation it can solvate. Therefore, 18-crown-6 has high affinity for potassium cation, 15-crown-5 for sodium cation and 12-crown-4 for lithium cation. Examples of some common crown ethers can be seen below in Figure 1.23.

Fig 1.23 has been removed due to third party copyright. The unabridged version of the thesis can be viewed at the Lanchester Library, Coventry University

Figure 1.23 Example of some crown ether chemical structures (Claff, 2003).

1.11.2 Cryptands

Modified crown ethers with some of the oxygen atoms replaced by nitrogen atoms are called cryptands. The cryptands are much more diverse in their reactions because the visitor molecule can be a cation, anion or neutral species. They are used in the synthesis of other molecules and also have significant biological importance. Cryptands can work in an organism to maintain osmotic pressure in cells, move these metals to different parts of the organism, or transfer across membranes. However, the majority of uses for cryptands are as catalysts or helpers to push reactions forward

that would not typically react. Examples of some commonly used cryptands can be seen below in Figure 1.24.

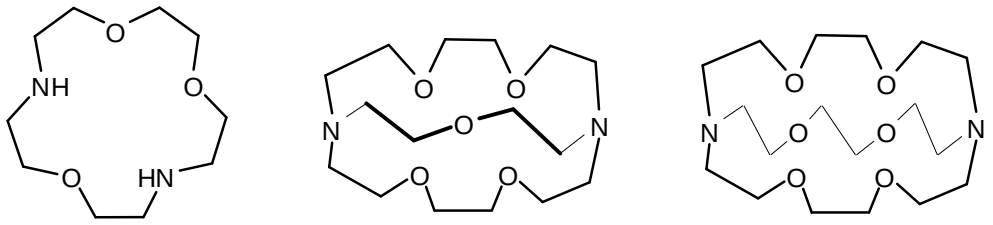

Figure 1.24 The chemical structure of kryptands 21, 221 and 222.

The reason that these molecules are called cryptands is the way the ligand entirely wraps its self around the visitor molecule/atom, acting like a crypt. Once the visitor molecule is attached to the cryptand the molecule is called a cryptate. These molecules are three dimensional analogues of crown ethers, but are more selective and complex the visitor molecule or ion much more strongly because they use both nitrogen and oxygen atoms in the binding; whereas crown ethers use only oxygen atoms. Their encapsulation mode is similar to the crown ethers by the fact that their co-ordination makes them size-selective; cryptands of different sizes strongly discriminate among alkali metal cations (e.g. Na^+ vs. K^+ on the basis of the best fit to the cryptand's cavity. Cryptands form many of their most important complexes with lanthanides and alkali & alkaline earth metals. In 1987 Pederson and his associates Cram and Lehn received the Nobel Prize for Chemistry for their efforts in discovering and determining uses of cryptates and crown ethers in the field of supra-molecular chemistry (Pedersen, 1988). PMPS particles are similar to cryptands because they also contain both oxygen and nitrogen atoms that can coordinate with ions in solution, but with the added advantage in that they seem to be able to co-ordinate to possibly any element in the periodical table, either neutral, ionic or cationic.

1.11.3 Calixarenes

The incorporation of benzene rings into crown ethers led to the synthesis of more complex ring systems such as bis(p-phenylene)-34-crown-10, which in turn led to the development of a group of compounds known as calixarenes (Fig. 1.25) (Claff, 2003).

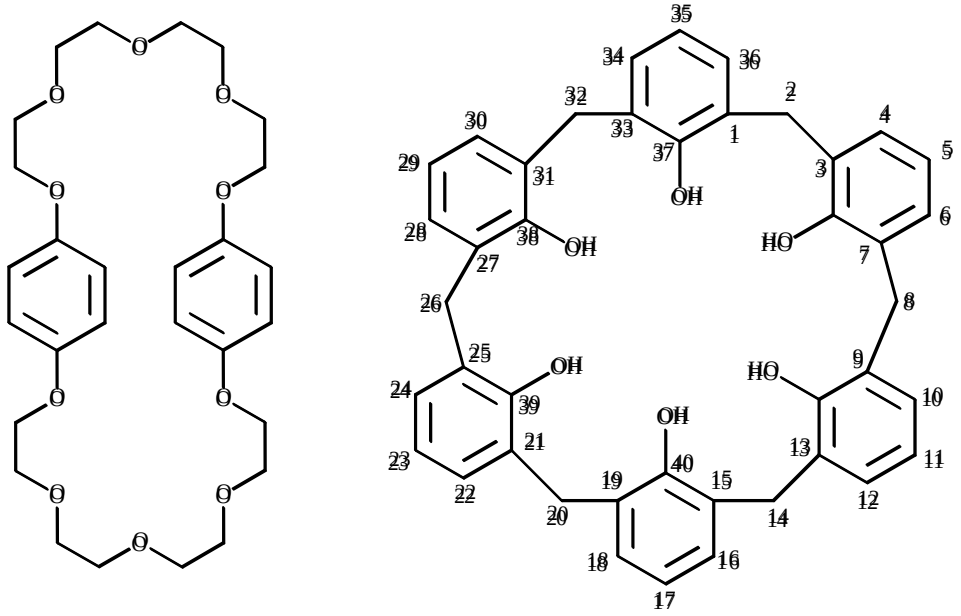

Figure 1.25 Chemical structures of bis(*p*-phenylene)-34-crown-10 and calix[6]arene.

Adolf von Baeyer pioneered the chemistry of calixarenes in 1872 although he was unable to determine its structure and did not realise its potential. John Cornforth, in 1955, was the first person to realize the potential of calixarenes as a basket. The first commercial use of calixarenes was in the 1950's when a company called Petrolite produced a range of calixarene products for use as demulsifiers in the oil industry. Other commercial applications for calixerines include enzyme mimetics, ion sensitive electrodes or sensors, selective membranes, non-linear optics and in HPLC stationary phases. The word calixarene was first used by David Gutsche in 1975 and is derived from calix or chalice, because they resemble the shape of a vase, and from the word arene that refers to the aromatic building block. They have hydrophobic cavities that

can hold smaller molecules or ions, i.e. a molecular sieve. The aromatic components are derived from phenol, resorcinol or pyrogallol and the aldehyde most often used is simply formaldehyde. The chemical reaction is an electrophilic aromatic substitution followed by an elimination of water and then a second aromatic substitution. The reaction can be acid catalysed or base catalysed. They are crystalline solids that have high melting points and are only found to be sparingly soluble. They can exist in different chemical conformations because of rotation around the methylene bridges. Conformations can be locked in place by substituents replacing the hydroxyl groups, thus increasing the rotational barrier. Alternatively placing a bulky substituent on the upper rim also locks a confirmation (Solomons and Fryhle, 2000). Calixarene nomenclature is straightforward and involves counting the number of repeating units in the ring and include it in the name. A calix[4]arene (Fig. 1.26) has four units in the ring and a calix[6]arene has six units (van Dienst *et al*., 1993).

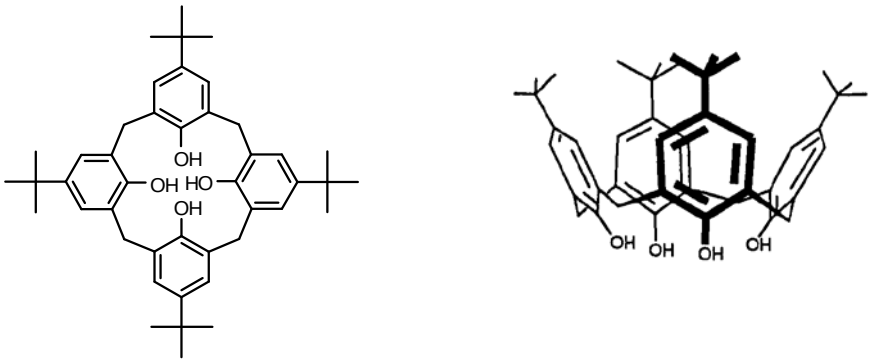

Figure 1.26 Chemical structure of calix[4]arene.

Calixarenes are able to form complexes with metal ions, anions and neutral molecules (Nachtigall *et al*., 2002) making them excellent candidates for the design of receptor sites for the specific recognition of guest moleucles. Calixarenes have both an upper and a lower rim and much attention has been focused on attachments to the *p*-carbons at the upper rim and phenolic oxygens at the lower rim. It has been

reported that oxygen containing macrocycles are effective for extracting alkali and alkaline earth metals. In acidic conditions attached sulfur atoms may be protonated and hydrogen bond to chromate/dichromate anions. As a result Memon *et al. (*2005) synthesized two new polymeric resins with sulfur-derivated functionalities for the extraction of heavy metal cations and dichromate anions. Van Dienst *et al*. (1993) succeeded in the selective functionalization of both the upper and the lower rim of calix[4]arene for use in non linear optics, organ imaging, ion sensitive field transistors and transport through supported liquid membranes. Matthews *et al*. (2001) synthesises a novel particulate system carrying (carbamoylmethylphosphine oxide) CMPO ligands pre-organised on a calixarene scaffold for successful removal of europium, americanum and caesium from simulated nuclear waste streams. Delmau *et al*. (1998) also report calix[4]arenes bearing four CMPO moieties on their upper rim where the phosphorus atoms are substituted with phenyl groups, are not only excellent extractants for trivalent lanthanides and actinides, they also exhibit remarkable selectivity based mainly on the size of the cations. This selectivity can reach nearly three orders of magnitude and remains even under strongly acidic conditions. It does not yet allow complete actinide–lanthanide group mixture separations but the separation factors could be useful for the selective extraction of actinides or light lanthanides from heavy lanthanides. Sliwa (2002) reviews many calixarene complexes forming with transition metals as well as lanthanides and actinide ions and reports them to be extremely beneficial in the extraction of nuclear waste and they also make excellent fluorescent chemosensors for optical detection of transition metal ions.

Bodenant *et al*. (1999) synthesized a bispyrenyl calix[4]arene-based receptor incorporating two hydroxamic acid functionalities that appeared to be specific for the

optical detection of Cu^{2+} and Ni^{2+} metal ions in solution. The synthesis of the receptor was based on the utilization of pyrene-labelled, *O*-protected hydroxylamines that represent versatile building blocks for the generation of fluorescent siderophore-based chelators. **(**A **s**iderophore (Greek for iron carrier) is an iron chelating compound secreted by micro-organisms). The compound was shown to exist in deuterated chloroform solution at room temperature as a mixture of mainly two conformers, namely, the cone and partial-cone species (partial-cone/cone ratio ca. 57/43) (Fig. 1.27).

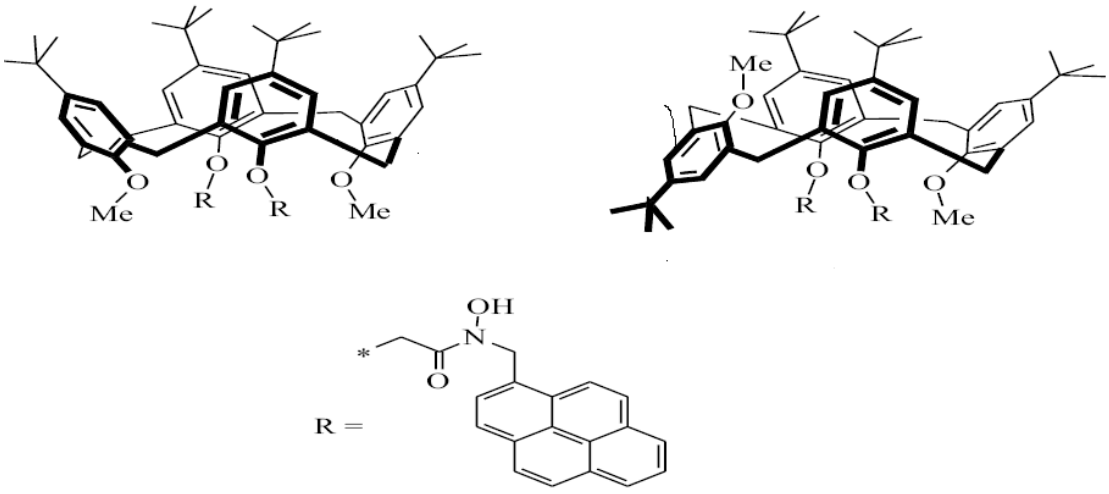

Figure 1.27 Cone and partial cone structure of copper and nickel selective calix[4]arene.

When in solution the product exhibited a dual fluorescence emission spectrum, which resulted from intramolecular interactions between the pyrene nuclei in the excited state. In a 20/80 mix of water and methanol the fluorescence intensity was shown to be sensitive to proton concentration and to the presence of transition-metal ions. Addition of Cu^{2+} and Ni^{2+} metal cations induced a dramatic quenching of fluorescence producing a novel photoresponsive ligand, belonging to a new class of sensitive chemosensors for the selective detection of transition-metal species in aqueous media.

There had been much attention focused on the various functionalities of the phenolic oxygen atoms on the lower rim and on the benzene rings of the upper rim but no products containing phosphate had been studied. Phosphonate and phosphine derivatives are already known to be useful extracting agents for metal ions and as potential ligands for transition metal catalysis in organic synthesis. Kyoda *et. al*. (2006) developed a new range of calix[4]arenes possessing phosphorous groups at the upper rim directly introducing them to the benzene rings. They synthesized a variety of novel calix[4]arene derivatives containing four phosphonate or phosphine oxide groups at the upper rim and four alkyl ether groups at the lower rim. These products also exhibited cone and partial cone structures (Fig 1.28).

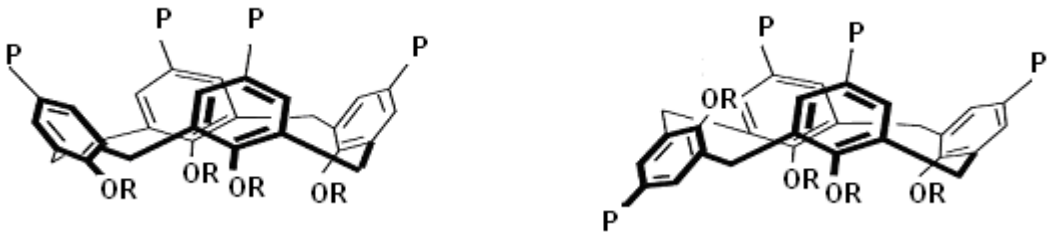

R = n-propyl ether and P = diphenylphosphine

Figure 1.28 Cone and partial cone structure of iron selective calix[4]arene.

All of the products showed a high selectivity and large ability for ion pair extraction of iron(III) chloride with the calix[4]arenes with four diphenylphosphine oxide groups and four n-propyl ether groups giving the best results.

1.11.4 Resorcinarenes and cavitands

Resorcinarenes (Fig. 1.29) are macrocycles, or a cyclic oligomers, based on the condensation of resorcinol (1,2-dihydroxybenzene) and an aldehyde. They are a type of calixarene. Baeyer was the first person to synthesize resorcinarenes whilst researching dyes in the late 19th century, but never classified them. Gutsche and Bohmer attempted to classify them as calixarenes by calling them

calix[4]resorcinarenes or resorcinol-derived calix[4]arenes. Others have called them hogberg compounds or simply octols or resorcarenes. Only very recently was the name resorcinarene suggested (Sliwa and Deska, 2002). The chemistry of resorcinarenes is now well established after much research. Their synthesis, conformational behaviour and complexation properties have been found to be useful building blocks in chemistry. Bridging the phenolic hydroxyl groups in resorcinarenes gives rise to a family of very rigid host molecules known as cavitands. Combining cavitands with calix[4]arenes gives a new family of molecules called carcerands which have nanometer-sized cavities. This has opened the way to a new type of molecular switch based on hindered mobility of the guest molecule (Saito *et al*., 1999).

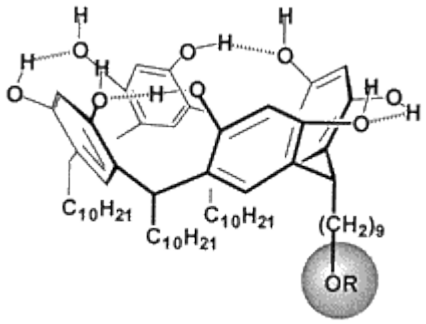

Figure 1.29 Chemical structure of a resorcinarene.

1.11.5 Cyclodextrins and porphorines

Cyclodextrins make up a family of cyclic oligosaccharides, composing of five or more α-D-glucopyranoside units. They are produced from starch by means of enzymatic conversion. Schardinger identified the three naturally occurring cyclodextrins -α, -β, and –γ in the mid 1970's (Loftsson and Duchêne, 2007).

Typical cyclodextrins create a cone shape. thus denoting:

- α-cyclodextrin: six sugar ring molecule (Fig. 1.30)
- β-cyclodextrin: seven sugar ring molecule
- γ-cyclodextrin: eight sugar ring molecule

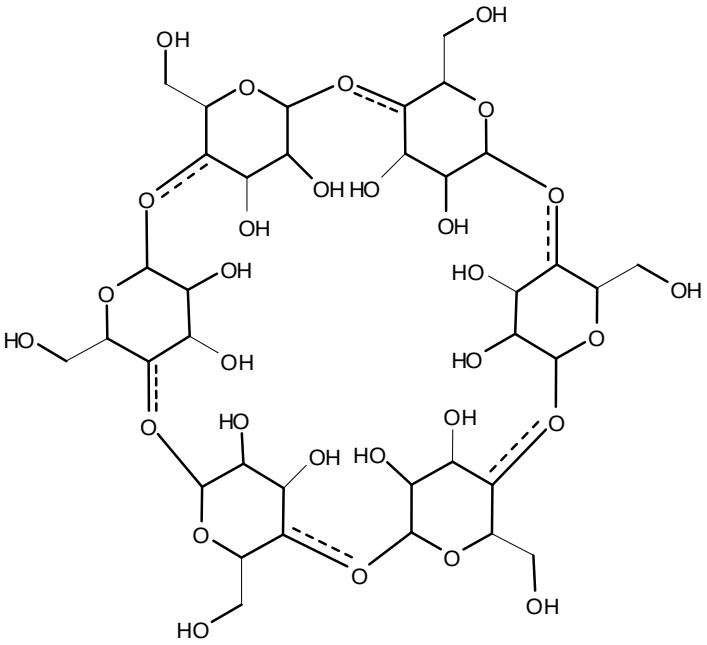

Figure 1.30 Chemical structure of α-cyclodextrin.

Over the last few years they have found a wide range of applications in food, pharmaceutical and chemical industries as well as agriculture and environmental engineering. It is also the chief active compound found in Procter and Gamble's deodorizing product "Febreze" (Proctor and Gamble, 2001).

A porphyrin is a heterocyclic macrocycle derived from four pyrrole-like subunits interconnected via their α carbon atoms via methylene bridges (=CH-) producing a highly conjugated system, and is consequently deeply coloured. The name porphyrin comes from a Greek word for purple. The macrocycle has 22 π electons. Many porphyrins occur in nature, such as in chlorophyll in green leaves and haemoglobin in red blood cells (Fig.1.31).

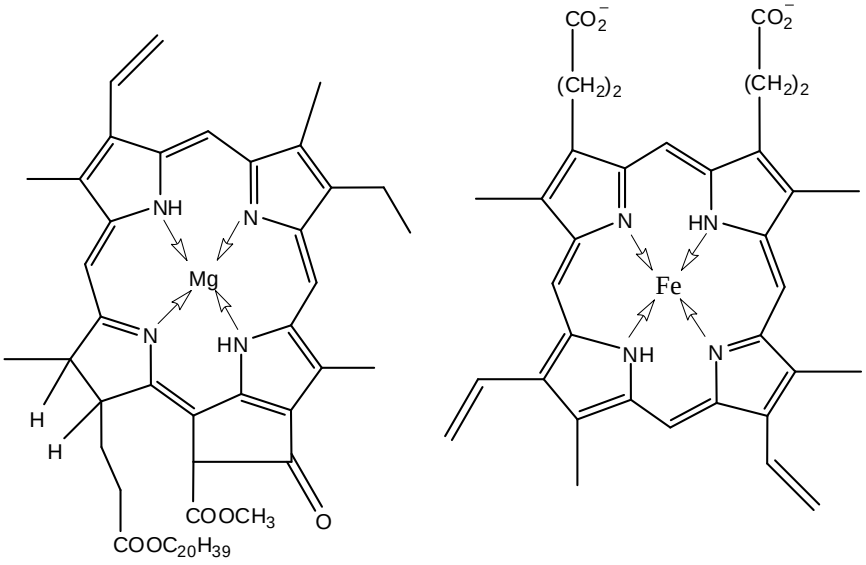

Figure 1.31 Chemical structures of naturally occuring porphyrins chlorophyll and haemoglobin.

Porphyrins bind metals to form complexes. The metal ion, usually with a charge of 2^+ or 3^+, resides in the central N_4 cavity formed by the loss of two protons. Most metals can be inserted. A porphyrin in which no metal is inserted in its cavity is sometimes called a free base. Some porphyrin derivatives follow Hückel's rule, but most do not. Although natural porphyin complexes are essential for life, synthetic porphyrins and their complexes have limited utility (Ritter, 1996, Miessler, 2004).

1.12 Summary of sorbent materials

Comparisons of sorbents are difficult because of inconsistencies in the data reported. It can be deducted however that inexpensive, effective and readily available materials can be used in place of more expensive activated carbon or ion exchange resins for the removal of heavy metals from solution. However, there are no products, naturally occuring or man-made, currently being reported that can successfully sorb almost any element in the periodic table like the PMPS particle can.

Chapter Two

Introduction to Squaraines

2.1 History of poly(1-methylpyrrol-2-ylsquaraine)

Poly(1-methylpyrrol-2-ylsquaraine) (PMPS) particles (Lynch *et al*., 2005) are synthesized by condensing 3,4-dihydroxycyclobut-3-ene-1,2-dione (squaric acid) with 1-methylpyrrole (Treibs and Fritz, 1957) producing a blue-black insoluble powder (Fig. 2.1). It was first synthesized in 1965 by Triebs and Jacob and studied in more depth in 1966, when they synthesized various pyrrole, 1-methylpyrrole and phenol derivatives with free α-positions, by a polycondensation reaction using a molar ratio of 2:1 in ethanol at 70^{o}C or by prolonged standing at 20^{o}C with catalytic amounts of perchloric acid. All reactions produced blue to blue-green insoluble polymers (Treibs and Jacob, 1965, Treibs and Jacob, 1966).

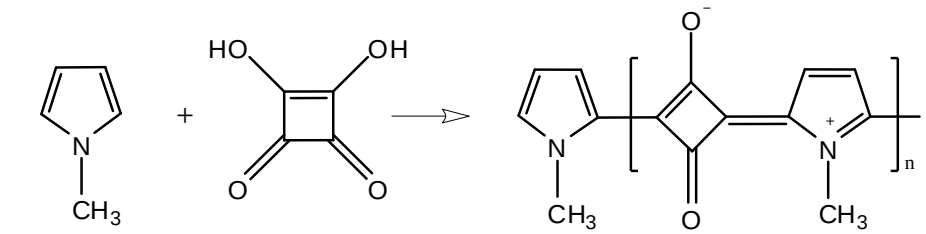

1-methylpyrrole squaric acid

Figure 2.1 Chemical synthesis of poly(1-methylpyrrol-2-ylsquaraine) PMPS.

This type of squaraine reaction involves an acid catalysed condensation mechanism and requires the use of either pure alcohol solvents or solvent mixtures containing alcohols. Subsequently PMPS particles can be prepared by refluxing the two components in any such solvent. More recent syntheses have been made by refluxing equimolar amounts of the pyrrole derivative and squaric acid with 1-butanol as the solvent (Yu *et al*., 1990), followed by washing the initial product with ethyl acetate to remove any soluble low molecular weight materials (Lynch *et al*., 2001). Most pyrrole-squaraine reactions are self-catalysed by the squaric acid, although in some cases the addition of acetic acid is required. Other squaraine condensation reactions sometimes require the removal of the produced water by the aid of chemical

drying agents or Dean and Stark apparatus, but for alkylpyrroles the reaction proceeds simply by refluxing in the alcohol-based solvent and the removal of water is not necessary (Lynch *et al*., 2005).

2.2 Syntheses of squaric acid

The chemical formula of squaric acid is $C_4H_2O_4$ (Fig. 2.2) and CAS number 2892-51-5. It is called squaric acid because its four carbon atoms form a square and it is one of the oxocarbonic acids. It appears as a creamy white crystalline powder, and has a melting point of 293°C (Fisher Scientific, 2007).

Fig 2.2 has been removed due to third party copyright. The unabridged version of the thesis can be viewed at the Lanchester Library, Coventry University

Figure 2.2 Structure of squaric acid (Maahs and Hegenberg, 1966).

Squaric acid was first synthesized in 1959, using chlorotrifluoroethylene (Fig. 2.3) (Park *et al.*, 1959). The first step in the synthesis was the heating of fluorinated ethylenes to produce a stable cyclobutane ring. The cyclisation process is exclusively a “head to head” or “tail to tail” joining to form only one isomer, (Mukkanti and Periasamy, 2005) which dimerizes on dechlorination with zinc to perfluorocyclobutene. This is then converted into 1,2 diethoxytetrafluorocyclobutene, which is finally hydrolysed with strong acid (Maahs and Hegenberg, 1966).

Fig 2.3 has been removed due to third party copyright. The unabridged version of the thesis can be viewed at the Lanchester Library, Coventry University

Figure 2.3 Synthesis of squaric acid (Park *et al*., 1959).

Figure 2.4 shows a simpler method for the production of squaric acid, which was devised in the early 1960's by using the more commercially available 1,2-dichlorotetrafluorocyclobutene that reacts with methanol to form 1-chloro-3,3-difluoro-2,4,4-trimethoxycyclobutene. Treatment of this with hydrochloric acid leads to good yields of squaric acid.

Fig 2.4 has been removed due to third party copyright. The unabridged version of the thesis can be viewed at the Lanchester Library, Coventry University

Figure 2.4 Simpler method of squaric acid synthesis (Park *et al*., 1962, West *et al*., 1963).

The preparation of squaric acid from hexachlorobutadiene (an undesirable by-product in the manufacture of perchlorinated hydrocarbons) can be carried out in one single step without the need to isolate the intermediates (Fig. 2.5) and with yields of up to 40% make this process viable for synthesis on the industrial or semi-industrial scale.

Fig 2.5 has been removed due to third party copyright. The unabridged version of the thesis can be viewed at the Lanchester Library, Coventry University

Figure 2.5 Proposed industrial synthesis of squaric acid (Maahs and Hegenberg, 1966).

It was suggested that the dianion of squaric acid should be regarded as a member of a series of novel aromatic compounds (West *et al*., 1960).

2.3 Reactions of squaric acid

Squaric acid undergoes many different types of reactions besides making polysquaraines. When squaric acid reacts with univalent metals, e.g. potassium, it forms readily soluble salts in water, whereas when it reacts with bivalent and tetravalent metals the product is insoluble. The salts of bivalent metals exist as dihydrates and those of trivalent metals are trihydrates. The salts of bivalent metals manganese, iron, cobalt, nickel, magnesium and zinc have been proven to have the same structure except for small differences caused by the size of the radii of the metal ion being observed only in the lattice parameters (Maahs and Hegenberg, 1966). West *et al*. (1963) postulated a chain structure (Fig. 2.6) for the salts of the general formula $M^{II}C_4O_4 \cdot 2H_2O$ where M is a bivalent metal. Maahs and Hegenberg at the time did not know the structure for the trivalent metal squarates. Many years later they were given the general formula $M^{III}C_4O_4(OH).3H_2O$ (Chesick, 1981). Reactions with alcohols give acetates and free squaric acid whereas ammonia gives acetamide and diammonium squarate (Maahs and Hegenberg, 1966).

Fig 2.6 has been removed due to third party copyright. The unabridged version of the thesis can be viewed at the Lanchester Library, Coventry University

Figure 2.6 West's postulated chain structure for bivalent metal squarates (West *et al*., 1963).

When reacted at room temperature with oxidizing agents, such as nitric acid or bromine, squaric acid undergoes a ring cleavage to form oxalic acid and carbon dioxide. In cold conditions (0^oC) the ring remains intact and the product obtained is cyclobutaneoctol, the tetrahydrate of cyclobutanetetrone (Fig. 2.7). When reacted with sulfur dioxide it is converted back to squaric acid (Maahs and Hegenberg, 1966).

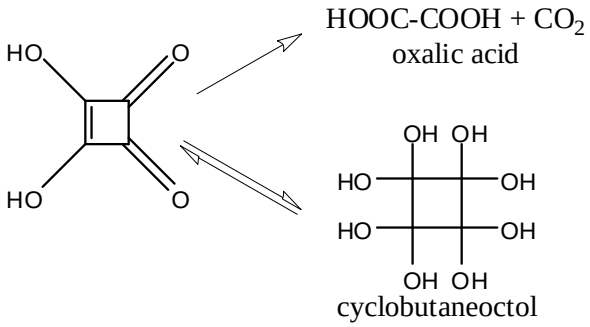

Figure 2.7 Squaric acid reaction with oxidizing agents.

The reaction which produces the PMPS particles is an equimolar condensation reaction between 1-methylpyrrole and squaric acid in 1-butanol which was first undertaken to synthesize squaraine dyes (previously known as cyclotrimethine dyes) in which the cyclobutene ring is substituted in positions 1 and 3 producing a blue black insoluble powder. If the pyrrole derivative is unsubstituted in position 2 and substituted in position 5 a red-violet dye is produced (Fig. 2.8). If position 2 and 5 are both occupied, e.g. by alkyl groups, no reaction will occur (Treibs and Jacob, 1965, Treibs and Jacob, 1966).

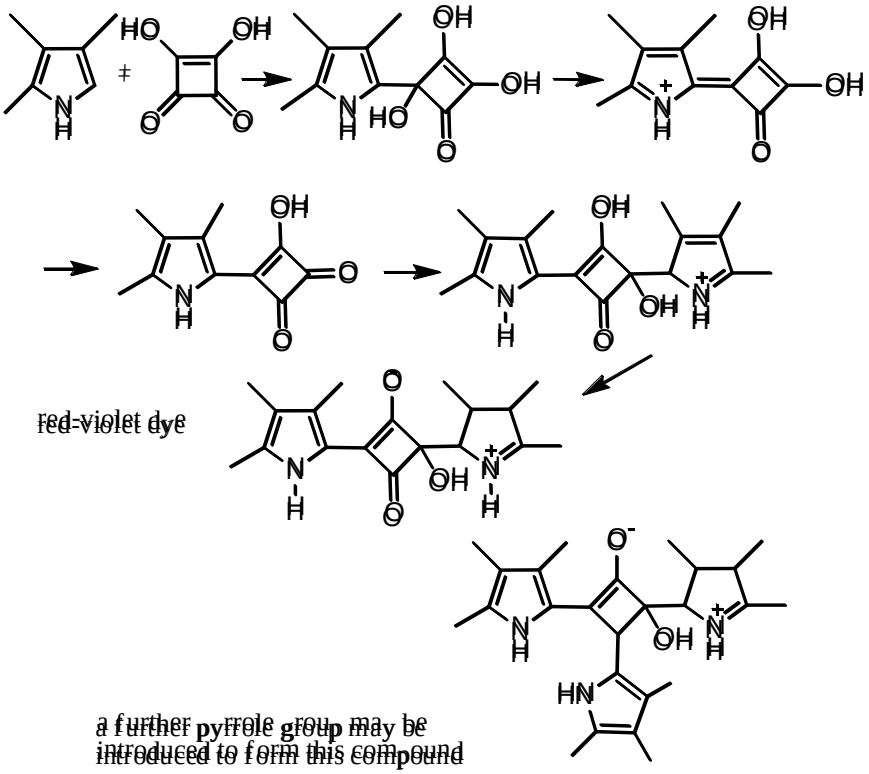

Figure 2.8 Reaction mechanism for the red-violet dye.

Poly(pyrrol-ylsquaraine)s are known to consist of three possible structural units (Fig. 2.9) with the 1,3-squarate being the desired main product. Lynch *et al*. (2001) reports that the 1,2-squarate groups only significantly occur from reactions performed in solvent systems where the produced two molar equivalent (per squarate) of water has not been removed, and when the mobility of the pyrrole ring is hindered, such as by long 1-alkyl chains or by attachment to another polymer backbone.

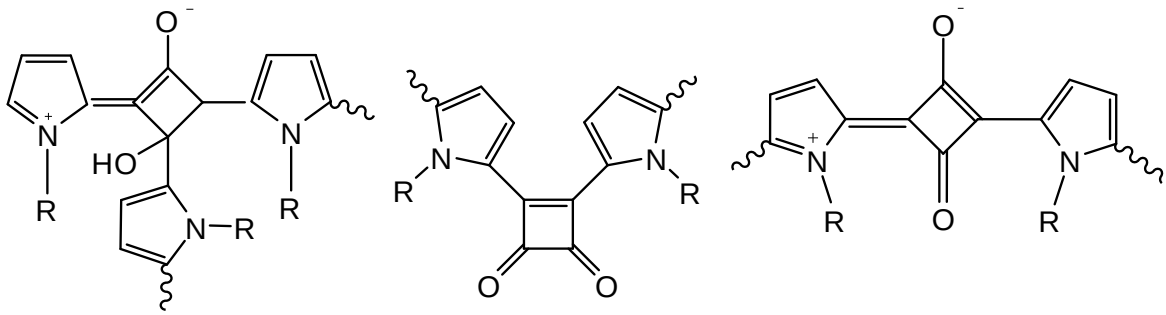

1,2,3-squarate 1,2-squarate 1,3-squarate

Figure 2.9 The three structural units of poly(pyrrolylsquaraine).

The 1,2,3-squarate is synthesized in low-molecular weight bis(pyrrolyl)squaraines by reacting a third mole of the pyrrole with the existing squaraine. It is easy to determine between the 1,2 and 1,3 squarates using infrared spectroscopy. The 1,3-species gives rise to a very strong C-O peak above 1600 cm^{-1} and either one or two medium peaks around 1750 cm^{-1} define the 1,2-groups. The 1,2,3-squarates should exhibit a strong C-O stretch ca. 1100 cm^{-1}, from the tertiary C-OH, but with a pyrrole-based material a medium-strong peak is also expected from conjugated HC-CH stretching, they should also have a smaller C-O stretch above 1600cm^{-1} due to the inclusion of the third pyrrole ring and the production of C-OH. The PMPS produce a large peak at 1600 cm^{-1} with only a small peak at 1750 cm^{-1} indicating that the 1,3 squarates are the major structural units with only a small amount of the 1,2 squarates.

2.4 Polysquaraine review

Squaraines belong to an important class of organic dyes with intense absorption and emission properties in the visible to near-IR wavelength region. These optical properties give interesting excited-state properties and a variety of materials that could be useful for a wide-range of applications such as photoconductors in organic solar cells, xerographic sensitises and near-IR absorbers in organic optical disks (Jyothish *et al*., 2004, Tatarets *et al*., 2005). They have been researched for use as fluorescent probes and labels, colouring agents for photoelectrical conversion elements and photochemical batteries, in electrophotography, and optical data storage that utilise the photophysical properties of these dyes (Tatarets *et al*. 2005). They have also been researched for use in biological labelling and photodynamic therapy. Their low band gaps and non-linear optical properties have also caused much interest (Ajayaghosh, 2005). Over the past few years many researchers have attempted to synthesize conjugated polymers with low optical band gaps (Eg), since they are thought to have good basic electrical conductivity. They represent the simplest models of molecular wires. Extension of conjugation in organic dyes would be expected to result in polymers with near infrared absorption.

The main reason for the lack of interest in squaraines is the fact that they are highly insoluble. Ayyappanpillai Ajayaghosh *et al*. have spent many years researching the properties of squaraine-based near-IR dyes, low band gap polymers, and cation sensors. In 1997 they began research into improving the solubility of PMPS by using *N*-alkyl chain substituted pyrroles instead of 1-methylpyrrole, to enable better opportunities for looking into their structure and properties. This led to the synthesis of several *N*-alkyl chain substituted pyrroles by reaction of the corresponding alkyl halide with pyrrole under phase transfer conditions.

Polysquaraine dyes **a** and **b** (Fig. 2.10) were synthesized by reacting equimolar amounts of the corresponding *N*-substituted pyrroles and squaric acid in a 2:1 mixture of 1-butanol and benzene as solvent. These two products were found to be soluble in a range of organic solvents enabling them to be analysed by infra red (IR), nuclear magnetic resonance (NMR) and ultra violet (UV) spectroscopy.

Fig 2.10 has been removed due to third party copyright. The unabridged version of the thesis can be viewed at the Lanchester Library, Coventry University

Figure 2.10 Chemical synthesis of soluble polysquaraine dyes (Ajayaghosh *et al*., 1997).

The IR data revealed a strong absorption band around 1620 cm^{-1} showing that the polymers have a resonance stabilised zwitterionic structure. The NMR spectra confirmed the proposed structures. The electrical conductivities were estimated to be around 10^{-6} S/cm, which could be further enhanced upon doping with appropriate dopants. The data were also comparable with that of several squaraine dyes with analogous structures. The conclusion of the analysis was that they had successfully synthesized soluble, alternate donor-acceptor co-polymers that had zwitterionic squaraine repeat units with interesting optical and electronic properties, which appeared to be potential candidates for several applications (Ajayaghosh *et al*., 1997). Chenthamarakshan *et al*.(1999b) experimented with 1-dodecyl and 3-dodecylpyrroles. They report that the polycondensation of 1-dodecyl and 3-dodecyl-substituted pyrroles with squaric acid led to the formation of copolymers with isomeric repeating units of 1,3-substituted zwitterionic and 1,2-substituted diketonic structures (Fig. 2.11).

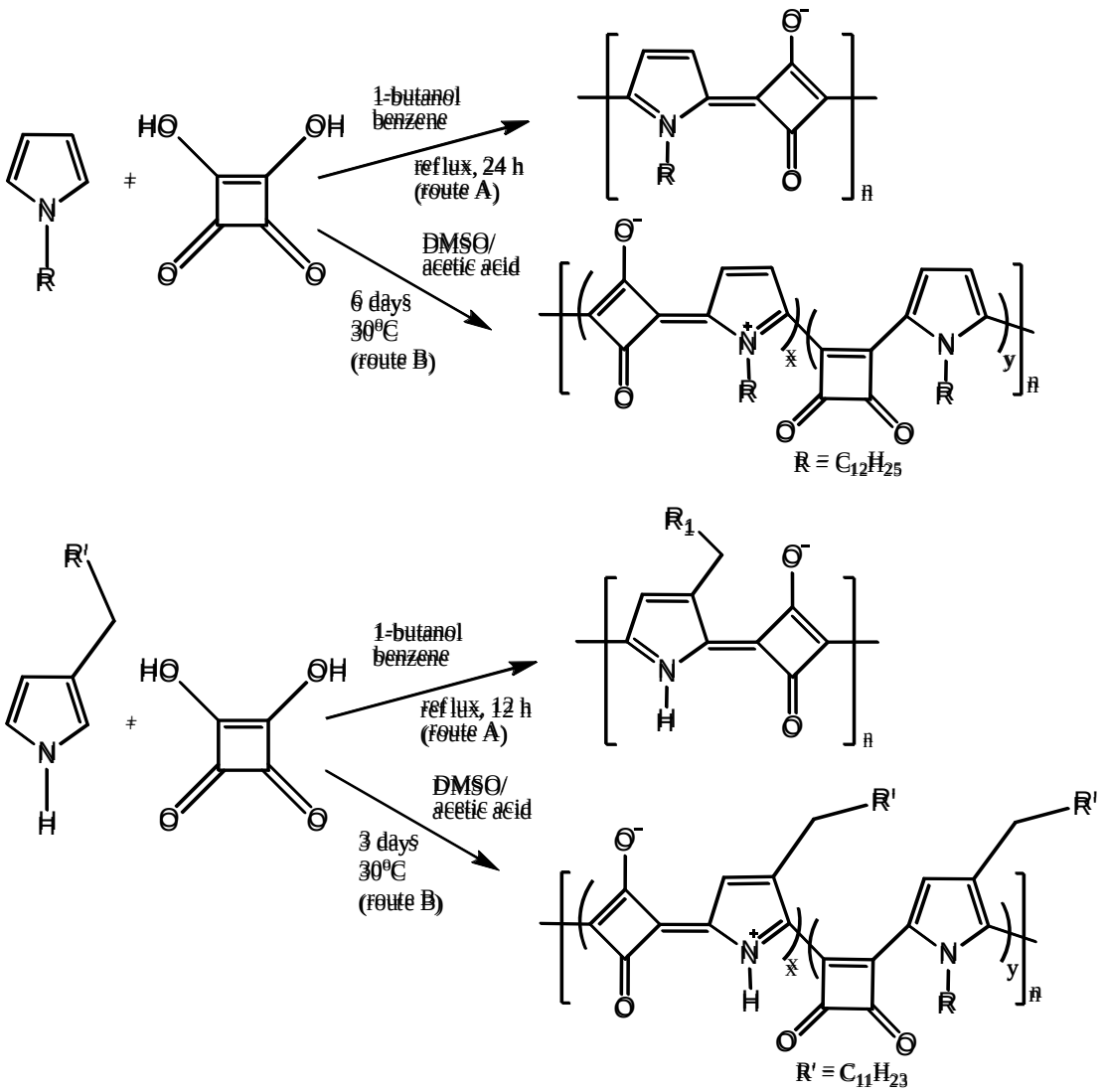

Figure 2.11 Chemical synthesis of 1-dodecyle and 3-dodecylpyrrole squaraines.

Reactions using 1-butanol/benzene mixtures under azeotropic reflux conditions gave low molecular weight deep blue polymers that mainly consisted of zwitterionic repeating units. The same reactants were stirred in acetic acid/DMSO at room temperature in the dark and produced a deep green relatively high molecular weight polymer with distinctively different physical properties, probably attributed to the presence of both 1,3-substituted zwitterionic and 1,2-substituted diketonic repeating units. IR and UV-visible spectral analysis confirmed the structures. The electrical conductivities of the acetic acid/DMSO reaction product showed better values than the 1-butanol/benzene reaction product. The values were 2.4 x 10^{-6} and 8

x 10^{-6} S/cm for the 1-butanol benzene and 2.5 x 10^{-6} and 2.3 x 10^{-5} S/cm for the acetic acid/DMSO. Thus 3-dodecylpyrroles obtained by polycondensation with squaric acid in acetic acid/DMSO gave the maximum conductivity without any external doping (Chenthamarakshan *et al*., 1999b)

In 2001 Ajayaghosh *et al*. did further research on low optical band gap polysquaraines and reported the polycondensation of 2,5-dialkoxydivinylbenzene-bridged bispyrroles with squaric acid to produce extensively conjugated polymers with strong near-infrared (NIR) absorption of around 800-1000 nm. One of the products (Fig. 2.12) showed a significantly low band gap (Eg) of 0.79 eV and with an intrinsic conductivity of 5.3 x 10^{-4} S/cm.

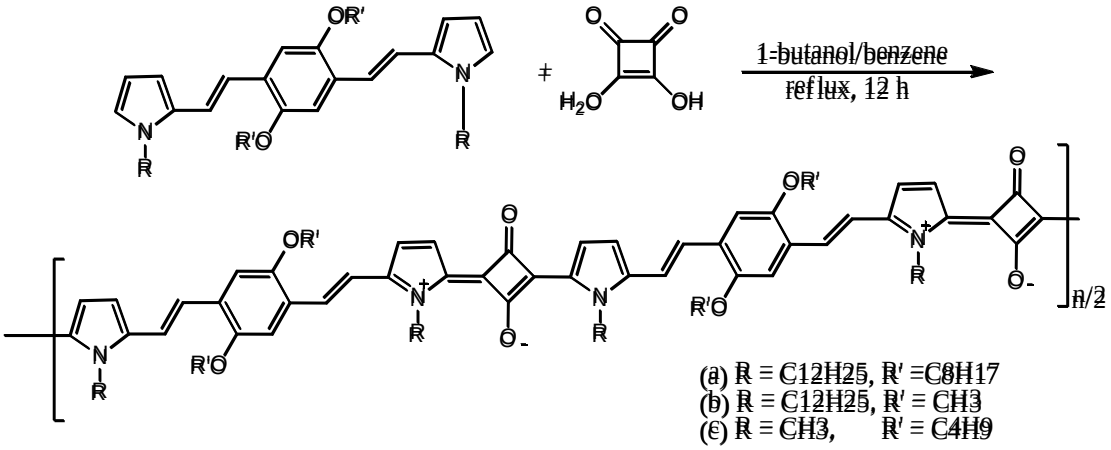

Figure 2.12 Chemical synthesis of a low optical band gap polysquaraine.

Ajayaghosh concluded that optical and electronic properties of polysquaraines could be significantly altered to the low band gap region when coupled with a strongly electron-donating conjugated moiety. A high degree of conjugation and planarization of the polymer backbone was suggested by the broad and structured NIR absorption spectra of the polysquaraine. They predicted a wider use of the present approach for the designing of new π-conjugated materials with novel optoelectronic properties (Ajayaghosh and Eldo, 2001).

In 2002 further research reported the reaction to be an A-B type co-polymerisation of squaric acid and 1,4-dialkoxydivinylbenzene-bridged bispyrroles, which resulted in zwitterionic polysquaraines with resonance stabilized quinoid structures. Incorporation of an electron donating conjugated moiety between each squaraine dye repeat unit had a dramatic influence on the optical and electronic properties of the resulting polysquaraines due to an enhanced donor-acceptor-donor (DAD) interaction. The solution UV-Vis-NIR absorption maxima of the new polymers, between 772 and 1040 nm with ground-state onset absorptions ranging from 1140 to 1300 nm, is unusual for conjugated polymers and is a signature of their low band gaps. Varying the length of the alkyl side chains could change the intrinsic conductivities of these polymers from between 10^{-7} - 10^{-4} S/cm. The solubility inducing alkyl side chains play a decisive role in the molecular packing, which control the optical band gap and conductivity of the reported polysquaraines. This is one of the simplest strategies for the synthesis of NIR absorbing conjugated polymers with extremely low band gaps that are soluble and intrinsically semi-conducting (Eldo and Ajayaghosh, 2002).

The following year (2003) Ajayaghosh and workers reported on the synthesis of redox-switchable squaraines comprising of a central squaraine unit joined to vinyl aromatic end groups (Fig. 2.13).

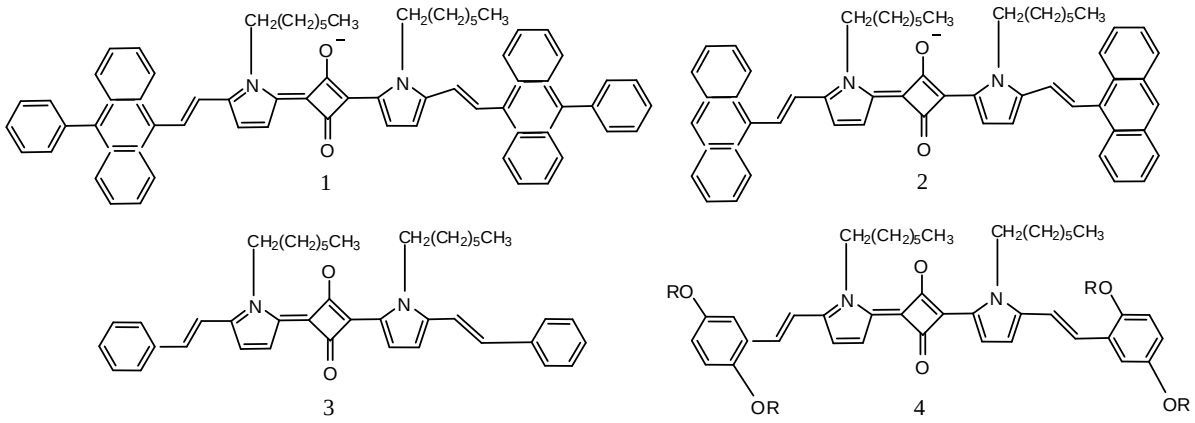

Figure 2.13 Chemical structures of redox-switchable squaraines.

Structure 3 showed a red shift in the absorption maximum from 547 to 687 nm in toluene and structure 4 showed a further red shift of 13-20 nm in toluene, depending upon the length of the alkyl side chains. When measured in the solid state they showed broad absorption from the 600 to 1000 nm range with different absorption maxima, the intensities of which are dependent upon the length of the side chains. Structure 1 showed interesting redox behaviour characteristic of a class III mixed-valence system. Cyclic voltammograms revealed that structure 1 also possess limited electrochemical but maximum chemical reversibility, suggesting that the phenylanthracenyl units were stabilising the radical cations and di-cations. Ajayaghosh predicted that oxidation leads to an electronic situation at the mixed-valence radical cation stage in which the positive charge is localized on the vinylpyrrole subunits. Further calculations carried out on the geometry and charge distribution of structure 1 in different oxidation states revealed that the pyrrole-vinyl subunits have to be regarded as effective redox centres in the oxidative process (Buschel *et al*., 2003, Ajayaghosh, 2005).

Ajayaghosh's team experimented with several π-conjugated water-soluble conducting oligosquaraines. The polycondensation of squaric acid with a water soluble pyrrole derivative containing an *N*-propanesulfonate pendant group (Fig. 2.14) produced dark green precipitates which appeared to have electrical conductivities in

the range of 10^{-5} S/cm without any external doping (Chenthamarakshan and Ajayaghosh, 1998b).

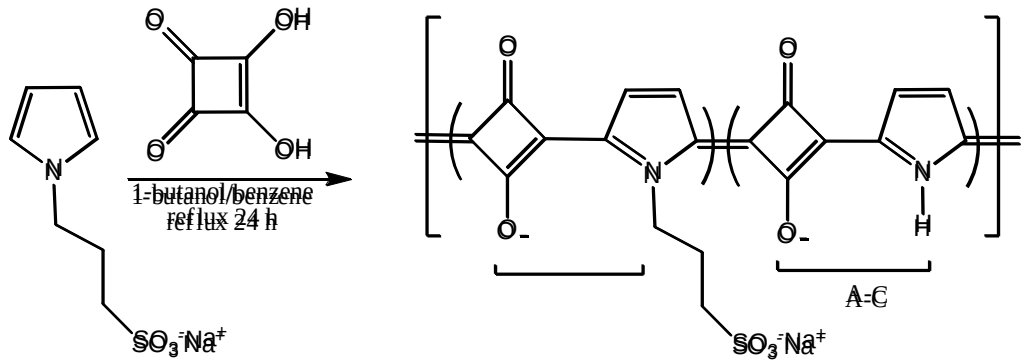

Figure 2.14 *N*-propanesulfonate squaraine derivatives.

Chenthamarakshan and Ajayaghosh then went on to research fluorescent chemosensors made by using a π-conjugated squaraine that contained flexible oxyethylene chains (molecular wire), which reversibly bind specific cations. They are analogous to crown ethers by the fact that it is oxygen atoms that coordinate with the metal ions. They showed significant enhancement in fluorescence emission, which appeared to be specific only for lithium ions in micro-molar quantities (Fig. 2.15).

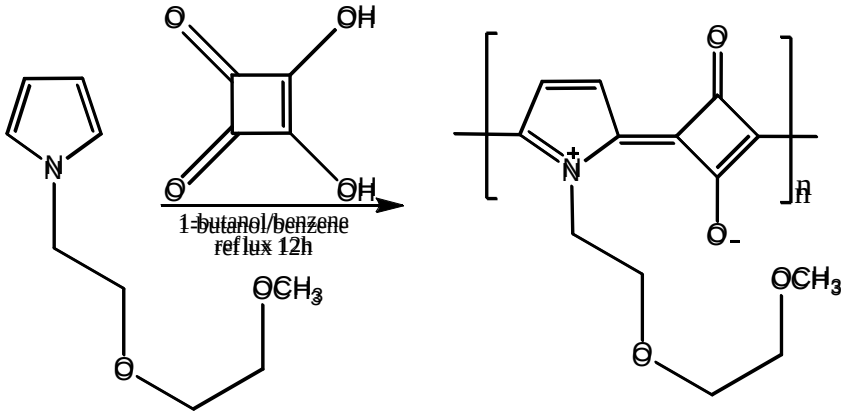

Figure 2.15 Chemical synthesis of fluorescent sensor.

When micro-molar quantities of alkali metal ions were added to a DMSO solution of the new sensor the absorption maximum was enhanced with a marginal red shift. With potassium and sodium the enhancement was only 8% but the squaraine molecular wire showed a massive 92% enhancement when lithium was

added in the form of lithium perchlorate. The proposed structure of the lithium complex can be seen in Figure 2.16.

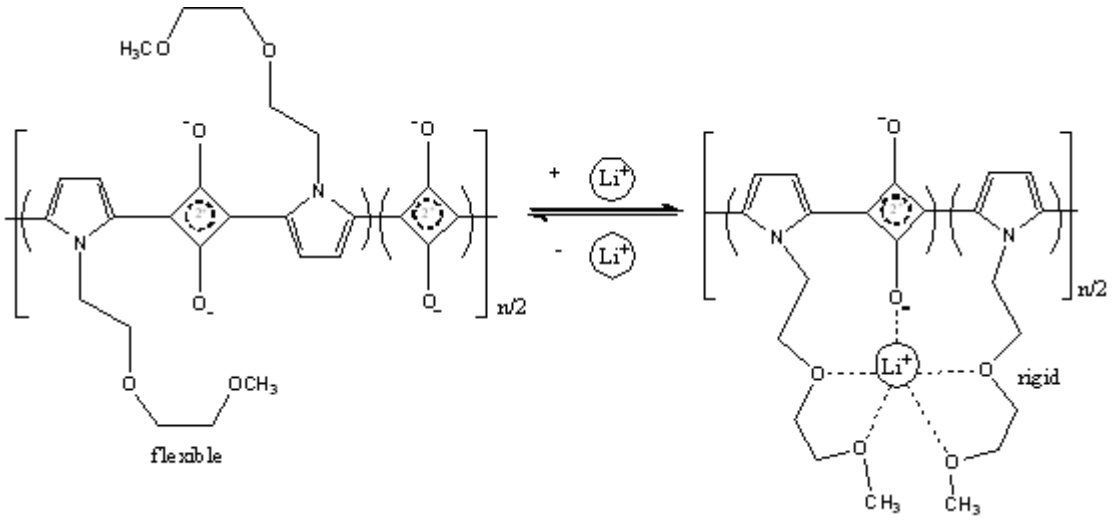

nonplaner (lower fluorescence) planer (higher fluorescence)

Figure 2.16 Chemical synthesis of a lithium ion sensor.

The huge specificity of the sensor for lithium was attributed to the optimum chain length of the binding sites and the electron affinity of lithium facilitating a better complexation (Chenthamarakshan and Ajayaghosh, 1998a, Chenthamarakshan *et al*., 1999a).

Ajayaghosh's team then moved on to synthesize a bichromophoric podand complex that appeared to be specific for calcium ions whilst using a "crown ether/cryptand like structure". The light-blue product in Figure 2.17 became intense purple blue upon addition of $Ca(ClO_4)_2$, which is visible to the naked eye (Ajayaghosh *et al*., 2002, Arunkumar *et al*., 2005). Addition of other cations such as Na^+, K^+, Mg^+, or Sr^+ did not show any visible colour change (Ajayaghosh, 2003). The sensor is suspected to fold its podand arm around the metal ion with all of the oxygen atoms and the nitrogen atoms coordinating with the Ca^{2+} ion analogous to a cryptand. The structure of the calcium sensor and the coordination of the nitrogen

and the oxygen atoms were proven by H^1 NMR analysis. The compound binds in a ratio of 1:1 with the calcium ion (Ajayaghosh and Arunkumar, 2005).

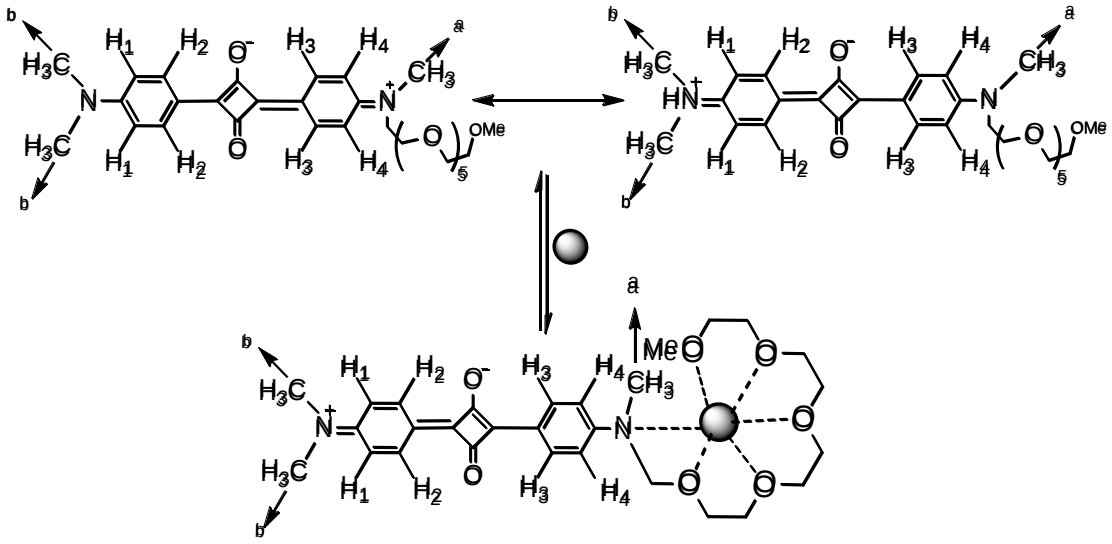

Figure 2.17 Chemical synthesis of a calcium ion sensor.

Arunkumar *et al. (*2004) working with Ajayaghosh synthesized three different squaraine complexes that had one, two and three oxygen atoms in the podand chain. They too showed high selectivity towards alkaline earth metal cations, particularly magnesium and calcium. From absorption and emission analysis they established that with the one and two oxygen complexes magnesium ions form 1:1 folded complexes and calcium ions form 1:2 sandwich dimers (Fig. 2.18). The complex containing three oxygen atoms formed weak 1:1 folded complexes with magnesium, calcium and strontium ions.

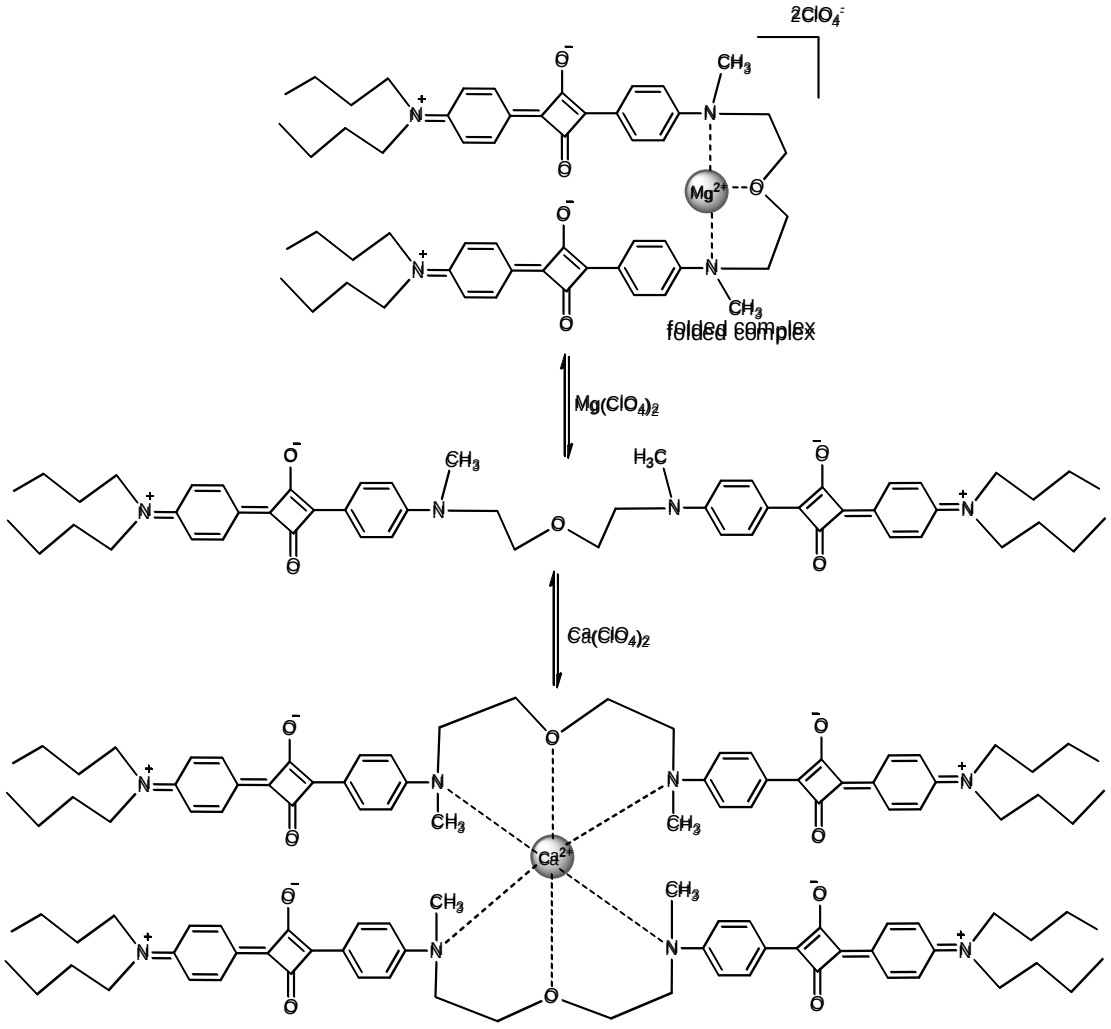

Figure 2.18 Chemical synthesis of alkaline earth metal chemosensors.

Balbo Block and Hecht (2004) were simultaneously researching novel non-conjugated polysquaraines with crown ether type structures consisting of isolated chromophores bridged by variable receptor linkers. They synthesized a number of compounds that claimed to have alternating receptor and squaraine chromophore units that undergo significant conformational changes controllable by physical and chemical stimuli such as temperature, solvent polarity and by addition of various cations. They report that such a receptor would supposedly wrap itself around the metal in a crescent fashion, leading to a dramatic change of its own conformation. Balbo Block *et al*. (2004) also reported on the attempted synthesis of poly(m-

phenylene-alt-squaraine)s. They intended to synthesize crown ether type complexes that would be intrinsically conducting as well as IR-emitting polymers based on donor-acceptor substituted polysquaraines. The reaction failed because of exceptionally low reactivity of the investigated compounds, which was put down to intramolecular hydrogen bonding. The majority of the remaining research into polysquaraines involves investigations into their conductance due to low optical band gaps or the use of strong donor acceptor repeating units because they are classed as π-conjugated polymers.

Conjugated polymers have been applied in diverse items such as photoreceptors for diode lasers, laser optical recording, laser printing, photo labelling, organic solar cells and DNA sequencing (Ajayaghosh, 2003). MacDiarmid, Shirakawa, and Heeger brought conjugated polymers to the fore in 1977 when they discovered that chemical doping of these materials resulted in increases in electronic conductivity over several orders of magnitude. They were awarded the Nobel Prize in 2000 for their work on conjugated and conducting polymers, specifically for recognizing that polyacetylene could be made to conduct (Heeger *et al*., 2000). Conjugated polymers have a framework of alternating single and double carbon–carbon or carbon–nitrogen bonds. Single bonds are referred to as σ-bonds, and double bonds contain a σ-bond and a π-bond. All conjugated polymers have a σ-bond backbone of overlapping sp^2 hybrid orbitals. The remaining out-of-plane p_z orbitals on the carbon and nitrogen atoms overlap with neighbouring p_z orbitals to give π-bonds. The characteristics of the π-bonds are the source of the semi-conducting properties of these polymers. First, the π-bonds are delocalised over the entire molecule; and then, the quantum mechanical overlap of p_z orbitals actually produces two orbitals, a bonding (π) orbital and an antibonding (π*) orbital. The lower energy

π-orbital produces the valence band, and the higher energy π*-orbital forms the conduction band. The difference in energy between the two levels produces the band gap that determines the optical properties of the material. The band gaps of most semi-conducting materials are typically between 0.1 eV and 2.2 eV (Wallace *et al*., 2000, Roncali, 1997).

Havinga *et al*. (1992, 1993, 1995) were one of the first research groups to synthesize conjugated polysquaraines. They reported band gaps as small as 0.8 eV by reacting squaric acid with benzo(1,2-4,5)di(1-alkyl 2-methyle-3,3-dimethyl pyrroline). It was found that the smallest band gap was found when in a combination in which the electro-negativity difference between donor and acceptor was greatest. In 1995 they synthesized several water-soluble squaraines with small band gaps of 0.7 eV that were stable at ambient conditions and could be doped to conductivities up to about 1 S/cm

At the same time Tol was working with poly-aminosquaraines and related compounds. He found that polymers containing squaric moieties could produce band gaps as low as 0.5 eV. He reported that poly-aminosquaraine was a donor/acceptor compound that has a band gap determined by the weak interactions between the highest occupied molecular orbital (HOMO) of the donor and the lowest unoccupied molecular orbital (LUMO) of the acceptor (Tol, 1994). In 1996 Brocks and Tol reported on other small band gap semi-conducting polymers made from squaraine dye molecules. They synthesized poly(aminodivinylsquaraine) which was found to give a low band gap of 0.2 eV (Brocks and Tol, 1996b, Brocks and Tol, 1996a).

In 1997 Lynch *et al*. found that the polycondensation of squaric acid with 1,2-(9-ethylcarbazol-3-yl)ethane and *N*-ethyliminostilbene in polyphosphoric acid yielded insoluble polymers which had substituted phosphate groups on the phenyl rings. The

phosphate groups were not ionic, hence no charge-balancing anions were present so neither of the polymers conducted electrically (Lynch *et al*., 1997a). The synthesis of a soluble poly(pyrrolylsquaraine) (Fig. 2.19) was achieved later that year (Lynch *et al*., *1997*b) by *N*-alkylation of pyrrole with 1-bromooctadecane and subsequent condensation with squaric acid. It was determined that increasing the alkyl chain length to eighteen carbon atoms increases the solubility of polysquaraines dramatically.

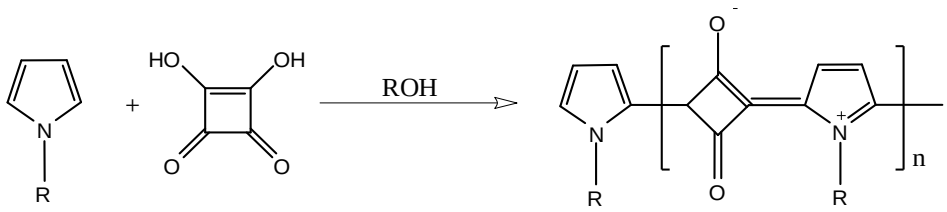

Figure 2.19 Chemical sythesis of a **s**oluble poly(1-octadecylpyrrole-2-yl) squaraine.

Poly(1-octadecylpyrrole-2-yl) squaraine was found to have good solubility in common organic solvents such as chloroform. It was also found to be surface active with the possibility of being used as a Langmuir-Blodgett film (Geissler *et al*., 1997) (Lynch *et al*., *1997*b). A Langmuir-Blodgett (LB) film is a set of layers of organic material one molecule thick (monolayers) deposited on a solid substrate. A solid substrate is lowered into the water, breaking through the Langmuir film and, provided that certain criteria have been met, the Langmuir film attaches itself to the substrate, coating it in a mono-molecular layer. Once the first layer has been deposited, further layers will be deposited on each subsequent pass of the substrate through the air-water interface. Multilayers can therefore be deposited to produce a film, the thickness of which is the product of the individual molecular chain length and the number of times that the substrate has crossed the air-water interface. Such films exhibit various electrochemical and photochemical properties (Zhang *et al*., 2003).

The separation, identification and subsequent second-order properties of poly(1-octadecylpyrrol-2-yl)squaraine and bis(1-octadecylpyrrol-2-yl)squaraine (Py) and its comparison with bis(3,5-dimethyl-1-octadecylpyrrol-2-yl)squaraine (Me-Py) was reported (Lynch *et al*., 1997b). Poly(1-octadecylpyrrol-2-yl)squaraine represents the first example of second harmonic generation (SHG) from a centro symmetric, alternating donor-acceptor polymeric chain. Second harmonic generation (SHG) occurs when a beam of monochromatic light impinges on a surface. The lack of symmetry at the surface (or a buried interface) can lead to the generation of light at a frequency twice that of the incident light (i.e. the second harmonic). The detected second harmonic light is of particular interest in studying buried interfaces as most surface science techniques cannot access such structures. SHG can provide information on the electric field at an interface) (Walker, 2007). Analysis of poly(1-octadecylpyrrol-2-yl)squaraine indicated that it was primarily a 1,3-substituted squaraine system, but a percentage of 1,2-squarate substitutions were present making the chemical structure presented in Figure 2.20 (Lynch *et al*., 1997b).

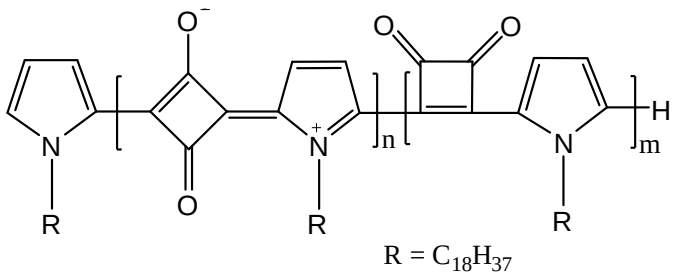

Figure 2.20 Revised chemical structure for poly(1-octadecylpyrrol-2-yl)squaraine.

The experimentally observed SHG in squaraines is thought to arise from a surface induced orientation effect. Results show that a higher SHG intensity is achieved if the squaraine head-group is essentially perpendicular to the surface. However, it was unclear if there was any interaction between the hydrophilic surface and the squarate oxygen. If the interaction between the surface hydroxyl groups and

the squarate oxygens gives rise to the molecular hyperpolarisability then head-groups aligned perpendicular to the surface would be preferred for strong SHG. The following year Lynch studied bis(5-ethyl-1-octadecylpyrrol-2-yl)squaraine (Et-Py) and bis(3,5-dimethyl-4-ethyl-1-octadecylpyrrol-2-yl) (MeEt-Py) (Fig. 2.21) as possible Langmuir-Blodgett (LB) monolayers.

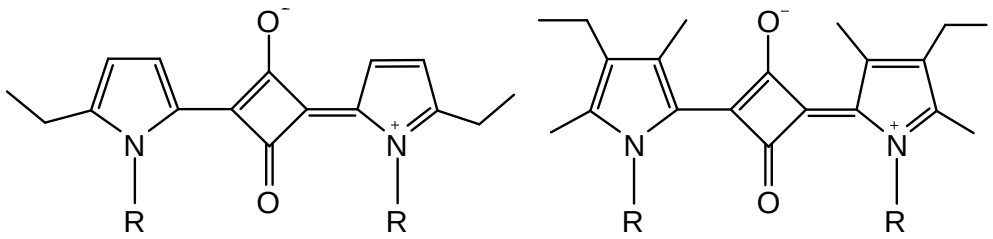

Figure 2.21 Chemical structures of bis(5-ethyl-1-octadecylpyrrol-2-yl)squaraine (Et-Py) and bis(3,5-dimethyl-4-ethyl-1-octadecylpyrrol-2-yl) (MeEt-Py).

When compared with the previously reported dyes, bis(1-octadecylpyrrol-2-yl)squaraine (Py) and bis(3,5-dimethyl -1-octadecylpyrrol-2-yl) (Me-Py) it was found that the bis(1-octadecylpyrrol-2-yl)squaraine (Py) exists as a mixture of 1,2- and 1,3-squarates as shown in Figure 1.20 for the structure of poly(1-octadecylpyrrol-2-yl)squaraine. The Me-Py was the only product of the four that formed ordered films when deposited using the Langmuir-Blodgett (LB) technique (Lynch *et al*., 1998b).

There are two possible isomers of Me-Py (*cis* and *trans*), Lynch reports that ^{1}H and ^{13}C NMR specta indicate that it most likely exists only in the *trans* form (Fig. 2.22). This was thought to be due to steric hindrance of the 4-methyl groups and the *N*-alkyl chains around the squarate oxygens (Lynch *et al*., 1997b).

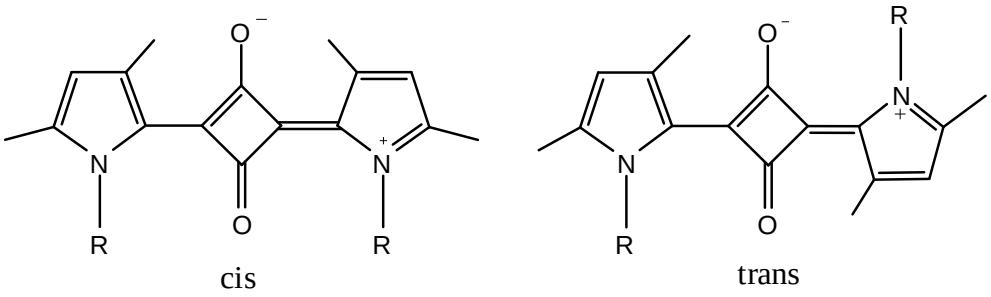

Figure 2.22 Chemical stuctures of the isomers of bis(3,5-dimethyl -1-octadecylpyrrol-2-yl) (Me-Py).

Bonnett *et al*. (2004) report a different reason for *N*-unsubstituted pyrroles to exist as *trans* isomers. They believe that *trans* isomers maximise intramolecular hydrogen bonding. Arguments for this formulation were given in the journal, including the analogy with 2,5-bis(4-ethyl-3,5-dimethylpyrrol-2-yl)-1,4-benzoquinone, for which an X-ray structure is presented. Bonnett also synthesized various derivatives of bis(5-arylpyrrol-2-yl)squaraines. Solutions of the new bis(5-arylpyrrol-2-yl)squaraines were found to have intense, sharp absorption bands shifted to the red. Condensation of squaric acid with arylpyrroles possessing fused ring systems, and condensation with 2-styrylpyrrole, gave chromophores with high values for λ_{max} and ε_{max}. They report that some of these chromophores appear to be suitable for further structural elaboration to give materials having potential in optoelectronic and photodynamic applications.

Lynch *et al.* (1998a) attempted to produce a more processible poly(pyrrol-2-ylsquaraine) by forming a copolymer of poly(pyrrol-2-ylsquaraine) with polymethylmethacrylate. Two synthetic routes were utilised, the first included formation of the polysquaraine and then polymerising the attached methacrylate groups to form the desired product and the second proceeded via the preformed methacrylate polymer, containing *N*-alkylpyrrole side chains, which was then condensed with squaric acid. The first route produced an insoluble product, which meant further polymerisation was prevented. Partial solubility during the second

procedure did allow bissquaraines to be formed which did exhibit fluorescent properties but the desired processible poly(pyrrol-2-ylsquaraine) was not achieved.

Lynch *et al*. (2001) then went on to synthesize six oligo(1-methylpyrrole) polysquaraines and studied their electrical conduction properties. The oligomers used were 1-methylpyrrole, the dimer, the trimer, the tetramer, the hexamer and a mixture of 6-12 1-methylpyrrole units long. Only the tetramer polysquaraine ($Sq.Py_4$) (red-purple colour) conducted, the first three (dark blue coloured) being essentially insulators. As stated earlier (page 75 Fig. 2.9) poly(pyrrolylsquaraine)s are known to consist of three basic structural units (1,2,3-squarate, 1,2-squarate and 1,3-squarate) with a dominance of the 1,3-squarate being desired. For conduction to occur a significant percentage of the 1,3-squarates in the polymer need to be present. They are highly resonant and give rise to the low band gap features. They also exhibit electro-positive and electro-negative regions in squaraines that are directly responsible for the close-stacked order in the solid state.

Ellis (2001) studied the properties of bis(*N*-hexylpyrrol-2-ylsquaraine) and poly(*N*-hexylpyrrol-2-ylsquaraine) prepared using four solvents; methanol, ethanol, isopropanol and 1-butanol. Calculation of the percentage yields showed that 1-butanol produced a much larger quantity of product than the other solvents, as can be seen in Table 2.1 below.

Table 2.1 Yield of poly(*N*-hexylpyrrol-2-ylsquaraine).

Solvent	Polymer Yield (%)
Methanol	2.2
Ethanol	9.0
Isopropanol	4.5
1-Butanol	38.0

Infra-red spectra were identical for all four polymers, indicating that the solvent did not alter the final product in any way other than to vary the yield. The

insolubility of the polymers prevented any further analysis of these moieties so the reaction time was shortened to two hours, thus resulting in an increased production of the dimer bis(*N*-hexylpyrrol-2-ylsquaraine). The resulting products synthesized were found to be oils and not solids. The dimers were once again produced using the four different solvents. Ellis reports that the nuclear magnetic resonance (NMR) spectra obtained was similar for dimers produced using the methanol, ethanol and the IPA solvents but different for the dimers produced using the 1-butanol solvent. It was speculated that the 1-butanol could be having a direct effect on the isomerism of the product obtained. It was also found that all four NMR spectra showed the presence of solvent peaks suggesting that solvent molecules were tightly bound to the squarate ring, probably caused by hydrogen-bonding through the squarate oxygen atoms. The proposed hydrogen bond association between methanol and the squarate unit is shown in Figure 2.23. It was proposed that a similar association exists for the other alcohol-dimer systems.

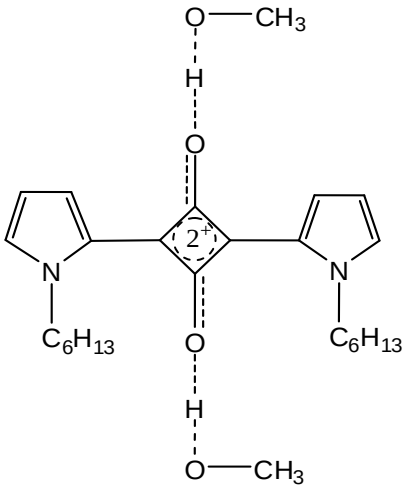

Figure 2.23 Hydrogen bonding between squarate oxygen atoms and methanol.

Further analysis of the spectra revealed that the more volatile the alcohol the larger the number of molecules bound to the squarate as can be seen in Table 2.2 below.

Table 2.2 Number of solvent molecules bound to each squarate unit.

Solvent	Molecules bound
Methanol	2-3
Ethanol	3
IPA	14-15
1-Butanol	~10

Ellis's theory for the high number of solvent molecules apparently bound to the squarate units is that some sort of aggregation occurs between the 1-butanol and the squarate oxygen atoms the same as when centrosymmetical squaraine molecules exhibit frequency doubling properties to produce second harmonic generation (SHG) and the formation of Langmuir-Blodgett films.

It was the research into more processible poly(pyrrol-2-ylsquaraine)s that led to the development of PMPS particles. The specific structure that the particles consist of has been previously published, but with very little chemical data being reported (Treibs and Jacob, 1965, Lynch *et al*., 2001, Ajayaghosh, 2003). Previous investigations at Coventry University have shown that PMPS particles can be used as a sacrificial template to produce hollow silica spheres. This was achieved by immersing the PMPS particles into a solution of 9:1 tetraethyl orthosilicate (TEOS): ethanol that allowed the silicate precursor to adhere to the surface of the PMPS particles. Subsequent treatment with hydrochloric acid caused the TEOS to polymerise around the particles forming a shell. When the particles were exposed to thermal heat at 660^{o}C the PMPS is calcined leaving hollow silica spheres. Undergraduate research carried out at Coventry shows that if a metal salt were added to the acid during the polymerisation stage then the resulting silica spheres would contain traces of the metal encapsulated inside, although no quantification data has previously been carried out (Fellows, 2003, Wilcock, 2004, Sethi, 2004). The PMPS particles appear to be very physically and chemically robust, not being cracked when

frozen (liquid nitrogen) and crushed, and not being either dissolved or decomposed in common solvents or corrosive materials (except for an acid / peroxide mixture) (Lynch *et al*., 2005).

In February 2004, Coventry University initiated the process to patent the production of PMPS particles. The patent was initiated because of industrial interest from a company called Addmaster (UK) Ltd who specialise in polymer additives. Addmaster recently supported an EPSRC CASE award based on the development of polymer matting, containing slow release phosphorus media, with the intention of being incorporated into Coventry University's porous pavement system, to sustain a bio-film of oil-degrading micro-organisms (Spicer, 2006).

Chapter Three

Analytical

Instrumentation

3.1 Analytical procedures

The most commonly used techniques for the analysis of metallic elements in samples are based on atomic spectroscopy. As the name implies these techniques involve electromagnetic radiation that is absorbed by and/or emitted from atoms in a sample. There were three types of equipment available for analysis of elements during this project. The preferred method of analysis was the inductively coupled plasma - optical emission spectrometer (ICP-OES). Flame atomic absorption spectrometer (AAS) and flame photometers were also used for some of the analyses.

3.2 Inductively coupled plasma – optical emission spectroscopy

Inductively Coupled Plasma – Optical Emission Spectroscopy (ICP-OES) is a major technique for elemental analysis. It can be used for elemental chemical analysis for all of the metallic elements in the periodic table. The degree of analysis can cover very high concentrations down to very low concentrations. Parts per billion or in many cases parts per trillion in solutions can be measured. Quantitative analysis involves calibrating the instrument with a series of appropriate solution standards and then measuring signals from the samples of interest. The sample to be analysed, if solid, is normally first dissolved and then mixed with water before being analysed.

An ICP-OES instrument consists of a sample delivery system, inductively coupled plasma (ICP) to generate the signal, one or more optical spectrometers to measure the signal, and a computer for controlling the analysis. Atoms in the plasma emit light (photons) with characteristic wavelengths for each element. This light is recorded by the optical spectrometer and when calibrated against standard solutions the technique provides a quantitative analysis of the original sample.

The ICP is reported to reach temperatures as high as 10,000 K with the sample experiencing useful temperatures between 5,500 K and 8,000 K. These temperatures allow complete atomisation of elements, minimizing chemical interference effects. The device that produces the plasma is commonly referred to as the ICP torch. There are various torch designs available and the rate of argon consumption can be between 5 and 20 litres per minute depending on the chosen design. The torch consists of two to four concentric quartz tubes through which argon gas flows. The largest tube often has a diameter of about 2.5 cm. The top of this tube is cooled by water in an induction coil that is powered by a radio-frequency generator capable of producing 0.5 to 2 kW of power at approximately 27 to 41 MHz. A spark from a Telsa coil ignites the plasma. When the radio frequency (RF) power is applied through the coil an oscillating magnetic field is formed. The plasma is created when the argon is made conductive by exposing it to an electrical discharge, which creates seed electrons and ions. Inside the induced magnetic field, the charged particles (electrons and ions) are forced to flow in a closed annular path. As they meet resistance to their flow, heating takes place and additional ionisation occurs. The process occurs almost instantaneously, and the plasma expands to its full dimensions.

The sample is injected as an aerosol though the centre of the hole. This characteristic of the ICP confines the sample to a narrow region and provides an optically thin emission source and a chemically inert atmosphere. This results in a wide dynamic range and minimal chemical interactions in an analysis. Argon is also used as a carrier gas for the sample (Tecmec, 2005). The resulting ions then interact with the fluctuating magnetic field produced by the induction coil. The argon ions once formed in the plasma are capable of absorbing sufficient power from an external source to maintain the temperature at a level at which further ionisation sustains the

plasma indefinitely (Skoog *et al*., 1999, Skoog *et al*., 1998). The liquid sample is introduced via a nebuliser into the plasma torch. The nebuliser turns the analyte liquid into droplets. The largest droplets fall out into a drain in the bottom of a spray chamber and the finest droplets are carried by argon gas flowing between 0.3 to 1.5 litres per minute into the plasma. Atomisation occurs within the plasma. Atoms get excited to atomic and ionic states. Rich spectra are produced because of the presence of both atomic and ionic lines. Because of their different excitation energies, different emission lines will have maximum intensities at different vertical positions in the plasma (Boss and Fredeen, 2004). Figure 3.1 shows a typical torch assembly and a photograph of an actual plasma torch.

Fig 3.1 has been removed due to third party copyright. The unabridged version of the thesis can be viewed at the Lanchester Library, Coventry University

Figure 3.1 Inductively coupled plasma torch assembly and photograph of a plasma torch (Tecmec, 2005).

3.3 Atomic absorption spectroscopy

Atomic Absorption Spectroscopy (AAS) is a form of quantitative and qualitative analysis for over seventy elements. It is the process that occurs when a ground state atom absorbs energy in the form of light of a specific wavelength and is elevated to an excited state. The amount of light energy absorbed at this wavelength will increase as the number of atoms of the selected element in the light path

increases. The relationship between the amount of light absorbed and the concentration of analyte present in known standards can be used to determine unknown concentrations by measuring the amount of light they absorb. Instrument readouts can be calibrated to display concentrations directly. It is preferable for the sample to be in solution when analysed (Taylor *et al.*, 1994) but under certain circumstances solids and slurries can be analysed (Sahuquillo et al., 2003). The basic layout of an atomic absorption system is shown in Figure 3.2.

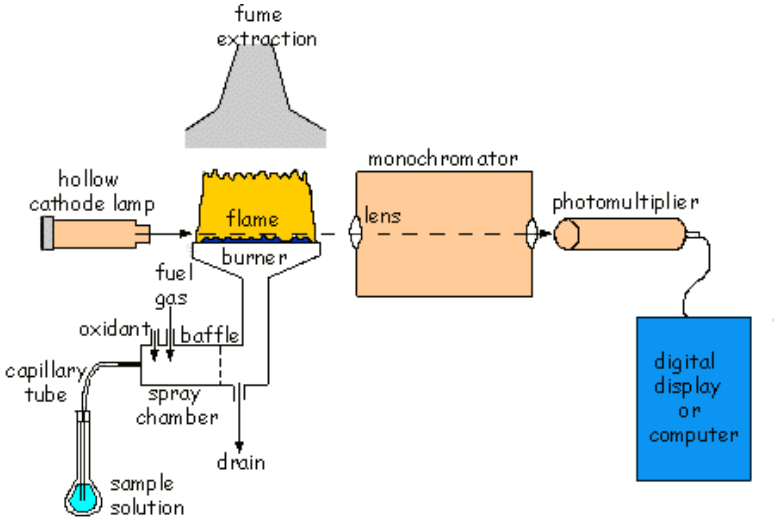

Figure 3.2 Schematic of an atomic absorption spectrometer.

The light source is usually a hollow cathode lamp (HCL), which emits radiation at resonance wavelength of the analyte element and is of a very narrow band-width (0.001 nm). Since the HCL is constructed of the analyte element (or an alloy of it) the radiation will be specific to that element only. The oxidant gas (acetylene or nitrous oxide) flows into the nebuliser and creates a partial vacuum which causes the solution containing the analyte element to be aspirated into the nebuliser, via a plastic capillary tube, and is then converted into an aerosol. The oxidant/aerosol is then swept into the spray chamber where mixing with the fuel gas occurs. The mixture is then forced into the flame that is of a sufficiently high

temperature to cause the atomisation of the analyte element. The free atoms thus formed absorb radiation from the HCL, which is focused through the centre of the flame and about 5-10 mm above the burner slot. The radiation that has now been attenuated by an amount related to the concentration of free atoms in the flame (and hence in the solution) now enters the monochromator. This allows only a narrow region of the spectrum, typically 0.5 nm centred on the pre-selected wavelength of the resonance line of the analyte element to pass into the photo-multiplier. This amplifies the resulting display. The output can also be processed by a data handling system, typically a computer. The absorbance of the element is directly proportional to the path length in the flame and to the concentration of atomic vapour in the flame in accordance with the Beer Lambert Law.

A major disadvantage of atomic absorption is that a different radiation source is required for each element. The wavelengths of radiation given off by the source are the same as those absorbed by the atoms of the flame. Atomisation is the most crucial step in flame spectroscopy and the one that limits the precision of this method. For this reason it is very important to select the correct type of fuel and oxidant so that a suitable flame can be achieved. The flow rate of both the oxidant and the fuel are an important variable in AAS and require careful control to vary each over a wide range so that optimal atomisation conditions can be achieved. Flow rates are usually measured using a rotameter. This consists of a tapered, graduated, transparent tube that is mounted vertically with the smaller end down. A lightweight float that is conical or spherical in shape is lifted by the gas flow; its position is determined by the flow of the gas. The actual control of the flow is done by means of a double diaphragm pressure regulator followed by a needle valve (Skoog *et al*., 1998, Skoog *et al*., 1999).

3.4 Flame photometer

Flame photometry, also called flame atomic emission spectrometry, is a relatively old instrumental analysis method (Kentucky, 2005). Kirchoff and Bunsen first investigated the principles of flame emission spectroscopy in the 1860's. Its origins came from Bunsen's flame colour tests for the qualitative identification of select metallic elements (Kirchhoff and Bunsen, 1860). Lundengardh refined the technique in the 1920's by incorporating a nebuliser and electro optical detector, which paved the way to modern quantitative analysis (Sherwood, 2007) .

As an analytical method, atomic emission is a fast, simple, and sensitive method for the determination of trace Group I and II metal ions in solution. The method is relatively free of interference from other elements because of the very narrow (ca. 0.01 nm) and characteristic emission lines from the gas-phase atoms in the flame. Typical precision and accuracy for analysis of dilute aqueous solutions with no major interference present are about ±1-5% relative. The method is suitable for metallic elements that are easily excited to higher energy levels at the relatively cool temperatures of typical flames; mainly sodium, potassium and lithium, some photometers can also analyse calcium, rubidium, caesium, copper, magnesium and barium. Metalloids and non-metals generally do not produce isolated neutral atoms in a flame, but rather mostly neutral, polyatomic radicals and ions. Therefore, non-metallic elements are not suitable for determination by flame emission spectroscopy, except for a very few and under very specialized conditions. Flame photometry is a highly empirical method of analysis. Many different experimental variables affect the intensity of light emitted from the flame, necessitating careful and frequent calibration to acheive good results (Kentucky, 2005).

The components of a typical flame photometer can be seen in Figure 3.3. The aqueous sample is aspirated into the Nebuliser where it is vaporised and mixed with air and fuel in the mixing chamber. Here it encounters baffles designed to prevent all but the smallest droplets reaching the flame. Larger droplets hit the baffles and are eliminated through the drain tube. The fine aerosol mist, now mixed with the gas, approaches the heat of the flame where the water content evaporates until only microscopic particles of hydroxides or oxides of the elements to be measured feed into the flame. Here they are thermally dissociated into molecules or atoms, the heat from the flame then energises the electrons. As the energised species pass into a cooler part of the flame they lose energy in the form of light of characteristic wavelength as the atoms return to their "ground state" (Higson, 2004).

Fig 3.3 has been removed due to third party copyright. The unabridged version of the thesis can be viewed at the Lanchester Library, Coventry University

Figure 3.3 Schematic of a Flame Photometer (Reallabware.com, 2006).

There is a big disadvantage when measuring sodium on the flame photometer because it is not possible to get a straight calibration line when analysing at high concentrations. This is because when sodium atoms are heated in the flame they become excited and then relax into their ground state. The energy released is seen as a yellow flame. When many atoms are in close proximity, as in high concentration,

the emitted light can cause adjacent atoms to become excited by absorbing the emitted light instead of it falling on to the detector. Thus the higher the concentration, the less light proportionally falls on to the detector. This phenomenon is known as sodium self absorption (Sherwood, 2006). However, the biggest issue for the flame photometer is the low flame temperature, which limits atomisation.

3.5 Conclusion

The AAS gives reliable data but is a more time consuming instrument to use due to having to change the hollow cathode lamp each time a different element is analysed, since the type of lamp depends on the metal being analyzed. The AAS is also limited to the range of elements it can analyse when a full set of hollow cathode lamps are unavailable. The flame photometer is the simplest and also the cheapest instrument to use, however it is limited to the Group I and II elements of the periodic table. The most convenient and reliable instrument to use (by far) for the analysis of metallic elements was the ICP since it is capable of analysing all of the metallic elements in the periodic table. It could also be set up to measure different elements at the same time.

Chapter Four

Adsorption Studies

Results and Discussion

4.1 Synthesis of the PMPS polymer particles

Equimolar amounts of 1-methylpyrrole and 3,4-dihydroxy-cyclobut-3-ene-1,2-dione (squaric acid) were boiled under reflux in 1-butanol (Yu *et al., 1990)* for sixteen hours (Fig. 4.1).

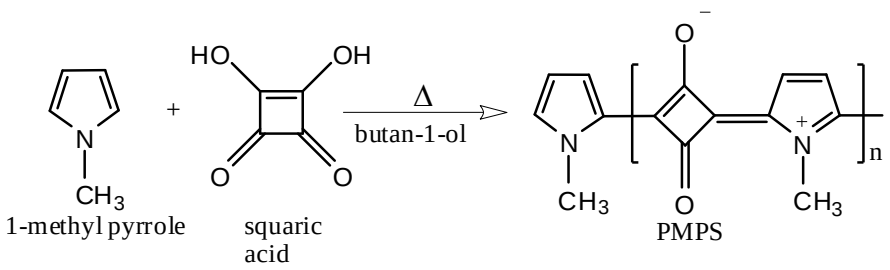

Figure 4.1 Chemical **e**quation for the chemical reaction of PMPS particles.

The product was collected using vacuum filtration and then washed repeatedly in ethyl acetate for two to three hours using a soxhlet extractor, to remove any low molecular weight and un-reacted materials (Lynch *et al.*, 2001). The product was then dried overnight in a heated cabinet (60^{o}C) to yield a fine dry blue-black powder. The ethyl acetate was saved and reused several times but the 1-butanol was discarded, as re-distillation was too time consuming and the volumes used did not warrant such an exercise.

Initial preparation of the beads was carried out by mixing 5 grams of squaric acid with 3.61 grams of 1-methylpyrrole in a 250 mL round-bottomed flask, half filled with 1-butanol. Quantities were then increased to 10 grams of squaric acid and 7.2 grams of 1-methylpyrrole in a 500 mL round-bottomed flask. If the amounts of squaric acid and 1-methylpyrrole are not equimolar the reaction does not produce the desired product. Too much 1-methylpyrrole caused the formation of the 1,2,3-squarate, which was unable to sorp effectively due to the negative oxygen anion no longer being able to co-ordinate. Too little 1-methylpyrrole causes the formation of low molecular weight and un-reacted materials that will get washed away during the

soxhlet process, thus leading to a poor yield. There is no foreseeable reason why the production cannot be scaled up to an industrial level although it is advisable for the reaction to be carried out in a fume cupboard as occasionally the reacting materials have been too volatile and have erupted through the condenser and out into the fume cupboard. The reason for this is probably due to over filling of the round-bottomed flask with 1-butanol.

4.1.1 pH of PMPS particles

The pH of 1 gram of blank PMPS beads stirred in 30 mL of water was found to measure pH 3.38 making them extremely acidic. Triebs and Jacob state that, "the acidity of squaric acid is maintained in the bridges producing intramolecular salts" (Treibs and Jacob, 1965). The PMPS particles can be structurally neutral but can also form Lewis acids.

4.1.2 The determination of water uptake by PMPS particles

0.5 grams of dry PMPS particles were weighed into a beaker, 50 mL of deionised water (25^{o}C) was added to the beaker and the contents mechanically stirred at room temperature for 2 hours. The PMPS particles were vaccum filtered until no more water could visably be removed and then re-weighed to determine the total water capacity. The beads weighed 1.5 grams meaning that when at full capacity they can absorb three times their own weight.

4.1.3 Swelling capacity of PMPS particles

0.5 grams of PMPS particles were weighed into a 10 mL measuring cylinder and the volume noted to be 4.5 cm^3. The cylinder was filled with deionised water,

covered with a watch glass and left to settle for 72 hours. The volume of beads fell to 4.0 cm^3. Therefore the PMPS beads do not swell. The 0.5 cm^3 drop in the volume would have been due to the particles becoming more tightly packed by the weight of the water.

4.1.4 Comparative studies of absorption vs adsorption

1 gram of both sand and PMPS particles were placed into separate beakers containing 30 mL of 2 molar sodium hydroxide and mechanically stirred for 30 minutes, after which time the samples were vacuum filtered and left to dry in a heated cabinet (60^oC) for 16 hours. Each sample was then added to 30 mL of ultra pure water and the pH of the solution was measured over a period of 30 minutes. The pH of the PMPS solution was 10 and the sand pH 9. Both solutions produced a constant pH reading during the 30 minutes of stirring. This suggests that the PMPS particles only adsorbed ions onto its outer surface in the same way that the solid sand particles did. A steady rise in pH would have been expected if absorption had occurred into the pores of the PMPS, unless some form of chemisorption had taken place, which would prevent the release of ions bound to active sites inside the PMPS particles. The term sorption refers to the action of absorption, adsorption and ion exchange and since it is not exactly clear how the PMPS particles works this is the term that will be used for the remainder of this paper.

4.2 Sorption methodology

The sorption experiments were all carried out as follows, unless otherwise stated; 1 gram of the selected elemental compound was dissolved as elemental salts (or oxides) separately in either deionised water, 0.1 molar hydrochloric acid or

concentrated hydrochloric acid. Each solvent was subjected to temperature variations of 4°C, room temperature (25°C ± 10%) and 50°C resulting in nine different variants. Once dissolved and the desired temperatures had been reached 1 gram of PMPS particles was added to each of the nine solutions and mechanically stirred for 30 minutes then filtered through vacuum and left to dry in a heated cabinet for 16 hours at 60°C.

The amount of element absorbed was determined by digestion of 100 milligrams of the prepared PMPS particles in acid peroxide solution using 50/50 (v/v) of 100 volume hydrogen peroxide and concentrated sulfuric acid, then diluted to 100 mL using deionised water once the digestion had taken place. The samples were then analysed using AAS, ICP-OES or flame photometer instruments, using initial standard solution concentration ranges of 0, 25, 50, 75 and 100 mg/L. Subsequently the solution concentrations were adjusted accordingly whenever results were found to be outside the calibration range, and the samples reanalysed. The standard solutions were always matrix matched with the samples. The purpose of matrix matching was so that the standard solutions would have an almost identical composition to the samples. Examples of calibration data can be found in Appendix 1.

A small number of samples were digested in a microwave oven using 30/70 v/v of 100 volume hydrogen peroxide and concentrated nitric acid to validate the digestion method. It was only possible to use 100 milligrams of each of the prepared samples for digestion because it would have been impossible to digest the whole of the prepared samples due to the extremely volatile nature of the digestion system. To be consistent with the spectator ions present and keeping them to a minimum, chloride salts were used whenever possible with water or hydrochloric acid as the solvent. There were a small number of occasions when this was not possible and an alternative

had to be found. The specific compounds and conditions used for sample preparation are listed below.

4.2.1 Group 1: Lithium, sodium, potassium, rubidium and caesium

Lithium samples were prepared using lithium chloride, lithium sulfate monohydrate and lithium hydroxide as the elemental salts. The chloride and the sulfate were prepared as stated in section 4.2. Lithium hydroxide pellets were dissolved in distilled water and made up to concentrations of 0.1, 1 and 5 molar solutions and then treated the same as in section 4.2. Sodium samples were prepared using sodium chloride, sodium nitrate and sodium hydroxide. Sodium chloride was dissolved in H_2O, 0.1 molar hydrochloric acid and 10 molar hydrochloric acid. The analysis of sodium chloride in concentrated acid was not possible as it is insoluble in concentrated hydrochloric, sulfuric and nitric acid. Sodium hydroxide pellets were dissolved in distilled water and made up to 0.1, 1 and 5 molar concentrations. Sodium nitrate was dissolved in 1 molar nitric acid. All of the sodium samples were then tested at the three different temperatures as stated in section 4.2. Potassium samples were prepared using potassium chloride and potassium hydroxide. The chloride salt dissolved in H_2O and 0.1 molar hydrochloric acid but would not dissolve in concentrated acid. It would not dissolve in 10 molar hydrochloric acid either for direct comparison with the sodium chloride. The strongest acid that the potassium chloride would dissolve in was found to be 6 molar. Potassium hydroxide pellets were dissolved in distilled water and made up to 0.1, 1 and 5 molar concentrations. Rubidium samples were prepared using rubidium chloride and caesium samples were prepared using caesium chloride, both salts readily dissolved in all of the solvents enabling the samples to be prepared as stated in section 4.2.

4.2.2 Group 2: Magnesium, calcium, strontium and barium

Magnesium samples were prepared using magnesium(II) chloride hexahydrate and magnesium sulfate heptahydrate and calcium samples were prepared using calcium chloride dihydrate, they were all prepared as stated in section 4.2. Strontium samples were prepared using strontium chloride hexahydrate. The H_2O and 0.1 molar hydrochloric acid samples were prepared as stated in section 4.2 but the strontium chloride hexahydrate failed to dissolve in concentrated, 10 molar or 5 molar hydrochloric acid, but was found to dissolve easily in concentrated sulfuric acid. Barium samples were prepared using barium chloride dihydrate. The H_2O and 0.1 molar hydrochloric acid samples were prepared as stated in section 4.2 but the barium chloride dihydrate failed to dissolve in the concentrated hydrochloric acid. Attempts to dissolve it in 10 molar and 5 molar hydrochloric acid also failed. However barium chloride dihydrate did surprisingly dissolve in concentrated sulfuric acid, after being stirred for 16 hours, and not react to form the expected barium sulfate. However, it was found that upon addition of further concentrated sulfuric acid during the digestion stage the barium did produced the expected insoluble complex of barium sulfate. This meant that the samples could not be acid digested using sulfuric acid. The alternative microwave digestion method had to be used which used nitric acid in place of the sulfuric acid. Nitric acid was also added to the standards to matrix match with the samples. This seems a very stange phenomenon considering that the concentrated samples were actually prepared using sulfuric acid, it would be assumed that barium sufate should have been created during the sample preparation, however the sample solutions were all clear.

4.2.3 Group 3: Scandium and yttrium

Scandium samples were prepared using scandium(III) chloride hydrate and yttrium samples were prepared using yttrium(III) chloride hexahydrate, both were prepared as stated in section 4.2. Lanthanum, cerium and ytterbium are grouped together as the lanthanides and are included separately in section 4.2.17 (page 121).

4.2.4 Group 4: Titanium, zirconium and hafnium

Titanium samples were prepared using titanium sulfate 45% wt solution in dilute sulfuric acid. The solution was first used as prepared taking three aliquots of 30 mLs and preparing PMPS particle samples at the three set temperatures. The solution was collected after filtration and diluted 50:50 with H_2O and three more PMPS samples prepared. The process was repeated a third time producing nine samples of varying concentration and temperature. Zirconium samples were prepared using zirconium(IV) chloride, hafnium samples were prepared using hafnium(IV) chloride and both were prepared as stated in section 4.2.

4.2.5 Group 5: Vanadium, niobium and tantalum

Vanadium was first prepared using ammonium meta-vanadate. This salt dissolved in concentrated hydrochloric acid and three samples were prepared at the varying temperature. However it proved to be insoluble in H_2O and 0.1 molar hydrochloric acid so an alternative salt had to be used. Vanadium samples were also prepared using vanadium(III) chloride and vanadyl sulfate. These salts dissolved in all three solvents and were all prepared as stated in section 4.2. All of the vanadium samples proved difficult to digest because when the concentrated sulfuric acid was added to the samples a violent reaction occurred producing effervescence causing the samples to froth out of the volumetric flasks. After several attempts the samples were

eventually all successfully digested, by cooling in ice and adding the acid very slowly and waiting for the reaction to subside before continuing the digestion. The niobium samples were prepared using niobium(III) chloride. The niobium dissolved easily in the concentrated hydrochloric acid but was not very soluble in H_2O or 0.1 molar hydrochloric acid. It was found that heating the Nb/H_2O solution caused a white precipitate to form, which was then unusable. The remaining solutions were left stirring for 16 hours and then filtered before being added to the PMPS particles. The tantalum samples were prepared using tantalum(V) chloride. This would only dissolve in hot concentrated hydrochloric acid so only three samples were prepared.

4.2.6 Group 6: Chromium, molybdenum and tungsten

Chromium samples were prepared using chromium(III) chloride hexahydrate and were prepared as stated in section 4.2. Molybdenum samples were prepared using molybdenum chloride, molybdenum oxide and ammonium molybdate. Molybdenum was found to be extremely insoluble. The molybdenum chloride, which was a brown powder, turned dark blue when added to water and dilute hydrochloric acid, and turned a red/brown colour when stirred in concentrated hydrochloric acid. After filtering the PMPS particles the concentrated solute collected was a green colour. All of the solutions were heated and stirred for 4 hours to ensure maximum solubility. The molybdenum still failed to dissolve completely so the solutions were filtered through glass wool to remove any remaining undissolved molybdenum particles, and then allowed to reach their correct temperatures before adding the PMPS particles and proceeding as stated in section 4.2. The molybdenum oxide would not dissolve in H_2O, 0.1 molar or concentrated hydrochloric acid or concentrated nitric acid. It did eventually dissolve in concentrated sulfuric acid after again being heated and stirred for 4 hours and then filtered through glass wool to

remove any remaining undissolved molybdenum oxide particles. The ammonium molybdate samples were prepared by dissolving in H_2O and concentrated ammonia. The ammonia produced endothermic reactions reducing the 4^oC solution down to –1^oC and reducing the 23^oC room temperature soluton down to 8^oC. The solutions were allowed to reach their correct temperatures before additon of the PMPS particles. The tungsten samples were prepared using ammonium tungstate, which also proved to be extremely difficult to dissolve. It would not dissolve in concentrated hydrochloric acid, sulfuric acid or nitric acid. It did however dissolve in H_2O and 0.1 molar hydrochloric acid. Attempts to dissolve it in 1 molar and 2 molar hydrochloric acid failed, even after heating, so it was not possible to produce a more concentrated solution.

4.2.7 Group 7: Manganese and rhenium

Manganese samples were prepared using manganese(II) chloride tetrahydrate and manganese(II) sulfate tetrahydrate and were prepared as stated in section 4.2. Rhenium samples were prepared using rhenium(V) chloride. The rhenium dissolved easily in the concentrated hydrochloric acid, however the H_2O and 0.1 molar hydrochloric acid samples were heated and stirred for 16 hours and then filtered and it appeared that very little of the rhenium had dissolved into these samples.

4.2.8 Group 8: Iron and ruthenium

Iron samples were prepared using iron(III) chloride and iron(III) chloride hexahydrate. Ruthenium samples were prepared using ruthenium(III) chloride hydrate, all samples were prepared as stated in section 4.2. The digestion of the ruthenium samples proved to be problematic. When hydrogen peroxide was added to

a volumetric flask containing a $RuCl_3$/PMPS sample a violent reaction took place producing a large amount of heat and gas, which resulted in cracking of the flask. To digest these samples it was necessary to cool the samples in ice then add the concentrated sufuric acid which caused no reaction, and then add the hydrogen peroxide very slowly and swirling gently waiting for the reaction to subside before adding more hydrogen peroxide.

4.2.9 Group 9: Cobalt, rhodium and iridium

Cobalt samples were prepared using cobalt chloride hexahydrate and were prepared as stated in section 4.2 except for the fact that there was only 7 grams of cobalt chloride available, which meant that instead of using 1 gram per sample only 0.75 grams were used. Rhodium samples were prepared using rhodium(III) chloride. The rhodium dissolved easily in H_2O and 0.1M hydrochloric acid but required heating and stirring for 16 hours and then filtering before using as stated in section 4.2. The Iridium samples were prepared using iridium(III) chloride hydrate. The iridium salt made a dark brown solution when added to all three solvents and failed to dissolve. Each sample was heated and stirred 16 hours and filtered before proceeding as stated in section 4.2.

4.2.10 Group 10: Nickel, palladium and platinum

Nickel samples were prepared using nickel chloride hexahydrate and platinum samples were prepared using platinum chloride, they were both prepared as stated in the section 4.2. Palladium samples were prepared using palladium chloride. Due to the high cost of the palladium salt there was only 2 grams of palladium chloride available for the analysis. To enable a full set of data to be obtained the salt was

divided into three enabling 0.33 grams to be dissolved into each of the three solvents. The samples at room temperature were prepared first and the solutions collected after filtration and reused at 4^{o}C and again at 50^{o}C. The heated samples were prepared last in case any of the solvent evaporated during preparation. So apart from reusing each of the dissolved salts three times the samples were prepared as stated in section 4.2. The palladium samples were extremely volatile during digestion. The samples had to be cooled in ice and the sulfuric acid added very slowly allowing the reaction to subside before continuing to keep the sample contained in the volumetric. The PMPS samples prepared in concentrated hydrochloric acid at room temperature were particularly difficult to contain and took three attempts before successful digestion was completed.

4.2.11 Group 11: Copper, silver and gold

Copper samples were prepared using copper chloride dihydrate as the elemental salt and were prepared as stated in the set method. Silver samples were prepared using both silver nitrate and silver sulfate. This was again due to difficulties in solubility. The silver nitrate salt was used to prepare samples dissolved in water and 0.1 molar nitric acid but for some strange reason refused to dissolve in concentrated nitric acid. The silver sulfate would not dissolve in water or 0.1 molar sulfuric acid, but would dissolve in concentrated sulfuric acid so the silver sulfate was used to prepare samples in concentrated acid. After filtration of the PMPS particles in silver sulfate dissolved in concentrated sulfuric acid the samples were left sticky and would not dry properly even after being left in a heated cabinet for three days. To enable the samples to dry the concentrated sulfuric acid had to be washed away. Stirring the PMPS samples in 0.1 molar sulfuric acid and then refiltering achieved

this. Both sets of samples were then analysed to obtain silver results at three varying concentrations.

Gold samples were prepared using gold(IV) chloride trihydrate as the elemental salt and were prepared as stated in the section 4.2. Gold was also analysed using pure gold metal dissolved in aqua regia and analysed only at the three temperature variations. The samples were prepared individually using the same gold solution. A problem with using the same solution more than once is that the concentration of the solution will be decreasing each time PMPS particles were added and the gold absorbed. Therefore the first sample prepared will have the highest concentration of gold ions and should therefore absorb the most gold. The samples were prepared in ascending temperature order, 4^{o}C, room temperature and then 50^{o}C.

4.2.12 Group 12: Zinc, cadmium and mercury

Zinc samples were prepared using zinc chloride and cadmium samples were prepared using cadmium(II) chloride monohydrate and cadmium sulfate. Mercury samples were prepared using mercury(II) chloride. A sample was also prepared using mercury nitrate in concentrated hydrochloric acid at room temperature. They were all prepared as stated in section 4.2.

4.2.13 Group 13: Boron, aluminium, gallium, indium and thallium

Boron samples were prepared using solid boric acid. Three concentrations of boric acid were used, 0.1 molar, 0.5 molar and 1 molar. The 0.1 molar solutions completely dissolved at all three variable temperatures. The 0.5 molar solutions were only soluble at room temperature and at 50^{o}C, precipitating out of solution when cooled. The 1 molar solution only dissolved when heated, two temperature variations

were prepared, at 28^{o}C and 50^{o}C. Boric acid was also dissolved in 0.1 molar hydrochloric acid and samples were prepared at room temperature and 50^{o}C, but was insoluble at 4^{o}C. It was insoluble in concentrated hydrochloric acid even when heated. Aluminium samples were prepared using aluminium(III) chloride hexahydrate and aluminium sulfate hexadecahydrate. The gallium samples were prepared using gallium nitrate and they were all prepared as stated in section 4.2. It was observed that all of the gallium sample solutions were clear except for the room temperature concentrated solution, which turned pale yellow, and the 50^{o}C concentrated solution, which turned deep yellow. The indium samples were prepared using indium(III) chloride tetrahydrate, they were all prepared as stated in section 4.2. The thallium samples were prepared using thallium sulfate dissolved in sulfuric acid. The concentrated acid solutions dissolved fine but the H_2O and 0.1 molar acid samples needed to be heated and stirred overnight and then filtered. Upon preparation of the 4^{o}C in H_2O sample the thallium sulfate crashed out of solution as soon as it was placed into the ice to cool, therefore it was abandoned, leaving only eight samples to test.

4.2.14 Group 14: Germanium, tin and lead

The germanium samples were prepared using germanium oxide. This was extremely insoluble. The solutions were heated and stirred for 16 hours then filtered. The filtered germanium was collected and weighed; it was found that on average only 0.2 grams of the initial 1 gram used had actually dissolved into solution. Tin samples were prepared using tin(II) chloride dihydrate. The tin proved to be very difficult to dissolve into solution. After trying, H_2O, 0.1 molar hydrochloric acid, concentrated hydrochloric acid, glacial acetic acid and concentrated sulfuric acid the most effective

solvent was found to be the concentrated hydrochloric acid. The solutions were stirred and heated for 4 hours and still needed filtering through glass wool to remove excess solid before the PMPS particles could be added. Three samples were prepared in concentrated acid at the normal temperature variations. Lead samples were prepared using lead(II) chloride and lead acetate. The lead acetate samples were prepared as stated in section 4.2 except that they had to be digested in the microwave using peroxide/nitric acid because the addition of sulfuric acid would have caused the insoluble product lead sulfate to precipitate out of the solution. The lead(II) chloride solutions needed to be heated, stirred and filtered before addition of the PMPS particles. These samples, once again could not be acid digested using sulfuric acid so were analysed as solid particles straight into the ICP.

4.2.15 Group 15: Phosphorous, arsenic, antimony and bismuth

Phosphorous samples were prepared using 30 mL of orthophosphoric acid mixed with 1 mL of ammonia solution (35% w.w. s.g. 0.88) to produce ammonium phosphate. The concentration of orthophosphoric acid was changed to produce three variants, using 5, 10 and 15 molar (conc.). The three temperature variants were used as stated in section 4.2. The samples prepared using concentrated orthophosphoric acid had to be washed with water after filtration to remove the excess acid to prevent the PMPS particles from sticking together. The vast difference in the data shows that the washing of the samples removed much of the sorbed phosphorous. The samples prepared using 10 molar acid gave the highest values because the 30% water content removed the necessity of washing after preparation. The 5 molar sample results were low because dilution of the acid reduces the amount of phosphorous available for sorption, although still higher than the concentrated samples that were washed.

Arsenic samples were prepared using arsenic(III) oxide as the elemental salt. The arsenic was very difficult to dissolve in water and 0.1 molar hydrochloric acid. Half of the normal amount of salt was added (0.5 g) to 30 mL each of H_2O and 0.1 molar hydrochloric acid and stirred for three days. The resulting solutions still needed filtering to remove excess arsenic that had not dissolved. The arsenic did dissolve in the concentrated hydrochloric acid as normal but to keep the results consistent with the other arsenic solutions 0.5 grams of salt was used. Once the solutions were made the PMPS samples were then prepared as stated in the section 4.2. Antimony samples were prepared using antimony(III) chloride as the elemental salt. Antimony proved to be very difficult to dissolve in dilute conditions, but was no problem in concentrated hydrochloric acid. Antimony in water and 0.1 molar hydrochloric acid was stirred for 16 hours and then filtered but hardly any of the antimony had dissolved. It was found that the lowest concentration of acid for dissolving antimony was 4 molar. PMPS samples were prepared using H_2O, 4 molar and concentrated hydrochloric acids at the three variant temperatures.

Bismuth samples were prepared using bismuth(III) chloride and bismuth(III) oxide. The bismuth(III) chloride was not soluble in H_2O or 0.1 molar hydrochloric acid but did dissolve in 2 molar, 5 molar and concentrated acid. The bismuth(III) oxide was not soluble in H_2O, 0.1 or 4 molar hydrochloric acid. It did dissolve in concentrated hydrochloric acid and 5 molar hydrochloric acid so only six samples of the oxide were prepared at the varying temperatures.

4.2.16 Group 16: Sulfur and selenium

Sulfur samples were prepared using ammonium sulfate and were prepared as stated in section 4.2. Digestion of the sulfur beads could not be done using sulfuric

acid so they were analysed as solid particles straight into the ICP. Selenium samples were prepared using selenium(IV) oxide as the elemental salt and were prepared as stated in section 4.2. The concentrated acid/PMPS solution at 50^{o}C produced a red vapour whilst being stirred and produced an orange filtrate afterwards, the room temperature filtrate was orange/yellow and the 4^{o}C filtrate was yellow. The filtrates from the H_2O and 0.1 molar hydrochloric acid were all clear; neither did they appear to produce any vapour whilst being stirred.

4.2.17 The Lanthanides: Lanthanum, cerium and ytterbium

Lanthanum samples were prepared using lanthanum(III) chloride heptahydrate as the elemental salt and cerium samples were prepared using cerium(III) chloride heptahydrate, ytterbium samples were prepared using ytterbium(III) chloride hexahydrate. They were all prepared as stated in section 4.2.

4.3 Spectroscopy equipment

The microwave digestion was performed using a Milestone, 1200 Mega HPR 600/10. The analytical data was obtained using either inductively coupled plasma - optical emission spectrometer (ICP-OES) (Perkin Elmer Plasma 400 or Optima 5300 DV) (section 3.2); atomic absorption spectrophotometer (AAS) (Unicam 939) (section 3.3); or a flame photometer (Corning 410) (section 3.4).

4.4 Quality control

Four calibration solutions and one zero standard (blank) were used to generate an accurate calibration curve. The range used depended on the concentration range of the different samples. Initial analysis was always run using the standard solution concentrations of 25, 50, 75 and 100 mg/L and then reanalysed using more appropriate concentrations whenever necessary. Spiked samples (fortified blanks) and also blank samples were routinely prepared along with each set of samples as a quality control procedure. For the preparation of the blank sample all the steps of the analysis were performed in the absence of any sample, i.e. PMPS particles with no salts added were digested using the same method as the rest of the sample batch. The spiked samples were blank samples which had a known concentration (50 mg/L) of analytical standard added. The purpose of preparing spiked and blank samples was to reveal errors due to interfering contaminants from the reagents and vessels used during the analysis. The acceptable error limit chosen was ± 5%. Whenever the quality control failed a review of the method was made and new samples prepared eliminating any errors due to contamination or from the chemicals not reacting as expected during digestion.

Due to the large number of elements under investigations and the number of variables used for each element it was not possible to carry out the standard procedure of three replicates for each sample. This was due to two reasons, time restraints and the high cost of some of the rare salts meant that only a small portion of elements would have been tested if each sample had been replicated. Since the main objective of the project was to establish a trend for absorption it was deemed necessary to investigate as many elements as possible. To compensate for this lack of replication six elements spread across the periodic table had each of their nine samples replicated at least three times over the course of the project. This ensured the precision of the methods used and it also checked that the quality of the PMPS particles being produced were consistent throught the whole of the research project. The elements

that were used for this quality control procedure were sodium, boron, manganese, iron, selenium and silver.

4.5 Microwave digestion

To check that the method of digestion was appropriate three of the PMPS/element samples were analysed using an alternative digestion method. The first analysis was carried out by digestion using the standard sulfuric acid/hydrogen peroxide method. A second set of samples were then prepared using nitric acid/hydrogen peroxide and a microwave oven for digestion and the results compared. The boron and selenium samples were prepared using the same volumes in each digestion but the iron samples were prepared using 300 mg of sample digested in the microwave oven and diluted to 25 mL, instead of 100 mg diluted to 100 mL, thus producing a much more concentrated sample. From Figure 4.2 below it can be seen that both methods of digestion produced almost identical results with the microwave digestion method being slightly reduced for the boron and selenium. This is due to more errors produced because of extra steps transferring samples into and out of the microwave containers rather than digestion directly into the volumetric flask as in the sulfuric acid / peroxide digestion.

The results for the iron samples used in the microwave digestion give a consistently higher concentration even after allowing for extra errors through using the microwave digestion technique. This is probably due to the increased amount of sample being digested, therefore decreasing the error margin, i.e. a possible 1% loss of sample would occur regardless of the sample size so the larger 300 mg samples would produce less error than the smaller 100 mg samples. The microwave digestion technique however does present a huge problem because the instrument only holds ten

samples. The normal number of samples is nine plus one blank and one spiked sample making a total of eleven samples. This means that the samples have to be digested in two stages, possibly producing secondary errors if the machine temperature or pressure varies between runs, or the blank sample has to be sacrificed in order to digest all of the samples at the same time. Whichever method is chosen it is compromising the quality control of the results therefore it is definitely preferential to use acid/peroxide digestion in terms of both time of sample preparation and quality control of the final results due to reduced errors produced.

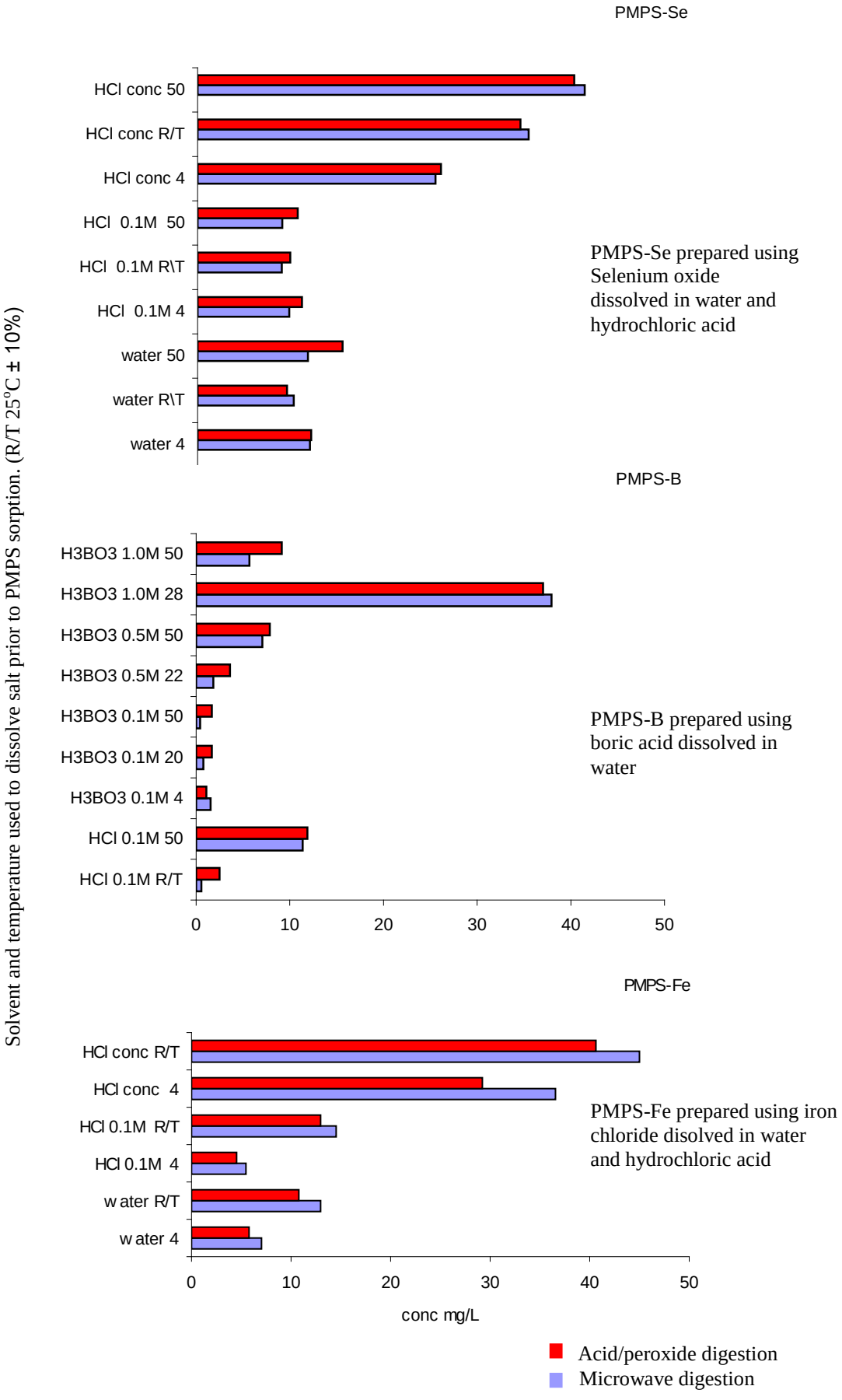

Figure 4.2 A comparison of results prepared by two different methods of digestion.

4.6 Sorption analysis

The results from the appropriate analytical equipment were calculated as mg/g and then as mmol/g (Appendix 2).

4.6.1 Group 1: Lithium, sodium, potassium rubidium and caesium

Table 4.1 Results for the PMPS particle sorption of Group 1 chloride salts (mg/g).

Solvent	Temp ^{o}C	Li	Na	K	Rb	Cs
H_2O	4	2.29	34.96	30.90	18.11	2.02
H_2O	25	9.51	34.62	35.67	21.43	1.68
H_2O	50	5.66	36.77	36.14	49.47	1.74
0.1M HCl	4	5.50	18.30	10.70	27.12	2.18
0.1M HCl	25	5.65	30.62	14.24	17.97	1.03
0.1M HCl	50	8.49	45.47	44.25	66.58	0.94
conc HCl	4	5.21	21.25	31.53	48.89	4.52
conc HCl	25	3.74	35.64	20.55	41.40	2.70
conc HCl	50	3.32	25.13	15.08	35.79	2.04

Analysis of the results for the alkali metals in Table 4.1 showed no obvious correlation of data between the elements. The variation of concentration or temperature did not seem to affect the results. The lithium and the caesium samples both gave a very low sorption whereas the sodium, potassium and rubidium samples all gave similarly comparable results. However, it can clearly be seen from Table 4.2 that altering the initial compound can vastly affect the ability for the ions to sorb into the PMPS particles. Neutral salts seemed to make no difference to the sorption when comparing the chlorides with the sulfates and nitrates, but the use of hydroxides made a vast difference. This is particulary noticeable for the potassium hydroxide at high concentration (which was 5 molar) producing a 10 fold increase in sorption. This phenomenon could be due to the fact that the PMPS particles have a very low pH

suggesting that the OH^- ions are attracted to the N^+ on the squaraine, which then leaves the O^- free to bind with the free alkali ions.

Table 4.2 Comparison of PMPS particle sorption using various group 1 elemental salts (mg/g).

Solvent Conc	Temp ^oC	LiCl	Li_2SO_4	LiOH	NaCl	$NaNO_3$	NaOH	KCl	KOH
low	4	2.29	3.70	14.62	34.96		50.81	30.90	50.46
low	25	9.51	2.20	13.62	34.62		48.92	35.67	48.05
low	50	5.66	2.50	12.60	36.77		46.52	36.14	38.81
med	4	5.50	3.20	35.43	18.30	25.04	88.86	10.70	129.50
med	25	5.65	7.90	42.31	30.62	21.04	92.29	14.24	133.40
med	50	8.49	5.30	43.76	45.47	33.59	99.91	44.25	137.10
high	4	5.21	2.70	69.84	21.25		135.25	31.53	149.60
high	25	3.74	7.50	54.79	35.64		116.39	20.55	143.90
high	50	3.32	8.20	59.73	25.13		117.64	15.08	159.00

4.6.2 Group 2: Magnesium, calcium, Strontium and Barium

Table 4.3 Results for the PMPS particle sorption of Group 2 chloride salts (mg/g).

Solvent	Temp ^oC	Mg	Ca		Sr	Ba	Solvent
H_2O	4	5.66	14.95		22.27	33.68	H_2O
H_2O	25	4.92	25.79		19.71	25.86	H_2O
H_2O	50	7.35	17.37		26.04	45.26	H_2O
0.1M HCl	4	4.80	23.03		10.63	26.55	0.1M HCl
0.1M HCl	25	7.29	11.52		20.57	43.14	0.1M HCl
0.1M HCl	50	1.08	6.66		17.79	13.29	0.1M HCl
conc HCl	4	1.25	12.81		8.03	9.20	conc H_2SO_4
conc HCl	25	1.38	14.05		7.73	0.48	conc H_2SO_4
conc HCl	50	6.06	19.45		5.39	3.45	conc H_2SO_4

A comparison of the results for the alkali earth metals in Group 2 (Table 4.3) gave a much more even spread of data. The results for the strontium and barium samples prepared in concentrated sulfuric acid were considerably less than the rest of the results and completely random forming no apparent pattern. This was because these samples needed to be washed off with dilute acid to remove excess concentrated

acid, which clung onto the PMPS particles and prevented them from drying out. Thus washing away some of the absorbed salt in the process. If the samples were not washed the PMPS particles formed sticky clumps that would not dry no matter how long they were left in the drying cabinet. Magnesium was sorbed into the PMPS particles using magnesium chloride and magnesium sulfate. A comparison of the results can be seen below in Table 4.4.

Table 4.4 Comparison of PMPS particle sorption using various magnesium elemental salts (mg/g).

Solvent	Temp ^{o}C	Cl^-	$(SO_4)^{2-}$
H_2O	4	5.66	15.48
H_2O	25	4.92	12.24
H_2O	50	7.35	14.38
0.1M HCl	4	4.80	10.66
0.1M HCl	25	7.29	12.75
0.1M HCl	50	1.08	1.80
conc HCl	4	1.25	10.01
conc HCl	25	1.38	10.21
conc HCl	50	6.06	11.10

The results in Table 4.4 show that the sulfate salts were more effective at sorption than the chloride salts, but overall both sets of magnesium results were still lower than the rest of the group.

4.6.3 Group 3: Scandium and yttrium

Table 4.5 Results for the PMPS particle sorption of Group 3 chloride salts (mg/g).

Solvent	Temp ^{o}C	Sc	Y
H_2O	4	2.47	3.41
H_2O	25	14.67	15.15
H_2O	50	16.16	0.00
0.1M HCl	4	4.99	1.23
0.1M HCl	25	3.50	1.48
0.1M HCl	50	2.59	0.00
conc HCl	4	6.22	8.68
conc HCl	25	11.26	3.82
conc HCl	50	5.24	8.99

The analysis gave unpredictable results with two yittrium samples not being sorbed. Lanthanum, cerium and ytterbium are grouped together as the lanthanides and are included separately in section 4.6.17 (page 142).

4.6.4 Group 4: Titanium, zirconium and hafnium

Table 4.6 Results for the PMPS particle sorption of Group 4 elements (mg/g).

Solvent	Temp ^{o}C	Zr	Hf
H_2O	4	5.21	10.05
H_2O	25	31.42	28.73
H_2O	50	11.27	44.54
0.1M HCl	4	17.46	9.10
0.1M HCl	25	18.38	27.36
0.1M HCl	50	27.78	31.00
conc HCl	4	18.88	34.38
conc HCl	25	26.52	39.43
conc HCl	50	41.31	24.29

Ti	Dilution
41.08	1:4 Ti/H_2O
54.66	1:4 Ti/ H_2O
52.96	1:4 Ti/ H_2O
54.66	1:1 Ti/ H_2O
47.70	1:1 Ti/ H_2O
53.83	1:1 Ti/ H_2O
79.98	Ti sol
86.09	Ti sol
88.47	Ti sol

The titanium results are much higher than the zirconium and hafnium results. This could be because the titanium was already dissolved in a solution of sulphuric acid when bought and the initial concentration of the solution could have been much higher than the standard method used to dissolve all of the other salts. The titanium

results also indicate that using the concentrated solution as prepared by the manufacturer produced a much higher adsorption value initially and dilution of the solution the first time reduced the sorption by nearly 50%, thereafter the second dilution made no difference.

4.6.5 Group 5: Vanadium, niobium and tantalum

Table 4.7 Results for the PMPS particle sorption of Group 5 elements (mg/g).

		V				
Solvent	Temp ^{o}C	NH_4	$(SO_4)^{2-}$	Cl^-	Nb	Ta
H_2O	4		7.49	26.39	7.47	
H_2O	25		16.41	21.72	8.81	
H_2O	50		14.86	23.41	20.79	
0.1M HCl	4		7.15	11.69	19.77	
0.1M HCl	25		15.76	19.89	20.57	
0.1M HCl	50		20.12	16.92	16.26	
conc HCl	4	16.60	15.49	8.29	36.16	19.90
conc HCl	25	17.69	10.11	12.88	53.57	17.33
conc HCl	50	32.14	13.02	19.41	50.67	15.73

The spread of data was fairly even for all three elements. The use of different salts for the vanadium did not make a great deal of difference except for the ammonium meta-vanadate in concentrated hydrochloric acid at 50^{o}C, which sorbed 32 mg/g, twice as much as some of the other vanadium samples.

4.6.6 Group 6: Chromium, molybdenum and tungsten

Table 4.8 Results for the PMPS particle sorption of Group 6 elements (mg/g).

Solvent conc	Temp ^{o}C	$CrCl_3$	NH_4W	$MoCl_3$	MoO_3	NH_4Mo
low	4	13.44	44.71	9.52		53.48
low	25	10.65	22.94	8.71		24.55
low	50	12.29	49.87	15.58		76.73
med	4	12.29	26.47	8.73		
med	25	14.78	44.06	11.85		
med	50	8.84	34.27	13.88		
high	4	11.53		14.81	6.88	41.48
high	25	13.45		29.99	6.17	38.06
high	50	7.98		39.98	7.58	28.99

The data show that the ammonium tungstate and ammonium molybdate absorbed better than the molybdenum chloride and the chromium chloride. This could be due to extra oxygen molecules in the ammonium providing more active sites to bind to the PMPS particles similar to the alkali hydroxides in Group 1. The molybdenum chloride and oxide data could possibly have been higher if more soluble salts could have been used, as the filtering of undissolved salts would have left a less concentrated solution.

4.6.7 Group 7: Manganese and rhenium

Table 4.9 Results for the PMPS particle sorption of Group 7 elements (mg/g).

Solvent	Temp ^{o}C	$MnSO_4$	Mn	Re
H_2O	4	47.54	5.38	87.65
H_2O	25	31.69	12.98	66.88
H_2O	50	23.51	18.83	76.08
0.1M HCl	4	30.20	18.34	78.68
0.1M HCl	25	32.97	13.22	78.76
0.1M HCl	50	34.63	15.25	69.12
conc HCl	4	38.05	21.55	68.19
conc HCl	25	40.16	8.56	87.58
conc HCl	50	36.84	9.12	107.34

The rhenium chloride, despite appearing insoluble, absorbed much more than the manganese salts. The manganese sulfate proved to be much better than the manganese chloride, once again showing that sulfates seem to be much more suitable salts for sorption into the PMPS particles. To confirm that the manganese sulfate results were correct another set of samples were digested, 14 months later; a comparison can be seen in Figure 4.3.

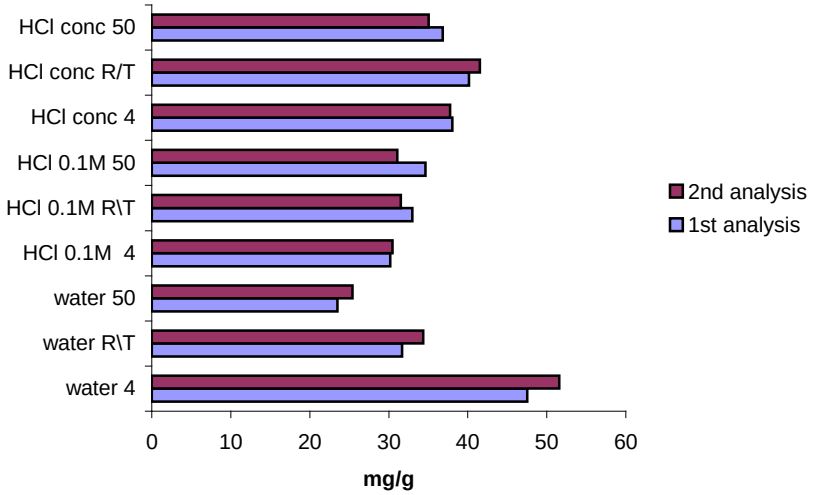

Figure 4.3 Comparison of separate batches of PMPS-Mn samples after storage.

The results in Figure 4.3 confirmed that the first set of data was correct and it also shows that samples do not alter when stored over a long period of time.

4.6.8 Group 8: Iron and ruthenium

Table 4.10 Results for the PMPS particle sorption of Group 8 elements (mg/g).

Solvent	Temp ^{o}C	$FeCl_3$	$FeCl_3.6H_2O$	Ru
H_2O	4	19.50	5.82	18.06
H_2O	25	29.72	10.72	8.43
H_2O	50	22.52		25.07
0.1M HCl	4	12.59	4.58	20.57
0.1M HCl	25	7.90	12.91	10.39
0.1M HCl	50	34.05		12.92
conc HCl	4	56.17	7.06	27.92
conc HCl	25	71.05	12.97	24.02
conc HCl	50	71.49		34.38

Iron(III) chloride hexahydrate was the first compound to be sorbed into the PMPS particles at the beginning of this project. Initially only two temperatures were examined, 4^{o}C and room temperature. Thereafter it was decided that the analysis should be carried out at three temperatures, since the literature review had revealed that high temparetures could help increase sorbtion levels (Atkins, 1998). Towards the end of the sorption studies it was decided that a complete set of iron chloride samples were needed as they were lacking the 50^{o}C samples. Attempts to prepare these samples using the same bottle of iron(III) chloride hexahydrate failed due to the compound now being insoluble. A replacement bottle of fresh iron(III) chloride was obtained, minus the hexahydrate, and a complete new set of samples was prepared. It can be seen from Table 4.10 that the new iron(III) chloride absorbed much more effectively than the iron(III) chloride hexahydrate. This indicates that the freshness of the compound to be sorbed has an effect on quality since the presence of water in the compound should have aided not hindered solubility. The ruthenium samples were comparable to the rest of the transition metals.

4.6.9 Group 9: Cobalt, rhodium and iridium

Table 4.11 Results for the PMPS particle sorption of Group 9 elements (mg/g).

Solvent	Temp ^{o}C	Co	Rh	Ir
H_2O	4	16.12	10.71	20.38
H_2O	25	6.63	20.36	41.88
H_2O	50	9.29	24.69	30.94
0.1M HCl	4	10.04	12.00	13.67
0.1M HCl	25	10.82	29.50	32.90
0.1M HCl	50	17.42	23.15	14.27
conc HCl	4	31.78	12.45	31.22
conc HCl	25	27.71	26.66	25.17
conc HCl	50	27.33	13.79	14.04

Table 4.11 shows that the elements in Group 9 were representative of the majority of the transition metal sorption data. The fact that only 7 grams of cobalt chloride were available for analysis, reducing the sample size from the normal 1 gram per sample down to 0.75 grams, did not seem to alter the results, cobalt still sorbed as well as the rhodium and iridium.

4.6.10 Group 10: Nickel, palladium and platinum

Table 4.12 Results for the PMPS particle sorption of Group 10 elements (mg/g).

Solvent	Temp ^{o}C	Ni	Pd	Pt
H_2O	4	13.52	9.12	15.62
H_2O	25	11.21	62.31	14.62
H_2O	50	24.38	73.84	31.54
0.1M HCl	4	5.83	6.23	27.62
0.1M HCl	25	17.01	23.74	37.73
0.1M HCl	50	20.03	64.46	56.36
conc HCl	4	12.01	46.80	37.95
conc HCl	25	25.77	57.17	32.21
conc HCl	50	18.65	42.89	58.32

Table 4.12 shows that the elements in Group 10 were representative of the majority of the transition metal sorption data. It would have been expected that the palladium samples prepared at room temperature should have sorbed the highest amount of element as these were the samples that were prepared first and would have had the highest concentration of palladium in the solution, with the 50^{o}C having the lowest concentration as they were prepared last. Analysis of Table 4.12 proves that there was sufficient palladium left in the reused solution to saturate the PMPS particles at 50^{o}C and produce the highest results for two out of three of the solvents.

4.6.11 Group 11: Copper, silver and gold

Table 4.13 Results for the PMPS particle sorption of Group 11 elements (mg/g).

Solvent conc	Temp ^{o}C	Cu	Ag	$HAuCl_4$	Au leaf
low	4	36.69	116.08	183.05	
low	25	22.13	87.99	312.77	
low	50	31.97	130.15	310.03	
med	4	41.98	104.03	189.42	
med	25	48.06	104.74	287.62	
med	50	53.99	69.45	318.74	
high	4	46.69	14.49	163.19	13.58
high	25	44.41	38.87	215.08	8.96
high	50	58.56	25.40	210.99	6.47

The elements in Group 11 sorbed very well. Copper being slightly above average compared to the rest of the transition metals, but the silver and gold samples proved to be excellent. The silver sulfate samples in concentrated acid gave poor results, this is probably due to the fact that the acid used had to be sulfuric, (because the use of hydrochloric acid produces insoluble silver chloride) and sulfuric acid does not filter out of the PMPS particles effectively necessitating the need to wash the acid off the particles so that they can dry to a fine powder. It is apparent from Table 4.13 that the washing process probably removed some of the metal ions that had been sorbed as well as the residual acid since other elements that have been prepared using sulfate salts have sorbed very effectively. The nitric acid that was used for the 0.1 molar samples appeared to be no more effective than dissolving the silver nitrate straight into H_2O.

The pure gold leaf metal dissolved in aqua regia sorption was very low and a definite decline in sorption can be observed with the repeated use of the solution as the sample first prepared was the 4^{o}C which is the highest sorption, then room temperature and finally the 50^{o}C sample absorbing the least of all. The presence of so

many spectator ions present in the aqua regia could have prevented the gold from sorbing into the PMPS particles since the gold chloride proved to be so much more effective. The samples prepared using water produced exceptional results because when the gold chloride is dissolved in water it is partially hydrolyzed to species such as $[AuCl_3OH]^-$ (Cotton and Wilkinson, 1962) and previous analysis has already revealed that hydroxide compounds absorb much better than neutral salts. However it was the 0.1M samples heated to 50^{o}C that produced the highest results. It is known that when gold(III) chloride is dissolved in concentated hydrochloric acid it forms tetrachlororoaurate(III) ion, $[AuCl_4]^-$, which is known to be one of the components in "liquid gold," a mixture of gold species in solution that will deposit a film of gold metal when heated (Rayner-Canham, 1999). The addition of 0.1 molar hydrochloric acid could produce a mixture of ions, maybe the hydroxide ions co-ordinate directly with the PMPS particles and then when heated the $[AuCl_4]^-$ ions are deposited onto the surface producing a film around the particles

4.6.12 Group 12: Zinc, cadmium and mercury

Table 4.14 Results for the PMPS particle sorption of Group 12 elements (mg/g).

Solvent	Temp ^{o}C	Zn	$CdCl_2$	$CdSO_4$	$HgCl_2$	$HgNO_3$
H_2O	4	46.32	31.56	9.72	193.12	
H_2O	25	59.10	36.38	44.18	224.82	
H_2O	50	63.55	44.63	19.90	240.60	
0.1M HCl	4	19.41	21.30	25.01	170.43	
0.1M HCl	25	19.65	49.13	23.08	166.13	
0.1M HCl	50	62.88	50.19	37.40	174.30	
conc HCl	4	63.69	41.86	46.43	107.39	
conc HCl	25	58.84	47.40	59.20	116.20	
conc HCl	50	70.35	75.98	71.31	131.14	140.35

Table 4.14 shows the zinc and cadmium samples to be comparable with the other transitional metals. The cadmium chloride does not appear to differ greatly from the cadmium sulfate. The PMPS particles do appear to favour mercury, producing excellent sorption properties for all of the samples with the water as the solvent at 50^{o}C producing the highest result.

4.6.13 Group 13: Boron, aluminium, gallium, indium and thallium

Table 4.15 Results for the PMPS particle sorption of Group 13 elements (mg/g).

		Al^{3+}							
Solvent	Temp ^{o}C	Cl^{2-}	$(SO_4)^{2-}$	Ga	In	Tl	B	Solvent	Temp ^{o}C
H_2O	4	8.73	1.56	5.25	16.79		2.50	0.1M HCl	25
H_2O	25	7.39	5.55	8.42	8.80	69.28	11.87	0.1M HCl	50
H_2O	50	8.21	5.33	18.48	22.48	106.49	1.10	0.1M H_3BO_3	4
0.1M HCl	4	9.19	2.29	6.91	15.23	75.89	1.67	0.1M H_3BO_3	20
0.1M HCl	25	1.70	3.36	20.04	7.20	51.68	1.68	0.1M H_3BO_3	50
0.1M HCl	50	9.67	5.47	22.69	8.46	55.12	3.62	0.5M H_3BO_3	22
conc HCl	4	6.17	2.66	42.90	26.42	4.15	7.88	0.5M H_3BO_3	50
conc HCl	25	6.92	5.47	77.85	23.69	4.61	37.02	1M H_3BO_3	28
conc HCl	50	9.49	8.05	71.56	35.75	7.32	9.13	1M H_3BO_3	50

Aluminium failed to sorb in any great quantities using either chloride or sulfate salts. The boron results were also very low except for the concentrated acid at room temperature. The indium results were slightly higher. The gallium and thallium seem to have opposite trends in the fact that gallium sorption increases as concentration and temperature increase, as expected in normal chemical reactions, however the thallium has the reverse trend, favouring H_2O as the solvent. There was no thallium sample prepared at 4^{o}C in H_2O because the thallium crashed out of solution when placed in ice to cool. The reason that the thallium sampled decrease in sorption is probably because the thallium samples in acid were prepared using sulfuric

acid. The concentrated samples required washing to remove surplus solvent so that the PMPS particles could dry thus probably washing away the thallium ions in the process.

4.6.14 Group 14: Germanium, tin and lead

Table 4.16 Results for the PMPS particle sorption of Group 14 elements (mg/g).

				Pb	
Solvent	Temp ^{o}C	Ge	Sn	Cl^-	CH_3COO^-
H_2O	4			1.34	33.33
H_2O	25	0.00		3.99	91.58
H_2O	50			8.98	106.00
0.1M HCl	4			1.05	34.05
0.1M HCl	25	0.00		0.77	85.63
0.1M HCl	50			1.52	113.31
conc HCl	4		65.44	29.02	16.68
conc HCl	25	0.00	87.50	29.99	26.96
conc HCl	50		93.56	124.55	23.51

The germanium salt used to prepare the samples was extremely insoluble which is probably why the results were zero. The tin samples that were able to be prepared seemed to sorb quite effectively. The lead samples proved to be very erratic with the lead acetate showing a preference for room temperature or hot water and dilute acid, in preference to cold or concentrated solvents. Initial observation of the lead chloride results would suggest that the solid particle analysis was unreliable in analysing PMPS particles until it was found that the very last result reported (conc HCl at 50^{o}C) was extremely high. To confirm this data a second set of results was obtained (Fig 4.4) clearly showing that lead chloride sorption has a strong preference for hot concentrated acid.

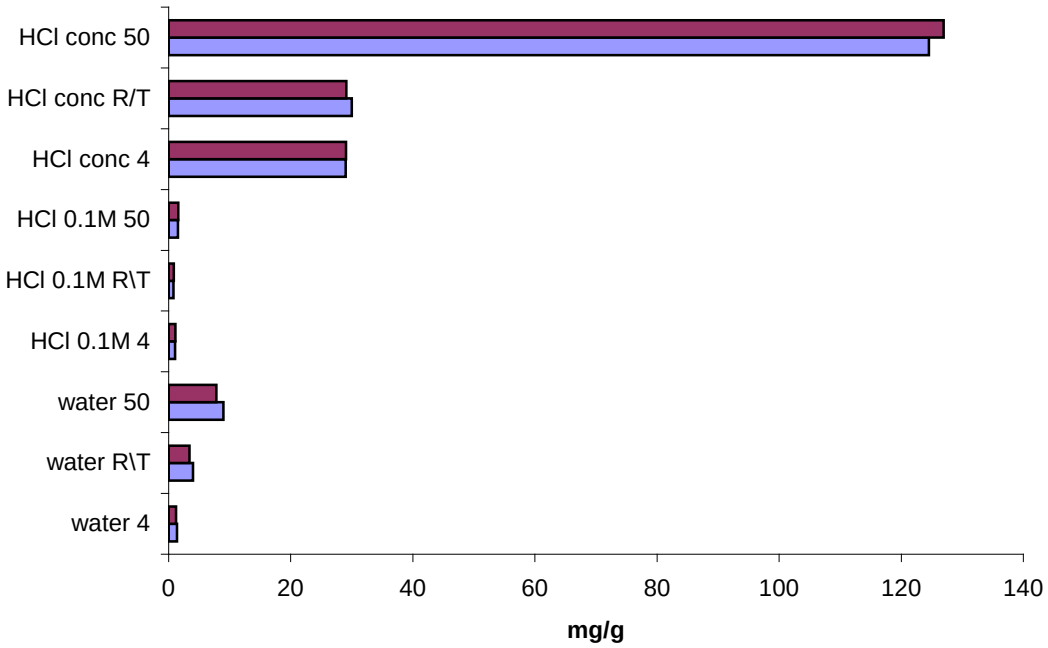

Figure 4.4 Duplicate results of solid particle analysis of PMPS particles containing lead chloride.

4.6.15 Group 15: Phosphorous, arsenic, antimony and bismuth

Table 4.17 Results for the PMPS particle sorption of Group 15 elements (mg/g).

Temp ^{o}C	Solvent	As	Sb	Solvent	Bi_2O_3	Solvent	P
4	H_2O	2.32	0.43			H_3PO_4 5M	53.77
25	H_2O	2.45	0.31			H_3PO_4 5M	108.73
50	H_2O	16.23	0.75			H_3PO_4 5M	74.04
4	0.1M HCl	10.29	27.44	5M HCl	13.18	H_3PO_4 10M	81.80
25	0.1M HCl	34.44	46.15	5M HCl	11.65	H_3PO_4 10M	164.93
50	0.1M HCl	12.58	44.07	5M HCl	14.18	H_3PO_4 10M	175.22
4	conc HCl	20.32	53.48	conc HCl	26.56	H_3PO_4 conc	40.82
25	conc HCl	55.38	96.20	conc HCl	23.69	H_3PO_4 conc	22.18
50	conc HCl	33.96	109.59	conc HCl	27.08	H_3PO_4 conc	45.46

The PMPS particles containing phosphorous (in the form of ammonium phosphate) gave a very high sorption rate compared to the rest of Group 15. There is no trend going down this group with phosphorous and antimony sorbing well above average whereas the arsenic and bismuth oxide show similar results, it was surprising

that the bismuth choride did not sorb into the PMPS particles. The arsenic, antimony and bismuth proved to be extremely difficult to dissolve in solution. The arsenic and antimony samples tested in H_2O show that solubility in water is very poor. It was surprising to see that the antimony sorbed at such high concentrations in the concentrated acid, double the amount sorbed in the 4 molar acid.

4.6.16 Group 16: Sulfur and selenium

Table 4.18 Results for the PMPS particle sorption of Group 16 elements (mg/g).

Solvent	Temp ^oC	S	Se
H_2O	4	18.20	86.16
H_2O	25	15.40	67.83
H_2O	50	11.70	109.93
0.1M HCl	4	24.30	79.02
0.1M HCl	25	14.80	70.23
0.1M HCl	50	23.50	75.94
conc HCl	4	4.60	184.48
conc HCl	25	8.20	244.74
conc HCl	50	10.50	285.47

The sulfur samples were disappointingly low. This could possible be down to the fact that the samples were analysed on the ICP as solid particles. If the particles were not of a fine enough quality, ie they were sticking together; they would not pass through the nebulizer and/or spray chamber for a reliable result to be obtained. The selenium samples did exceedingly well. The initial samples were acid digested. These same samples were redigested using the microwave technique and similar results were obtained. To confirm the validity of these high results a completely new batch of samples were prepared and acid digested using a fresh bottle of selenium oxide. Figure 4.5 below confirms that using fresh salts produces even higher results than previously obtained.

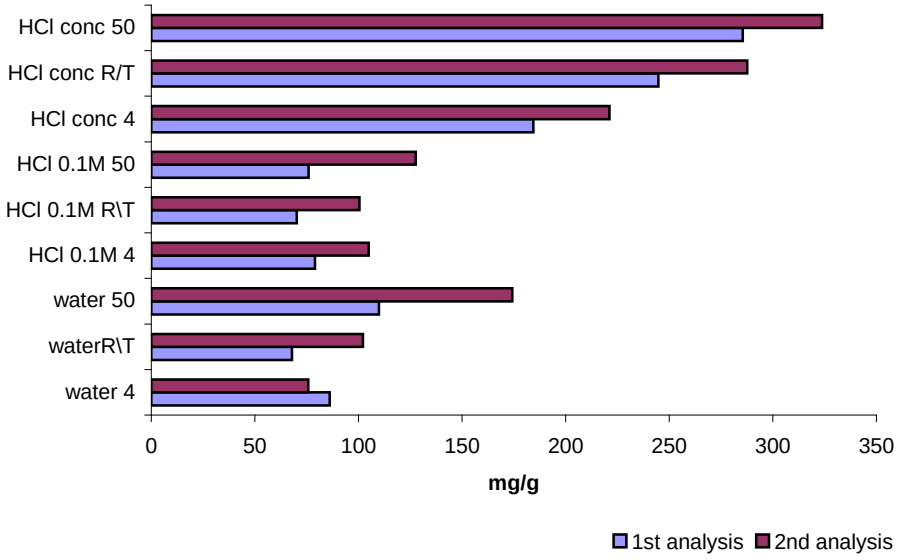

Figure 4.5 A comparison of two sets of data for PMPS-selenium sorption .

The compound selenium dioxide used for sorption into the PMPS particles structurally consists of a syndiotactic polymeric chain of alternating selenium and oxygen atoms, each selenium atom also bears a terminal oxide group (Fig. 4.6 a) (Cotton and Wilkinson, 1962).

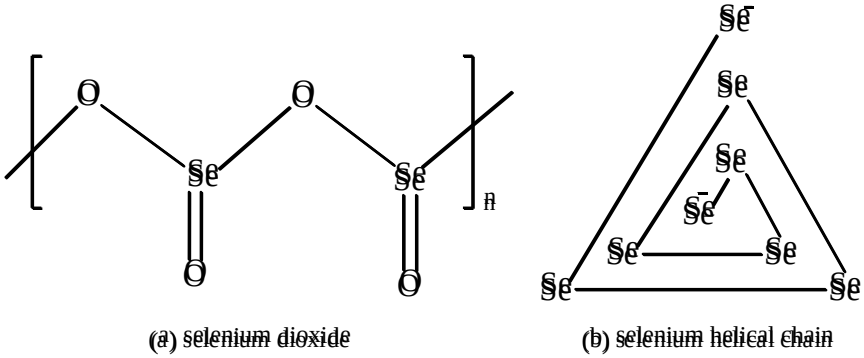

Figure 4.6 Chemical structures of selenium.

The selenium dioxide dissolves in water to form selenous acid (H_2SeO_3).

$$SeO_2 \rightarrow H_2SeO_3$$
$$H_2SeO_3 \rightleftharpoons H^+ + HSeO_3^-$$
$$HSeO_3^- \rightleftharpoons H^+ + SeO_3^{2-}$$

The addition of hydrochloric acid would have produced free selenium atoms

$$H_2SeO_3 + 4H^+ + 4e^- \rightleftharpoons Se$$

Selenim atoms are capable of forming infinite unbranched helical chains with a weak, metallic interaction between atoms in the adjoining chains (Fig. 4.6 b). It is possible that the H^+ ions on the selenious acid co-ordinate with the O^- ions on the PMPS particles leaving free O^- ions on the selenium molecules which could then either co-ordinate with the N^+ on the PMPS particles or rejoin another SeO_2 molecule forming chains of SeO_2, or further oxidation could have formed helical selenium chains, which attach to the PMPS particles. The chain formation would explain the high adsoption data found for the selenium.

4.6.17 The Lanthanides: Lanthanum, cerium, europium and ytterbium

Table 4.19 Results for the PMPS particle sorption of the lanthanides (mg/g).

Solvent	Temp ^oC	La	Ce	Eu	Yb
H_2O	4	1.36	19.49	19.26	34.97
H_2O	25	3.11	16.83	22.65	31.31
H_2O	50	1.81	9.78	22.63	32.50
0.1M HCl	4	1.98	14.31	29.86	25.71
0.1M HCl	25	1.50	12.75	5.87	28.36
0.1M HCl	50	2.53	21.54	37.36	24.97
conc HCl	4	6.65	9.46	34.74	30.72
conc HCl	25	2.84	8.51	25.52	36.35
conc HCl	50	3.51	21.93	24.93	43.66

Considering the similarity of the elemental salts i.e. all being trichlorides, lanthanum and cerium being heptahydrates and europium and ytterbium being hexahydrates, and having similar molecular masses it would be expected that the adsorption data would be comparable. There is an obvious trend of increase in adsorption along the lanthanide period.

4.7 Discussion of sorption results

Fifty-four elements were separately sorbed into PMPS particles, forty-three of which were investigated as chloride salts. This was done to limit interference from multiple spectator ions in an attempt to establish some form of pattern to explain the vast spread of data collected. On eleven occasions this was not possible either because the chloride salt was insoluble, hazardous or was unobtainable for various reasons. The elements where chloride salts were not available for sorption are listed in Table 4.20 along with the alternative compounds that were used instead.

Table 4.20 Elements that were not sorbed into PMPS particles as chloride salts.

Titanium	$Ti_2(SO_4)_3$ (liquid)
Tungsten	$(NH_4)_{10}W_{12}O_{41}.5H_2O$
Silver	$AgNO_3$
Boron	H_3BO_3
Gallium	$Ga(NO_3)_3.xH_2O$
Thallium	Tl_2SO_4
Germanium	GeO_2
Phosphorous	$NH_4H_2PO_4$
Arsenic	As_2O_3
Sulfur	$(NH_4)_2SO_4$
Selenium	SeO_2

Table 4.21 A record of the highest results found for each chloride element (except when unavailable) and optimum conditions necessary to obtain these results. The data is reported in mg/g and then converted into mmol/g and also the average ratio of each PMPS particle repeat unit per elemental atoms sorbed (calculations in Appendix 3), in order to establish any trend or pattern in the sorption data.

Element	Form	Solvent	Temp	mg/g	mmol/g	Ratio
Li	LiCl	H_2O	R/T	9.51	1.38	1: 0.08
B	1M H_3BO_3	H_2O	28	37.94	3.51	1: 0.33
Na	NaCl	0.1M HCl	50	45.47	1.98	1: 0.40
Mg	$MgCl_2.6H_2O$	H_2O	50	7.35	0.30	1: 0.06
Al	$AlCl_3.6H_2O$	HCl	50	9.49	0.35	1: 0.08
P	$NH_4H_2PO_4$	10M H_3PO_4	50	175.22	5.66	1: 1.54
S	$(NH_4)_2SO_4$	0.1M HCl	4	24.30	0.76	1: 0.21
K	KCl	0.1M HCl	50	44.25	1.13	1: 0.39
Ca	$CaCl_2.2H_2O$	H_2O	R/T	25.79	0.64	1: 0.23
Sc	$ScCl_3.xH_2O$	H_2O	50	16.16	0.36	1: 0.14
Ti	$Ti_2(SO_4)_3$	H_2SO_4	50	88.47	1.85	1: 0.78
V	VCl_3	H_2O	4	26.39	0.52	1: 0.23
Cr	$CrCl_3.6H_2O$	0.1M HCl	R/T	14.78	0.28	1: 0.13
Mn	$MnCl_2.4H_2O$	HCl	4	21.55	0.39	1: 0.19
Fe	$FeCl_3$	HCl	50	71.49	1.28	1: 0.63
Co	$CoCl_2.6H_2O$	HCl	4	31.78	0.54	1: 0.28
Ni	$NiCl_2.6H_2O$	HCl	R/T	25.77	0.44	1: 0.23
Cu	$CuCl_2.2H_2O$	HCl	50	58.56	0.92	1: 0.52
Zn	$ZnCl_2$	HCl	50	70.35	1.08	1: 0.62
Ga	$Ga(NO_3)_3.xH_2O$	HCl	R/T	77.85	1.12	1: 0.69
Ge	GeO_2	-	-	0.00	0.00	1: 0.00
As	As_2O_3	HCl	R/T	55.38	0.74	1: 0.49
Se	SeO_2	HCl	50	293.28	3.71	1: 2.59
Rb	RbCl	0.1M HCl	50	66.58	0.78	1: 0.74
Sr	$SrCl_2.6H_2O$	H_2O	50	26.04	0.30	1: 0.23
Y	$YCl_3.6H_2O$	H_2O	R/T	15.15	0.17	1: 0.13
Zr	$ZrCl_4$	HCl	50	41.31	0.45	1: 0.36
Nb	$NbCl_3$	HCl	R/T	53.57	0.58	1: 0.47
Mo	$MoCl_3$	HCl	50	39.98	0.42	1: 0.35
Ru	$RuCl_3.H_2O$	HCl	50	34.38	0.34	1: 0.30
Rh	$RhCl_3$	0.1M HCl	R/T	29.50	0.29	1: 0.26
Pd	$PdCl_2$	H_2O	50	73.84	0.69	1: 0.65
Ag	$AgNO_3$	H_2O	50	130.15	1.21	1: 1.15
Cd	$CdCl_2.xH_2O$	HCl	50	75.98	0.68	1: 0.67
In	$InCl_3.4H_2O$	HCl	50	35.75	0.31	1: 0.32
Sn	$SnCl_2.2H_2O$	HCl	50	93.56	0.79	1: 0.83
Sb	$SbCl_3$	HCl	50	109.59	0.90	1: 0.97
Cs	CsCl	HCl	4	4.52	0.03	1: 0.04
Ba	$BaCl.2H_2O$	H_2O	50	45.26	0.33	1: 0.40
La	$LaCl_3.7H_2O$	HCl	4	6.65	0.05	1: 0.06
Ce	$CeCl_3.7H_2O$	HCl	50	21.93	0.16	1: 0.19
Eu	$EuCl_3.6H_2O$	0.1M HCl	50	37.36	0.25	1: 0.26
Yb	$YbCl_3.6H_2O$	HCl	50	43.66	0.25	1: 0.38
Hf	$HfCl_4$	H_2O	50	44.54	0.25	1: 0.39
Ta	$TaCl_5$	HCl	4	19.90	0.11	1: 0.18
W	$(NH_4)_{10}W_{12}O_{41}.5H_2O$	H_2O	50	49.87	0.27	1: 0.44
Re	$ReCl_5$	HCl	50	107.34	0.58	1: 0.95
Ir	$IrCl_3.xH_2O$	H_2O	R/T	41.88	0.22	1: 0.37
Pt	$PtCl_4$	HCl	50	58.32	0.30	1: 0.51
Au	$HAuCl_4.3H_2O$	0.1M HCl	50	318.74	1.62	1: 2.81
Hg	$HgCl_3$	H_2O	50	240.60	1.20	1: 2.12
Tl	Tl_2SO_4	H_2O	50	106.49	0.52	1: 0.94
Pb	$PbCl_2$	HCl	50	124.55	0.60	1: 1.10
Bi	$BiCl_3$	HCl	50	0.00	0.00	1: 0.00

Analysis of Table 4.21 shows that the optimum conditions to use for the majority of the elements are concentrated acid at 50^{o}C. As stated in section 1.3 if the adsorbing particles attract one another, then they tend to cluster together in islands, and growth occurs at the borders, then when they are heated enough they undergo order-disorder transitions until the thermal motion of the ions overcomes the particle-particle interactions allowing the surface to become saturated (Atkins, 1998), thus the heated samples produce higher adsorption results. The PMPS particles could have absorption taking place inside the particles as well as adsorption onto its surface, making them act like micro sponges. As mentioned in section 1.11.2 the structure of PMPS particles is similar to cryptands because they both contain oxygen and lone pair nitrogen atoms that can co-ordinate with ions in solution. However the huge difference between a cryptand and PMPS particles is that cryptands are specific towards hard acids, particularly NH_4^+, lanthanoids, alkali metals, and alkaline earth metals, whereas PMPS particles are able to sorb almost every element in the periodical table whether neutral, ionic or cationic but they are also very specific towards the soft acid and base elements, which is the opposite to cryptands.

The data from Table 4.21 has been transferred onto period tables and colour coded for a visual display to aid the determination of any trends or patterns. From Table 4.22 below it can be seen that the alkali metals, the heavier transiton metals and the p-block elements absorbed the highest amount in mmol per kilogram of beads but there is no obvious trend visible. Tables 4.23 and 4.24 report the data in milligrams of element per kilogram of PMPS particles and average ratio of PMPS molecule repeat unit per elemental atoms sorbed respectively. It is easy to see that both these tables show the same spread of data indicating the same pattern of sorption. It is evident that Groups 11 –16 have a preference to absorb into the PMPS particles,

particularly the heavy elements that are toxic to man and also classed as soft acids and soft bases.

Table 4.22 Spread of data for the highest sorption of each element into the PMPS particles. Results are reported in millimoles of ions sorbed per gram of PMPS particles.

H																	He
Li 1.38	Be											**B 3.51**	C	N	O	F	Ne
Na 1.98	**Mg 0.30**											**Al 0.36**	Si	**P 5.66**	**S 0.76**	Cl	Ar
K 1.13	**Ca 0.64**	**Sc 0.36**	**Ti 1.85**	**V 0.52**	**Cr 0.28**	**Mn 0.39**	**Fe 1.28**	**Co 0.54**	**Ni 0.44**	**Cu 0.92**	**Zn 1.08**	**Ga 1.12**	**Ge 0**	**As 0.74**	**Se 3.62**	Br	Kr
Rb 0.78	**Sr 0.30**	**Y 0.17**	**Zr 0.45**	**Nb 0.58**	**Mo 0.42**	Tc	**Ru 0.34**	**Rh 0.29**	**Pd 0.69**	**Ag 1.21**	**Cd 0.68**	**In 0.31**	**Sn 0.79**	**Sb 0.90**	Te	I	Xe
Cs 0.03	**Ba 0.33**	*	**Hf 0.25**	**Ta 0.11**	**W 0.27**	**Re 0.58**	Os	**Ir 0.22**	**Pt 0.30**	**Au 1.62**	**Hg 1.20**	**Tl 0.52**	**Pb 0.60**	**Bi 0**	Po	At	Rn
Fr	Ra	**	Rf	Ha	Sg	Ns	Hs	Mt	Uun	Uuu	Uub		Uuq		Uuh		Uuo

*	**La 0.05**	**Ce 0.16**	Pr	Nd	Pm	Sm	**Eu 0.25**	Gd	Tb	Dy	Ho	Er	Tm	**Yb 0.25**	Lu
**	Ac	Th	Pa	U	Np	Pu	Am	Cm	Bk	Cf	Es	Fm	Md	No	Lr

Key elements not tested | 0 - 0.4 | 0.5 - 0.9 | > 1

Table 4.23 Spread of data for the highest sorption of each element into the PMPS particles. Results are reported in milligrams of ions sorbed per gram of PMPS particles.

H																	He
Li 10	Be											**B 38**	C	N	O	F	Ne
Na 46	**Mg 7**											**Al 10**	Si	**P 175**	**S 24**	Cl	Ar
K 44	**Ca 26**	**Sc 16**	**Ti 88**	**V 26**	**Cr 15**	**Mn 22**	**Fe 72**	**Co 32**	**Ni 26**	**Cu 59**	**Zn 70**	**Ga 78**	**Ge 0**	**As 55**	**Se 285**	Br	Kr
Rb 67	**Sr 26**	**Y 15**	**Zr 41**	**Nb 54**	**Mo 40**	Tc	**Ru 34**	**Rh 30**	**Pd 74**	**Ag 130**	**Cd 76**	**In 36**	**Sn 94**	**Sb 110**	Te	I	Xe
Cs 5	**Ba 45**	*	**Hf 45**	**Ta 20**	**W 50**	**Re 107**	Os	**Ir 42**	**Pt 58**	**Au 319**	**Hg 241**	**Tl 107**	**Pb 125**	**Bi 0**	Po	At	Rn
Fr	Ra	**	Rf	Db	Sg	Bh	Hs	Mt	Ds	Rg	Uub	Uut	Uuq	Uup	Uuh	Uus	Uuo

*	**La 7**	**Ce 22**	Pr	Nd	Pm	Sm	**Eu 37**	Gd	Tb	Dy	Ho	Er	Tm	**Yb 44**	Lu
**	Ac	Th	Pa	U	Np	Pu	Am	Cm	Bk	Cf	Es	Fm	Md	No	Lr

Key elements not tested | 0 - 49 | 50 - 99 | > 100

Table 4.24 Spread of data for the highest sorption of each element into the PMPS particles. Results are reported in average ratio of ions sorbed per PMPS repeat unit.

H																	He
Li 0.08	Be											**B 0.33**	C	N	O	F	Ne
Na 0.40	**Mg 0.06**											**Al 0.08**	Si	**P 1.54**	**S 0.21**	Cl	Ar
K 0.39	**Ca 0.23**	**Sc 0.14**	**Ti 0.78**	**V 0.23**	**Cr 0.13**	**Mn 0.19**	**Fe 0.63**	**Co 0.28**	**Ni 0.23**	**Cu 0.52**	**Zn 0.62**	**Ga 0.69**	**Ge 0**	**As 0.49**	**Se 2.52**	Br	Kr
Rb 0.74	**Sr 0.23**	**Y 0.13**	**Zr 0.36**	**Nb 0.47**	**Mo 0.35**	Tc	**Ru 0.30**	**Rh 0.26**	**Pd 0.65**	**Ag 1.15**	**Cd 0.68**	**In 0.32**	**Sn 0.83**	**Sb 0.97**	Te	I	Xe
Cs 0.04	**Ba 0.40**	*	**Hf 0.39**	**Ta 0.18**	**W 0.44**	**Re 0.95**	Os	**Ir 0.37**	**Pt 0.51**	**Au 2.81**	**Hg 2.12**	**Tl 0.94**	**Pb 1.10**	**Bi 0**	Po	At	Rn
Fr	Ra	**	Rf	Ha	Sg	Ns	Hs	Mt	Uun	Uuu	Uub		Uuq		Uuh		Uuo

*	**La 0.06**	**Ce 0.19**	Pr	Nd	Pm	Sm	**Eu 0.26**	Gd	Tb	Dy	Ho	Er	Tm	**Yb 0.38**	Lu
**	Ac	Th	Pa	U	Np	Pu	Am	Cm	Bk	Cf	Es	Fm	Md	No	Lr

Key elements not tested | 0 - 0.4 | 0.5 - 0.9 | > 1

A comparison to Rayner-Canham's table of soft acids from section 1.4 shows a very similar pattern to the results reported in Tables 4.23 and 4.24.

Table 4.25 A modified display of Table 1.3 to include the elements P, S, and Se that form soft bases as well as the hard, borderline and soft acids.

H																	He
Li	Be											**B**	C	N	O	F	Ne
Na	**Mg**											**Al**	Si	**P**	**S**	Cl	Ar
K	**Ca**	**Sc**	**Ti**	**V**	**Cr**	**Mn**	**Fe**	**Co**	**Ni**	**Cu**	**Zn**	**Ga**	**Ge**	**As**	**Se**	Br	Kr
Rb	**Sr**	**Y**	**Zr**	**Nb**	**Mo**	Tc	**Ru**	**Rh**	**Pd**	**Ag**	**Cd**	**In**	**Sn**	**Sb**	Te	I	Xe
Cs	**Ba**	*	**Hf**	**Ta**	**W**	**Re**	Os	**Ir**	**Pt**	**Au**	**Hg**	**Tl**	**Pb**	**Bi**	Po	At	Rn
Fr	Ra	**	Rf	Db	Sg	Bh	Hs	Mt	Ds	Rg	Uub	Uut	Uuq	Uup	Uuh	Uus	Uuo

*	**La**	**Ce**	Pr	Nd	Pm	Sm	**Eu**	Gd	Tb	Dy	Ho	Er	Tm	**Yb**	Lu
**	Ac	Th	Pa	U	Np	Pu	Am	Cm	Bk	Cf	Es	Fm	Md	No	Lr

Key Hard | Borderline | Soft | Borderline/Hard | Borderline/Soft

4.7.1 Analysis of mixed ion compounds

A further study to aid the explanation of the sorption of ions by PMPS particles was carried out which involved trials of PMPS particles soaked in equimolar amounts of mixed compounds containing hard, borderline or soft ions, which were then prepared and analysed as in section 4.2 to confirm that PMPS particles do preferentially select soft ions for adsorption. The first comparison undertaken involved the mixture of a soft acid and a borderline acid. To do this zinc, being a borderline acid was chosen to mix with silver, a soft acid. However it was not possible to use the zinc chloride due to the precipitation of insoluble silver chloride, no zinc nitrate salts were available at the time so it was necessary to use zinc and silver sulfate salts, unfortunately the silver sulfate salts do not absorb as well into PMPS particles as the nitrate salt so the performance of the silver was compromised. To prepare the mixed solution of zinc and silver ions it was necessary to first dissolve the silver sufate in concentrated sulfuric acid since it does not dissolve in H_2O or dilute acid and then dissolve the zinc sulfate separately in H_2O because it does not dissolve in dilute or concentrated acid. The two solutions were then slowly mixed together and the final concentration of the acid calculated. The results in Table 4.26 do however clearly show that PMPS particles have a preference for silver over zinc.

Table 4.26 Results for PMPS- zinc/silver sulfate mixed ion samples.

Concentration	Solvent	Temp ^oC	Mixed ions	
0.04M	8M H_2SO_4	50	$ZnSO_4$	$AgSO_4$
			0.01 mol/L	0.2 mol/L

The zinc/silver analysis was repeated twice more using zinc nitrate and silver nitrate since the silver adsorption is exceedingly high using nitrate salts. The first repeat was done using 0.1 molar solutions. The second repeat was done using a more concentrated solution of 0.5 molar. The individual salts were also tested using the

same 0.5 molar concentration solution as the mixed salts, to compare results. The samples were prepared by dissolving the salts in H_2O at room temperature.

Table 4.27 Results for PMPS- zinc/silver nitrate mixed ion samples (mol/L).

H_2O at room temp.	$Zn(NO_3)_3.6H_2O$	$AgNO_3$
0.5M Single solution	0.5	1.5
0.5M Mixed solution	0.6	1.5
0.1M Mixed solution	0.2	1.0

The results in Table 4.27 show that PMPS particles have a preference for silver over zinc in both concentrations of solution. It also shows that the PMPS particles absorbed the same amount of ions from each element whether in a mixed solution or single solutions. This could mean that if the PMPS particles acts like a molecular sieve it will have a number of cavities of varying sizes that are specific to ions of that size, i.e. one gram of PMPS particles contains 40> cavities specific to zinc nitrate whereas it has 170> cavities specific to silver nitrate, making the PMPS particles more selective towards the silver ions.

A borderline acid and a borderline/soft acid were compared next. Zinc and copper were used because copper is classed as borderline/soft acid depending on what it is co-ordinated with. The samples were prepared using 0.5 molar concentrations of salts dissolved in concentrated hydrochloric acid at 50^{o}C. This was because both zinc and copper ion sorption was highest using this process. The results in Table 4.28 below confirm that the borderline/soft copper adsorbed more than the zinc, although only marginally different it is still showing the preference towards soft acids.

Table 4.28 Results for PMPS- zinc/copper chloride mixed ion samples (mol/L).

Concentration	Solvent	Temp ^{o}C	Mixed ions	
0.5M	Conc HCl	50	$ZnCl_2$	$CuCl_2.2H_2O$
			0.8	0.1

The mixture of a soft acid with a hard acid was carried out using silver nitrate and sodium nitrate; 0.5 molar solutions of each salt were used but dissolved in H_2O at room temperature. It can be clearly seen in Table 4.29 that the soft silver ions have a much higher preference for adsorption than the smaller harder sodium ions.

Table 4.29 Results for PMPS- silver/sodium nitrate mixed ion samples (mol/L).

H_2O at room temp.	$AgNO_3$	$NaNO_3$
0.5M Mixed solution	1.0	0. 5

However the mixture of soft mercury ions with hard sodium ions did not follow the same pattern as the silver/sodium mixture. The samples were prepared using 0.5 moles of elemental salt dissolved in concentrated hydrochloric acid at 50^{o}C. It can be seen from Table 4.30 that the PMPS particles show preference towards the sodium ions and not the mercury ions.

Table 4.30 Results for PMPS- mercury/sodium chloride mixed ion samples (mol/L).

7M HCl at 50^{o}C	$HgCl_2$	NaCl
0.5M Mixed solution	0.1	0.9

A mixture of mercury and zinc ions also failed to give any conclusive evidence of PMPS particles showing preference towards the sorption of soft acids over hard or borderline acids. It can be seen from Table 4.31 that the PMPS particles show preference towards the borderline zinc ions over the mercury ions.

Table 4.31 Results for PMPS- mercury/zinc chloride mixed ion samples (mol/L).

Conc HCl at 50^{o}C	$HgCl_2$	$ZnCl_2$
0.5M Mixed solution	0.2	0.9

A mixture of mercury and selenium produced interesting results, bearing in mind that mercury is a soft acid and selenium is a soft base, it can be seen from Table 4.32 that the PMPS particles show an obvious preference towards selenium ions.

Table 4.32 Results for PMPS- mercury/selenium mixed ion samples (mol/L).

Conc HCl at 50°C	SeO_2	$HgCl_2$
0.5M Mixed solution	3.1	0.3

A mixture of selenium and zinc ions, soft base and borderline acid, (Table 4.33) and selenium and sodium ions, soft base and hard acid (Table 4.34) also confirms that PMPS particles are selective towards the soft base selenium ions.

Table 4.33 Results for PMPS- zinc/selenium mixed ion samples (mol/L).

Conc HCl at 50°C	SeO_2	$ZnCl_2$
Mixed solution	3.0	0.3

Table 4.34 Results for PMPS- sodium/selenium mixed ion samples (mol/L).

7M HCl at 50°C	SeO_2	NaCl
Mixed solution	2.3	0.8

A mixture of silver nitrate and selenium oxide was not possible because an insoluble product was formed when the two salts were mixed.

Due to the high cost of purchasing gold salts the solutions used for the sorption analysis were retained and used for the mixed ion analysis. Tables 4.35 and 4.36 below show that analysis of soft acid gold ions mixed with hard acid sodium and borderline acid zinc ions provide inconclusive evidence for PMPS particle selectivity towards soft acids. This could possibly be caused by a degredation of the gold solutions, thus preventing the gold ions from absorbing at their optimum, it was proved previously with repetitions of selenium and iron sorption that fresh salts perform more effectively than salts that have been stored over a period of time.

Table 4.35 Results for PMPS- gold/sodium chloride mixed ion samples (mol/L).

	$HAuCl_4.3H_2O$	NaCl
Mixed solution	0.1	0.4

Table 4.36 Results for PMPS- gold/zinc chloride mixed ion samples (mol/L).

	$HAuCl_4.3H_2O$	$ZnCl_2$
Mixed solution	0.1	0.7

4.8 Statistical analysis of results

To confirm this theory an indepth study of all of the data was undertaken using a statistical analysis programme called Minitab. A table containing all of the adsorption data can be found in Appendix 4. Analysis of Variation (ANOVA) was carried out for each element to determine whether the alteration of temperature and solvent concentration had any effect on adsorption. ANOVA for the whole of the data could not be done due to the variation of different solvents used. The results for the individual analysis, however, suggested that overall temperature or concentration changes were not significantly responsible for the amount of ions absorbed. When manufacturing a product it is necessary to produce products with minimum costs using easily obtainable and disposable or recyclable waste products. Therefore if a product can be made using water or dilute acid as the solvent and the reaction takes place at room temperature, even though productivity will be slightly less, it will be much cheaper to produce in the long run than a product that relies on concentrated acid, which is expensive and difficult to dispose of, and high temperatures that are difficult to maintain and are not energy efficient.

A variety of graphical data was produced to confirm that soft acids and bases sorb more effectively than hard acids. The first type of graph produced was a scatter plot because scatter plots are a visual display that shows any correlations between known variables. Correlations may be positive (rising), negative (falling), or null (uncorrelated). A line of best fit can be drawn in order to study the correlation between the variables if one exists. One of the most powerful aspects of a scatter plot,

however, is its ability to show nonlinear relationships between variables. Figure 4.7 shows a scatter plot of all of the sorption data in mg/g vs atomic number. It can clearly be seen that no line of best fit can be applied to this graph so the atomic number has no correlation to sorption. It can, however, clearly be seen that the green diamonds representing the soft acids or bases have a much higher sorption rate than the hard and borderline acids or bases. Incidently the hard acids (black circles) that have relatively high values were the hydroxide salts.

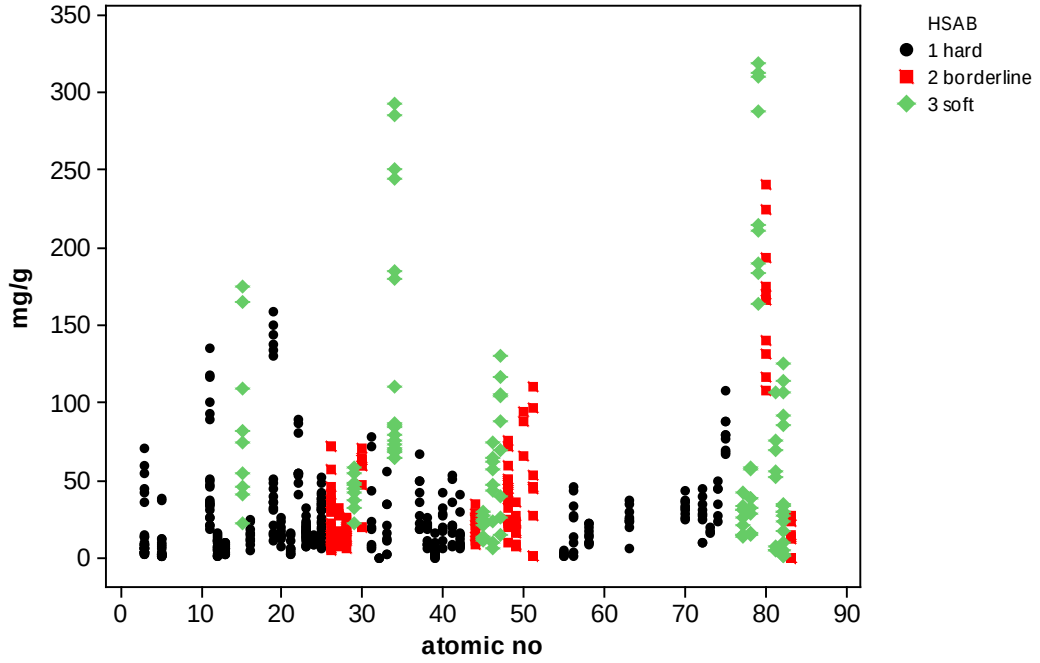

Figure 4.7 Scatterplot of mg/g vs atomic number for every sorption analysis.

Removing the hydroxide results from the scatterplot (Figure 4.8) and using only the optimum chloride results (except where chlorides were not available) shows a much clearer spread of data. It is clear that all of the elements that absorbed above 100 mg/g were actually soft acids or bases.

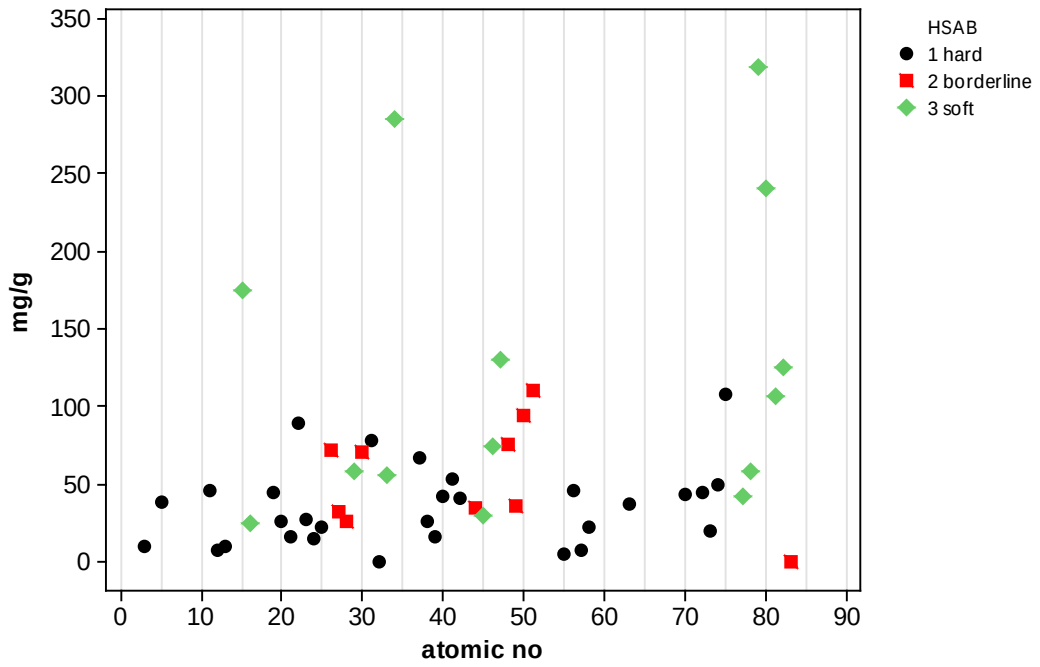

Figure 4.8 Scatterplot of mg/g vs atomic number for optimum chloride salts.

Empirical cumulative distribution function (cdf) graphs were generated, using the optimum sorption data. Figure 4.9 show plots of mg.g vs atomic number and mmol/g vs atomic number. These graphs evaluate and compare different sample distributions. The graph includes an empirical cumulative distribution function (ecdf) of the data, and a fitted normal cumulative distribution function (cdf). The stepped ecdf resembles a cumulative histogram without bars. Minitab plots the value of each observation against the percentage of values in the sample that are less than or equal to that value.

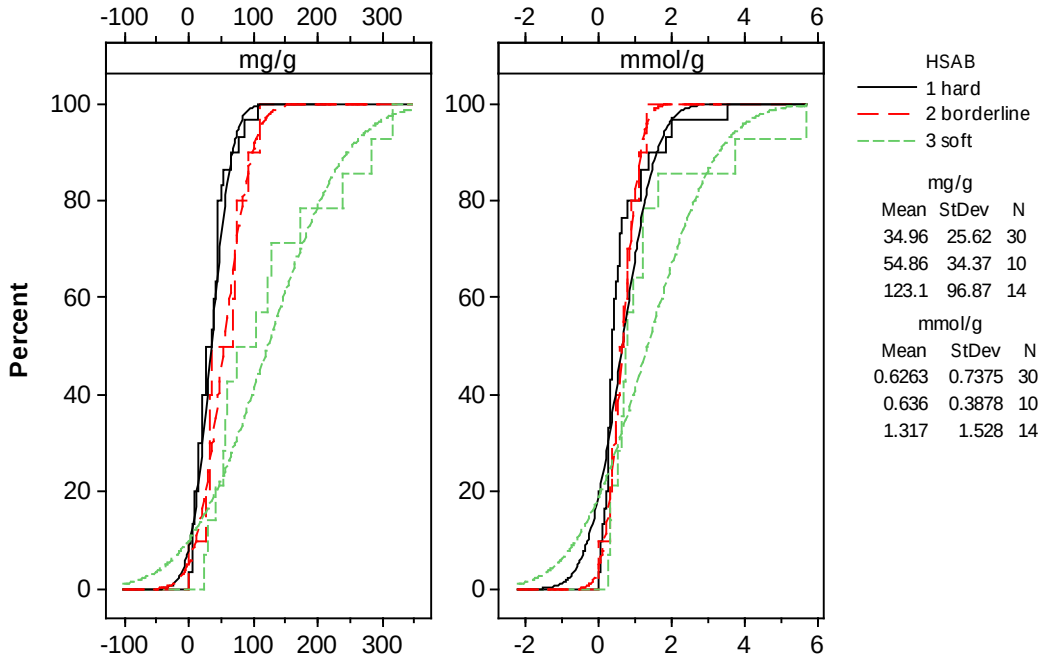

Figure 4.9 Empirical cumulative distribution function of mg/g and mmol/g.

From the above graphs it can be seen that the group of ions that achieved the highest percentage of sorption was the soft acids and bases. The data clearly gives the same evidence whether the analysis is carried out using mass or moles.

The final statistical analysis to be generated was interval plots of both mg/g vs HSAB and mmol/g vs HSAB. An interval plot consists of a bar showing 95% conficence intervals with a symbol somewhere along it representing the group mean. The use of individual standard deviations allows for the assessment of the group variability.

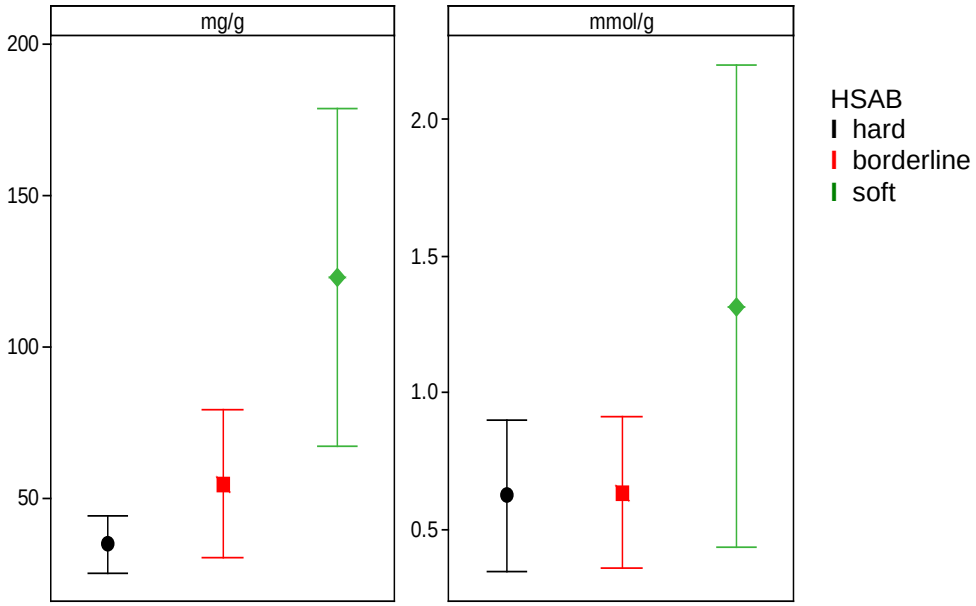

Figure 4.10 Interval plot of mg/g and mmol/g vs HSAB. Interval plots are especially useful for comparing groups by measuring the central tendency and variability of the data by calculating means with 95% confidence intervals.

It can be seen from Figure 4.10 that the means for the hard, borderline and soft acids and bases are relatively similar on both graphs, with the soft acids and bases being three times higher than both the hard and borderline acids and bases proving that PMPS particles do in fact have a preference for these types of ions. The outlying confidence intervals could be due to random errors and more research needs to be done to narrow down the confidence levels.

Chapter Five

Release Profile Studies

Results and Discussion

5.1 Introduction

The first section of this project has ascertained that PMPS particles are capable of sorbing many elements of the periodic table. The second part of this project focused on release profiles for a selection of these elements. It was necessary to investigate the release profiles of these elements to see whether the sorbed ions leached out of the PMPS particles, and if so how much and how fast, when subjected to an aqueous medium. The study focused on some of the elements that are commonly utilised in industry and also the soft acids and bases primarily because they had some of the highest sorption values and the fact that the majority are known to be particularly toxic to man.

5.2 Release methodology

Release experiments were performed by placing 100 milligrams of PMPS particles containing absorbed ions into an extraction thimble. Pure water was then dripped through the filter at a rate of approximately one drop per second. The equipment used to produce the release profiles can be seen below in Figure 5.1.

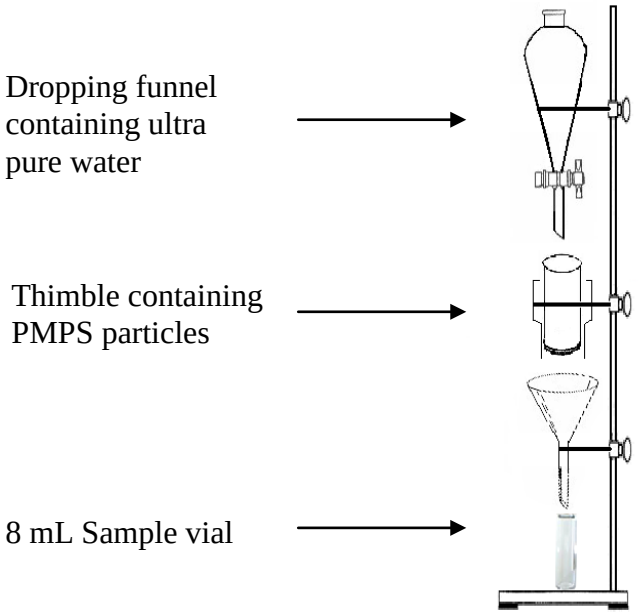

Figure 5.1 Release profile equipment set-up.

The filtrate was collected in aliquots of 2 mL over a time period of 1 hour and the samples were then subsequently analysed, using the same equipment as in the absorption analysis, to determine the percentage of element released, in relation to the amount initially absorbed into the PMPS particles, when subjected to an aqueous environment.

5.3 Release profile analysis

The release profiles of 11 elements were individually investigated (Table 5.1). The PMPS particle samples that were previously prepared for sorption analysis were used to create the release profiles, as the intial sorption capacities were already known. The samples with the optimum solvent and temperature conditions were chosen for the release profiles, except for the arsenic and cadmium samples.

Table 5.1 Percentage of ions leached from PMPS particles when individually introduced to aqueous conditons. The solvent and temperature columns show the original conditions that were used to prepare the elemental salts in readiness for sorbtion into the PMPS particles prior to the release profiles. (R/T = room temperature ~25^{o}C ± 10%). The amount of ions sorbed is the total volume of ions initially sorbed into the PMPS particles as stated in chapter four.

Elemental salt	Solvent	Temp ^{o}C	Amount of ions sorbed mg/g	% Ions Release
As_2O_3	H_2O	R/T	2.5	83.36
$CdCl_2.xH_2O$	H_2O	R/T	44.0	18.78
CsCl	Conc HCl	4^{o}C	4.5	21.53
$CuCl_2.2H_2O$	Conc HCl	50^{o}C	58. 6	65.92
$HAuCl_4.3H_2O$	H_2O	R/T	313.0	0.27
$PbCl_2$	Conc HCl	50^{o}C	124.0	58.45
$MnSO_4.4H_2O$	H_2O	4^{o}C	47.5	63.62
$HgCl_3$	H_2O	R/T	225.0	48.26
SeO_2	H_2O Conc HCl	R/T 50^{o}C	67.8 293.1	0.00 0.00
$AgNO_3$	H_2O	R/T	91.0	1.75
NaCl	0.1M HCl	50^{o}C	45.5	44.89

The samples chosen to create the release profiles for PMPS particles containing arsenic and cadmium were the ones prepared in water at room temperature. This was

because industrial use of these elements often requires a system that can remove ions out of aqueous solutions for water purification purposes.

It can be seen in Table 5.1 that the percentage of ions released from the PMPS particles varied enormously with arsenic having the highest percentage release down to selenium having zero release. To confirm the zero release for PMPS-Se particles two different samples were used for release profile analysis. The first PMPS-Se particle sample analysed was the one prepared using concentrated hydrochloric acid at 50^{o}C, because these conditions gave the highest adsorption data. This sample failed to release any of the absorbed ions even though the absorption rate was very high (293 mg/g). The analysis was repeated using the sample prepared in water at room temperature, just in case the selenium in the concentrated sample had formed a salt that was insoluble in water. This sample also failed to release any selenium ions whatsoever.

The gold and the silver ions were also retained very effectively by the PMPS particles. The combined release profiles for the PMPS particles containing gold and silver ions can be compared below in Figure 5.2. The results show that gold was only present in the first three 2 mL aliquots of water collected and that just over 0.25% of the 313 mg/g of sorbed gold was released during this time, thereafter no more gold was released during the remainder of the experiment, indicating that the PMPS particles still contained 312 mg/g of gold ions.

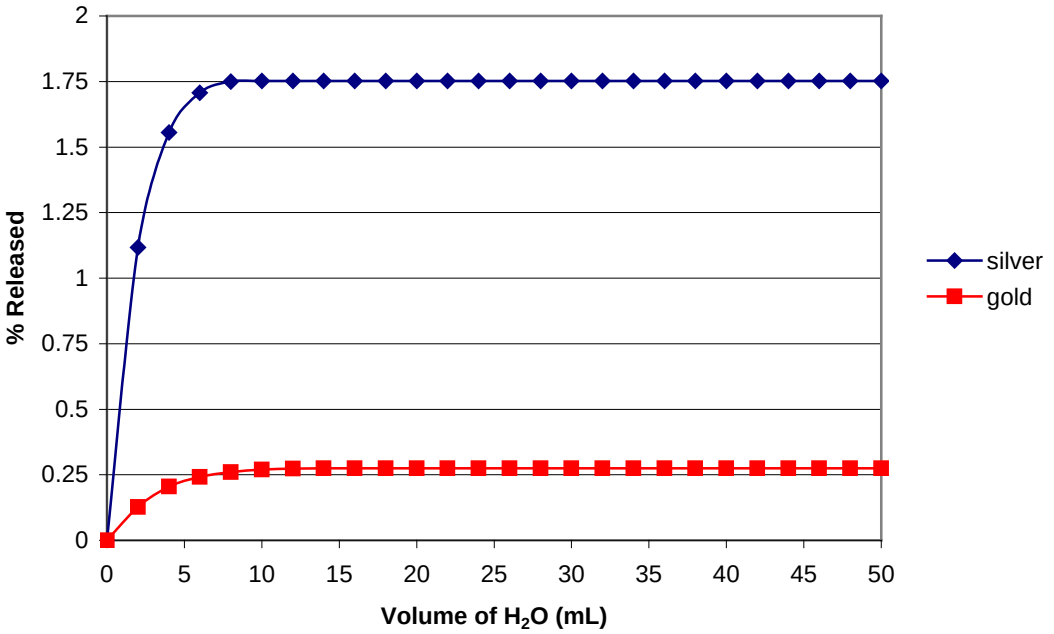

Figure 5.2 Release profiles of gold and silver ions from PMPS particles when water is dripped over the particles. The percentage released was calculated cumulatively.

The silver sample followed a similar trend with the silver ions once again only being released during the first three 2 mL aliquots. Although a slightly higher percentage of leaching, 1.75% of the 91 mg/g of ions sorbed, once the first three samples had been collected no more ions were present in any of the samples for the remainder of the experiment leaving 89 mg/g of silver ions still in the PMPS particles.

It can be seen in Figure 5.3 that the PMPS particles that contained cadmium sodium or caesium ions gave the next lowest release profiles. The release profile for PMPS particles containing cadmium was much slower than the previous ions tested taking seven 2mL aliquots of water before the PMPS particles stopped releasing ions. The total percentage of cadmium ions released was slightly higher. Even so at the end of the experiment only 19% of the 44 mg/g of cadmium ions that had initially been adsorbed were released back out of the PMPS particles, leaving 36 mg/g of cadmium ions still in the PMPS particles.

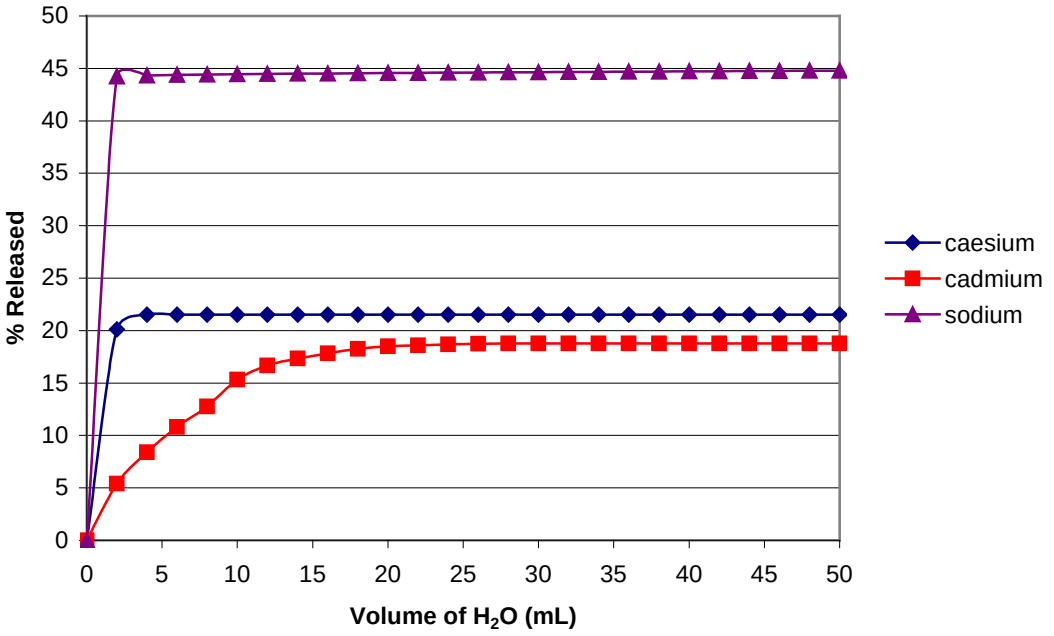

Figure 5.3 Release profile of cadmium sodium and caesium ions from PMPS particles when water is dripped over the particles. The percentage released was calculated cumulatively.

The caesium ions followed a similar profile to the PMPS particles containing gold or silver ions by quickly achieved a stable environment after the first 2 mL aliquot collection, but still only releasing marginally more ions than the cadmium, reaching a total of 21.5% release of the 4.5 mg/g of caesium ions initially sorbed leaving 3.5 mg/g of caesium ions still in the PMPS particles.

The sodium ions followed the same trend as the caesium by achieving a stable environment during the first 2 mL collection, after which no more ions were released but with a much higher percentage release of 44% of the initial 45.5 mg/g sorbed leaving only 25.5 mg/g of sodium ions in the PMPS particle. This could possibly be due to the sodium ions being easier to wash out of the PMPS pores because they are much smaller than the caesium ions.

Figure 5.4 gives the combined release profiles for the PMPS particles containing mercury or lead ions. The release of mercury ions was much slower than previous profiles but also much greater. Fifteen 2mL aliquots were collected over 30

minutes before a stable environment was achieved with 48% of the 225 mg/g of mercury initially sorbed leaching out of the PMPS particles leaving 117 mg/g of mercury ions still in the PMPS particles. The rate of leaching was fairly consistent and gradual, averaging 5 mg/L for every 2 mL sample collected.

The lead ions produced a similar profile to the mercury ions, also taking fifteen 2 mL aliquot collections before a stable environment was achieved. The percentage leached out was only 10% higher reaching a total of 58% of the 124 mg/g ions sorbed leaving 52 mg/g of ions still in the PMPS particles.

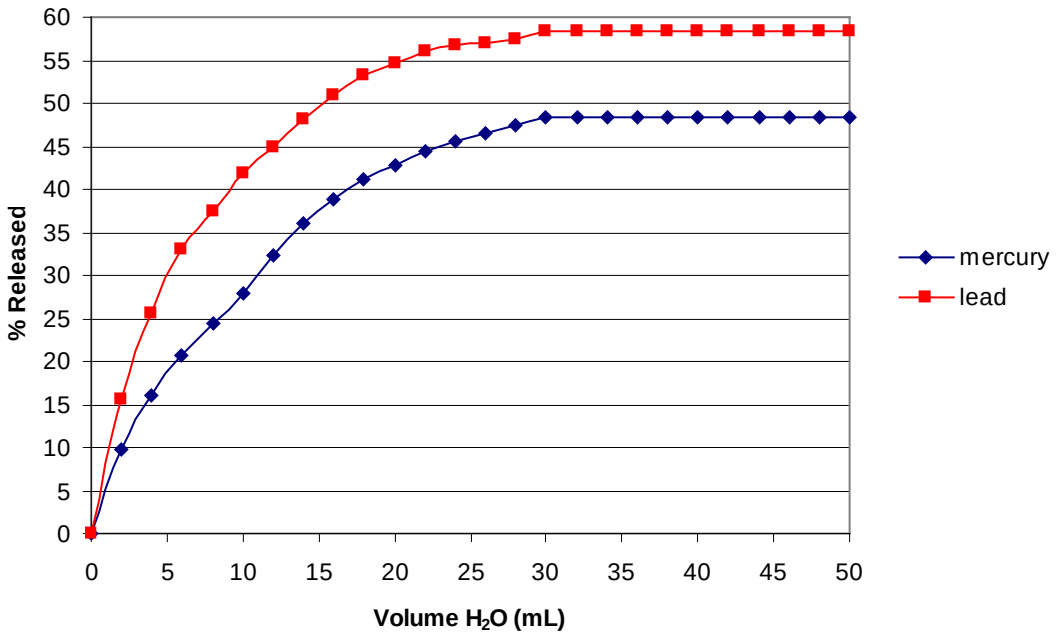

Figure 5.4 Release profile of mercury and lead ions from PMPS particles when water is dripped over the particles. The percentage released was calculated cumulatively.

Figure 5.5 gives the combined release profiles for the PMPS particles containing manganese or arsenic ions. The release profile for manganese ions follows a similar trend to the Group 1 elements, sodium and caesium, with a huge amount of ions being collected during the first 2 mL aliquot. The manganese however did not achieve a stable environment and continued to release ions at a steady rate during the

entire experiment time, suggesting that possibly a total 100% release could eventually have been reached if the reaction had been allowed to continue.

The PMPS particles containing asenic released the most ions reaching 83% of the original 2.5 mg/g of ions sorbed leaving a mere 0.4 mg/g of arsenic still contained in the PMPS particles.

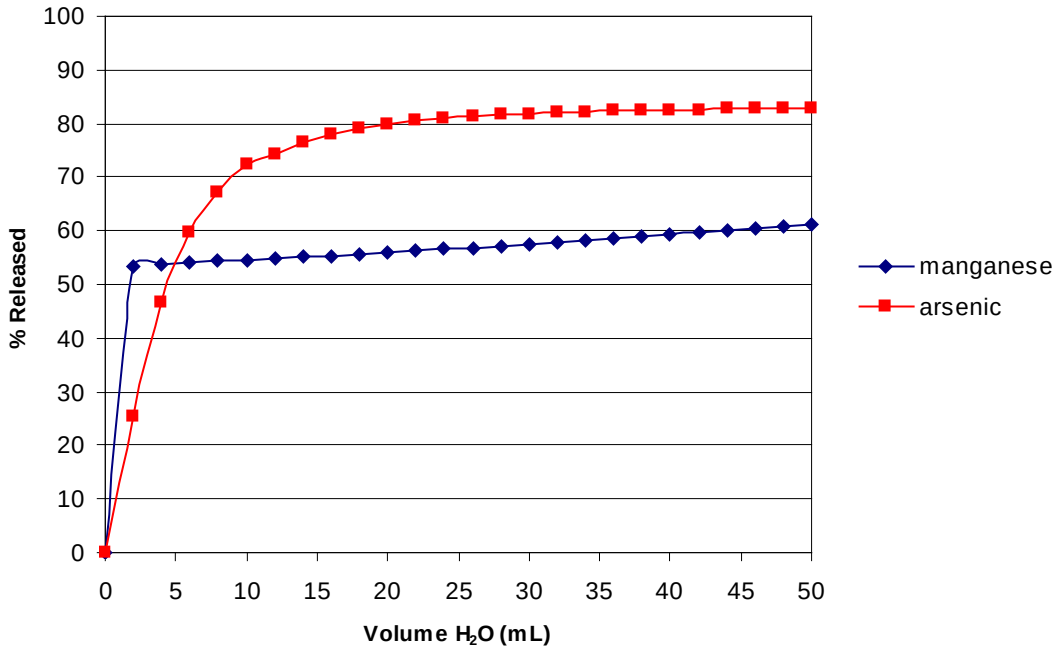

Figure 5.5 Release profile of manganese and arsenic ions from PMPS particles when water is dripped over the particles. The percentage released was calculated cumulatively.

Copper performed in a similar way to manganese reaching a release of 65% of the original 58.6 mg/g of copper ions sorbed into PMPS particles meaning that only 20 mg/g of copper was left in the PMPS particles. However the copper was still releasing after the total 50 mL volume had been collected. To see if any further leaching would take place the copper experiment was repeated using a refined method, which involved 1mL aliquots being taken for the first sixteen collections and then 8 mL aliquots thereafter until a total of 120 mL was collected over a period of 2.5 hours. Figure 5.6 shows that the copper did actually stop being released after the first hour (50mL) and that no more subsequent leaching occurred thereafter.

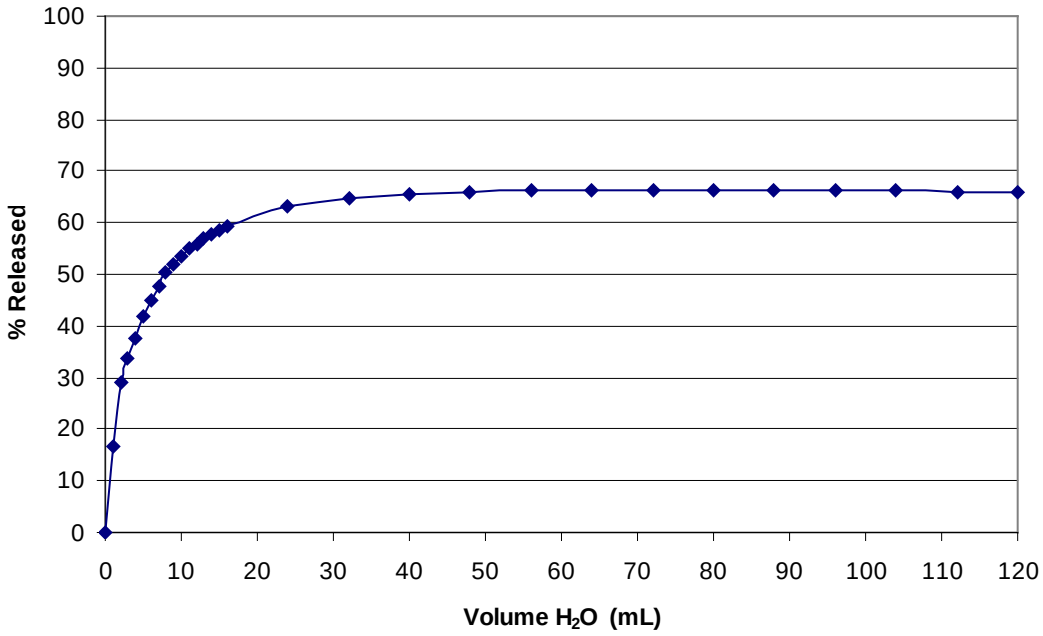

Figure 5.6 Release profile of copper ions from PMPS particles when water is dripped over the particles. The percentage released was calculated cumulatively.

5.4 Release profile summary

Grouping all of the release profiles together (Figure 5.7) shows that there appears to be two types of profile emerging. In the first type of profile the metallic ions leached out of the PMPS particles slowly over a period of time until equilibrium was reached whereupon no more ions were released. This happened for the arsenic, copper, lead, mercury, cadmium, silver and gold ions. In the second type of profile all of the free ions were released as soon as water was added, in the first 2 mL aliquot. This happened for the sodium and caesium ions. Manganese appeared to react this way as well, but then continues to release very slowly after the initial high release in the first 2 mL aliquot.

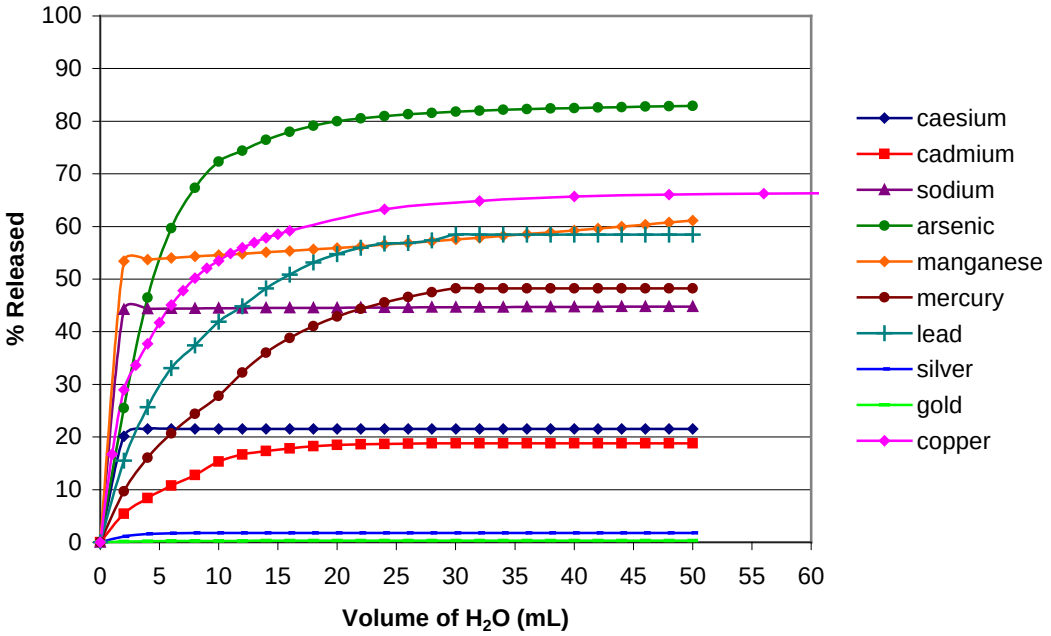

Figure 5.7 Release profiles for nine of the PMPS particle samples containing ions, grouped together for comparison. All profiles were studies over 1 hour totalling 50 mL of water collected in aliquots of 2 mL except for the copper profile which had 1 mL aliquots taken for the first 16 collections and then 8 mL collections for the remaining time, total collection time was 2.5 hours.

It would appear that the ions that have the gradual release profile are the heavier ions on the right hand side of the periodic table, which also means that they are soft acids or bases. The ions that have the second type of profile, where release was achieved in the first aliquot, were all hard acids. It was interesting to observe that arsenic had the highest percentage release despite having the lowest sorption uptake and selenium had the lowest (zero) percentage release despite having one of the highest sorption uptakes.

Chapter Six

Over-coating Studies

Results and Discussion

6.1 Over-coating of PMPS- copper particles

A 10 gram batch of PMPS- copper particles were prepared, as stated in section 4.2, with copper chloride dihydrate as the elemental salt using the optimum sorption conditions of 0.1 molar hydrochloric acid and stirred at 50^{o}C. This was sent to Addmaster Ltd who then incorporated the PMPS-Cu particles into a polypropylene sheet at a concentration of 1%. A sheet of polypropylene containing 1% of pure copper flake was also prepared under identical conditions. A series of tests were carried out on both sheets to determine the leachability of the copper from the polypropylene for the purpose of developing a slow release technique.

The first leach test involved cutting 1 cm x 3 cm strips of each sheet. Each strip was placed into a separate funnel and pure water dripped over the strips at a rate of one drop every 2-3 seconds. The water was collected in 8 mL vials over a period of 150 minutes, totalling fifty 8 mL samples. The samples were analysed using the Unicam atomic absorption spectrometer. None of the samples were found to contain any copper ions. The reason for not finding any copper ions in the samples was put down to the fact that possibly the polypropylene sheet had not had a long enough contact time with the water as it was dripped on, to allow the ions to leach out. Therefore the second test involved submersing the strips in 100 mL of pure water in a separating column, to increase the contact time, 8mL samples were taken every 1.5 hours for a period of 7.5 hours and the columns topped up with fresh water to keep the volumes constant. These samples also failed to contain copper ions. The test was repeated again using larger strips over a longer period of time. This time 2.5 cm x 13 cm strips were placed into measuring cylinders and submersed in 100 mL of pure water. A glass sample vial was placed on top of each sample to weigh it down (to prevent the sheet from floating). The cylinders were covered with parafilm to keep

out contaminants. Every twenty-four hours the water was drained off into a plastic sample bottle and 10 mL of concentrated nitric acid added as a preservative. This was repeated over a period of six days. The total amount of time the sheets were submerged was 187 hours. The samples were analysed on the Unicam atomic absorption spectrometer. It can be seen from Figure 6.1 below that the copper flake in polypropylene sheet started to leach out fairly fast, with the maximum amount being released in the first aliquot, and then over a period of time the amount lessened to almost zero.

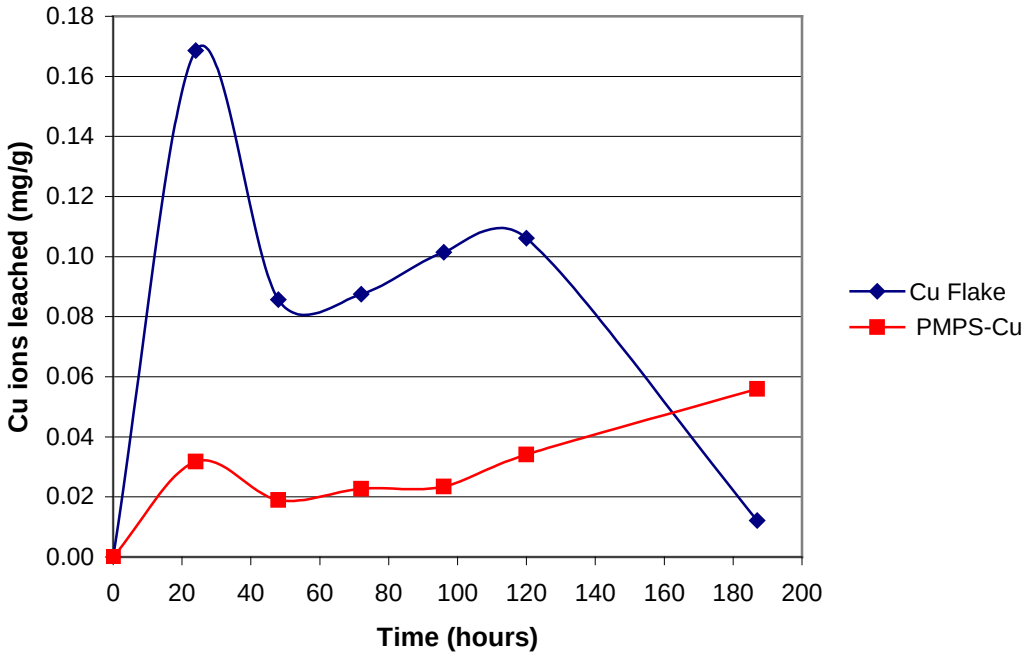

Figure 6.1 Leaching of copper ions from polypropylene sheets containing copper flake or PMPS-copper when submerged in water over a period of six days.

The leaching of the copper contained in the PMPS particles started more slowly and overall gave a lower and more consistent release profile over the length of the experiment with a gradual increase over time, the reverse of the copper flake. Therefore the PMPS particles do appear to help contain ions to facilitate slow release properties.

When the release profile of the PMPS-Cu incorporated into the polypropylene from Figure 6.1 is compared the original release profile previously reported for PMPS-Cu particles (Fig. 5.6, page 165) it is evident that the PMPS-Cu particles whether on their own or when overcoated with a polymer appear to have a slow release profile.

6.2 Over-coating of PMPS- sodium particles

The next phase of this project was to study the effects of encapsulating PMPS particles inside some sort of polymer to form a slow release matrix. Sodium hydroxide was chosen for this project because commercially many companies could potentially find this product useful, for example slow releasing drain cleaner. The first task was to find out which concentration of sodium hydroxide gave the maximum sorption into the PMPS particles. Four different concentrations were used; also two types of surfactant were investigated at varying concentrations to see if this would aid the sorption of the sodium hydroxide. To test the amount of sodium hydroxide the PMPS particles had taken up one gram of the previously prepared dry PMPS-NaOH was mechanically stirred into 30mL of each of the various polymer solutions for thirty minutes. The PMPS particles were then vacuum filtered and left to dry in a heated cabinet (60^{o}C) overnight, (unless stated otherwise). The dry PMPS particles were then added to 30 mL of pure water and mechanically stirred for three minutes, after which time the pH was measured. Table 6.1 shows the results for all of the variations carried out. Changing the concentration of the sodium hydroxide or the addition of surfactant did not have much effect on the maximum sorption of the sodium. The 1 molar concentration had a slightly higher sorption so this was the concentration chosen for all of the encapsulation experiments.

Table 6.1 Various concentration experiments to determine the optimum conditions for maximum sorption of aqueous NaOH into PMPS particles.

Varying concentration of NaOH	pH after 3 mins
Blank PMPS – no NaOH added	3.38
0.1M	9.90
1M	12.80
2M	12.50
5M	12.18
1M 0.1% sodium lauryl sulfate solution	10.78
1M 0.2% sodium lauryl sulfate solution	10.95
2M 0.2% sodium lauryl sulfate solution	12.60
2M with 0.2% C10 amine oxide	12.57
5M 1% sodium lauryl sulfate solution	11.81

A fifty gram batch of PMPS particles was first prepared with the 1 molar sodium hydroxide, to ensure consistency with the starting pH of the material. Table 6.2 lists the various polymers used to encapsulate PMPS-NaOH particles dissolved in various solvents.

Table 6.2 Results for polymer encapsulation of PMPS-NaOH.

Coating	pH after 3 mins
1% poly(methyl methacrylate) in toluene	9.25
5% poly(methyl methacrylate) in toluene	9.32
1% poly(methyl methacrylate) in chloroform	9.70
5% poly(ethylene methyl acrylate)-co-methacrylate in tetrahydrofuran	9.32
5% poly(ethylene methyl acrylate)-co-methacrylate in chloroform	9.84
1% poly(ethylene methyl acrylate)-co-methacrylate in toluene	8.10
1% poly(ethylene methyl acrylate)-co-methacrylate in toluene stirred for 5 hours	9.79
1% poly(ethylene methyl acrylate) in toluene	9.00
1% poly(ethylene methyl acrylate) in toluene	8.10
5% poly(ethylene methyl acrylate) in toluene	9.84
1% poly(ethylene methyl acrylate) in acetone	8.50
1% poly(ethylene methyl acrylate) in acetone	10.25
1% poly(ethylene methyl acrylate) in acetone stirred for 1 hour	9.84
1% poly(ethylene methyl acrylate) in acetone heated to 50^{o}C	10.43
1% poly(ethylene methyl acrylate) in acetone rotary evaporated	7.63
1% poly(ethylene methyl acrylate) in acetone rotary evaporated	9.90
0.5% poly(ethylene methyl acrylate) in acetone rotary evaporated	10.00
2% poly(ethylene methyl acrylate) in acetone	9.90
1% poly(ethylene methyl acrylate) in ethanol (not fully dissolved)	10.02
1% Polyvinyl chloride-co- Polyvinyl acetate in acetone	9.13
5% Polyvinyl chloride-co- Polyvinyl acetate in toluene	8.90

1% polystyrene in toluene	9.43
1% polystyrene in acetone	9.40
1% polystyrene in chloroform	8.92
1% polystyrene in chloroform rotary evaporated	**5.40**
1% polystyrene in chloroform rotary evaporated	**6.12**
2.5% polystyrene in toluene	8.73
4% polystyrene in toluene	8.79
5% polystyrene in toluene	7.56
5% polystyrene in toluene	10.12
5% polystyrene in toluene	10.52

It can be seen from the results in Table 6.2 that the over-coating of the PMPS-NaOH particles cannot be achieved by the method of stirring and filtering. This is probably because the vacuum suction removes the coating from the PMPS particles before it has had time to set. The only method that seemed to be plausible was the use of polystyrene dissolved in chloroform, using the rotovap to remove the excess solvent leaving behind the entire polymer to coat the PMPS particles. Unfortunately this method produced a solid block of polymer and not a powder, which was unusable because it could not be removed from the buchi flask. To test the pH of the product a spatula was used to scrape the sides of the flask to loosen the polymer from the sides and attempt to break it up into sections. The pure water was then added to the flask and the pH measured. This was the only measurement that actually remained acidic. The only problem was that when heated the polystyrene did not release any NaOH so the product would be useless. This is of course assuming that there was actually some NaOH still inside the PMPS/polystyrene product and that it had not been pulled out into the solvent during rotary evaporation.

Chapter Seven

Conclusions

and

Further Work

Conclusions

7.1 Sorption

The PMPS particles have been able to encapsulate almost all of the elements tested. The quantities vary enormously depending upon the conditions used to encapsulate the elements. Analysis of the sorption data shows that the highest rates are found on the right hand side of the periodic table, nominally Groups 11 - 16. The highest sorbing element, by far was gold, Group 11, which had results as high as 319 mg/g, the other elements tested in Group 11 also performed well with copper reaching between 22 and 59 mg/g and silver reaching a respectable 130 mg/g, therefore showing an increase of 45% for each element going down the group. Selenium, Group 16, had the second highest results with 285 mg/g although sulfur, the only other element tested from this Group failed to achieve anything nearly as remarkable only managing between 4 and 24 mg/g. Mercury, Group 12, came a close third with 241 mg/g. When compared with the other elements tested from this Group there is a huge difference since both zinc and cadmium only managed to sorb a maximum of 70 mg/g each.

The results for Group 13 were very erratic with boron, aluminium and indium sorbing very little and gallium and thallium sorbing well. Boron ranged from 1 to 38 mg/g, aluminium ranged from 1 to only 8 mg/g and indium ranging from 7 to 36 mg/g, whereas gallium sorbed from 5 to 78 mg/g and thallium 4 to 107 mg/g. The gallium was sorbed as gallium nitrate and the thallium as thallium sulfate. Following the trend two elements from Group 14 sorbed high values with tin absorbing 94 mg/g and lead 113 ppm mg/g, whereas germanium absorbed nothing at all. This was probably because the germanium oxide that was used was insoluble; it was also very old stock. Group 15 reached high sorption levels with phosphorous sorbing 175 mg/g

and antimony sorbing 110 mg/g. It is probable that the arsenic and bismuth results could be increased if more soluble salts could be found, as solubility was a problem for both these elements.

The trend for the highest sorption to occur in elements on the right hand side of the periodic table, i.e. the least cationic elements suggests that the acidic nature of the PMPS particles have a preference for binding to neutral or anionic atoms. This is clearly evident when the results of hydroxide salts in Group 1 are compared to the chloride salts of the same elements (Table 7.1).

Table 7.1 Comparison of lithium chloride/hydroxide sorption into PMPS particles (mg/g). The lithium hydroxide was prepared by dissolving solid LiOH pellets in water and the lithium chloride was prepared by dissolving LiCl salt in water or hydrochloric acid to achieve the appropriate concentrations.

Conditions	LiOH	LiCl	Conditions
0.1M 4^{o}C	14.62	3.74	water 4^{o}C
0.1M RT	13.62	2.20	water R\T
0.1M 50^{o}C	12.60	2.51	water 50^{o}C
1M 4^{o}C	35.43	3.18	HCl 0.1M 4^{o}C
1M RT	42.31	7.93	HCl 0.1M R\T
1M 50^{o}C	43.76	5.31	HCl 0.1M 50^{o}C
5M 4^{o}C	69.84	2.69	HCl conc 4^{o}C
5M RT	54.79	7.48	HCl conc R/T
5M 50^{o}C	59.73	8.18	HCl conc 50^{o}C

It can be seen from Table 7.1 that there is a huge difference in sorption between the lithium chloride and lithium hydroxide. The same trend can also be seen in Table 7.2 below comparing the sodium results. Although this trend only applies at high concentrations since the 0.1 molar sodium hydroxide results appear to be comparable to the chloride results in H_2O.

Table 7.2 Comparison of sodium chloride/hydroxide sorption into PMPS particles (mg/g). The sodium hydroxide was prepared by dissolving solid NaOH pellets in water and the sodium chloride was prepared by dissolving NaCl salt in water or hydrochloric acid to achieve the appropriate concentrations.

Conditions	NaOH	NaCl	Conditions
0.1M 4^{o}C	50.81	35.13	water 4
0.1M RT	48.92	34.59	water R\T
0.1M 50^{o}C	46.52	37.03	water 50^{o}C
1M 4^{o}C	88.86	18.34	HCl 0.1M 4^{o}C
1M RT	92.29	30.53	HCl 0.1M R\T
1M 50^{o}C	99.91	45.69	HCl 0.1M 50^{o}C
5M 4^{o}C	135.25	21.32	HCl 10M 4^{o}C
5M RT	116.39	35.67	HCl 10M R/T
5M 50^{o}C	117.64	25.11	HCl 10M 50^{o}C

The trend is also evident in Table 7.3 by comparison of the potassium results. Once again the weak 0.1 molar potassium hydroxide results are similar to the chloride results in H_2O but the 1 molar and 5 molar concentrations both show a huge change in sorption.

Table 7.3 Comparison of potassium chloride/hydroxide sorption into PMPS particles (mg/g). The potassium hydroxide was prepared by dissolving solid KOH pellets in water and the potassium chloride was prepared by dissolving KCl salt in water or hydrochloric acid to achieve the appropriate concentrations.

Conditons	KOH	KCl	Conditions
0.1M 4^{o}C	50.46	30.90	water 4^{o}C
0.1M RT	48.05	35.67	water R\T
0.1M 50^{o}C	38.81	36.14	water 50^{o}C
1M 4^{o}C	129.50	10.70	HCl 0.1M 4^{o}C
1M RT	133.40	14.24	HCl 0.1M R\T
1M 50^{o}C	137.10	44.25	HCl 0.1M 50^{o}C
5M 4^{o}C	149.60	31.53	HCl 6M 4^{o}C
5M RT	143.90	20.55	HCl 6M R/T
5M 50^{o}C	159.00	15.08	HCl 6M 50^{o}C

Analysis of the hydroxides also shows that there is evidence of an increase in sorption as concentration and temperature increase. This increase is visible for each of the single elements but is also true to say that a trend now exists for the increase in

sorption down the group as seen in Figure 7.1, which did not exist for the chloride salts.

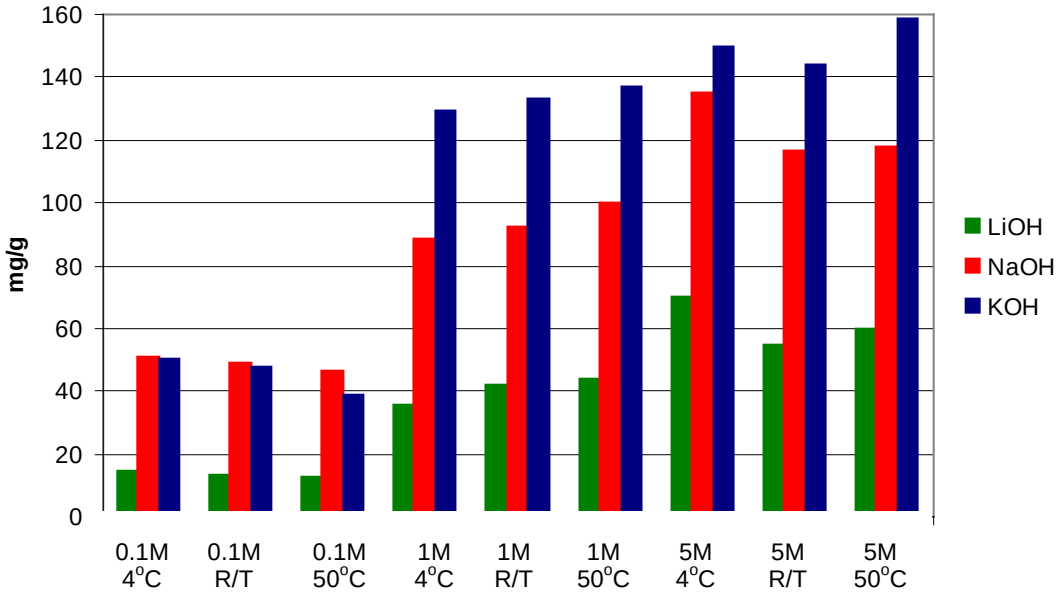

Figure 7.1 Analysis of Group 1 hydroxides sorbed into PMPS particles.

These results suggest that changing pH is a huge factor that affects the ability of PMPS particles to sorb ions but also shows that it is the least electronegative ions that have increased sorption.

Ammonium salts of vanadium and molybdum were analysed and compared to their corresponding chloride salts to see if there was any increase in sorption. It was found that ammonium vanadate dissolved in concentrated hydrochloric acid at 50^{o}C sorbed 32 mg/g, whereas the corresponding chloride salt performed best dissolved in water at 4^{o}C sorbed 26 mg/g. The ammonium salt was slightly higher but not a marked difference. Ammonium molybdate dissolved in H_2O at 50^{o}C sorbed 77 mg/g compared to the molybdenum chloride, dissolved in hydrochloric acid at 50^{o}C, which only achieved 40 mg/g, making the ammonium molybdate much more efficient. For comparison molybdenum oxide was also tested. This was difficult to dissolve and only managed to sorb 7 mg/g.

7.2 Release profiles

The results for the release profiles were very varied with selenium releasing absolutely nothing at all, gold and silver only releasing marginal amounts and other elements with variously increasing release profiles, arsenic being the highest at 83.4%. There does appear to be a difference in the way that ions reach their maximum release, it can be slow and gradual over a period of time or extremely quickly with all of the released ions being in the first aliquot. It would appear that the ions that have the slow gradual release profile are the heavier ions on the right hand side of the periodic table, which also means that they are soft acids or bases. The ions that have the second type of profile, where release was achieved in the first aliquot, were all positioned on the left hand side of the periodic table and are also classed as hard acids although there is no apparent trend for the amount of ions released.

Table 7.4 Percentage release profiles for selected elements.

H																
Li	Be											**B**	C	N	O	
Na 45	**Mg**	**Sc**										**Al**	Si	**P**	S	
K	**Ca**	**Y**	**Ti**	**V**	**Cr**	**Mn 64**	**Fe**	**Co**	**Ni**	**Cu 66**	**Zn**	**Ga**	**Ge**	**As 83**	**Se 0**	
Rb	**Sr**	*	**Zr**	**Nb**	**Mo**	Tc	**Ru**	**Rh**	**Pd**	**Ag 1.75**	**Cd 19**	**In**	**Sn**	**Sb**	Te	
Cs 22	**Ba**	**	**Hf**	**Ta**	**W**	**Re**	Os	**Ir**	**Pt**	**Au 0.27**	**Hg 48**	**Tl**	**Pb 58**	**Bi**	Po	

ions release in first aliquot **ions released gradually**

Group 1 elements sodium and caesium both reached their maximum release after the first 2 mL sample collection. Manganese also had a huge release in the first 2 mL sample but then continued to release ions very slowly throughout the duration of the analysis. Silver and gold were still fairly quick to reach their maximum release

levels with silver taking 8 mL and gold taking 14 mL, the copper however, took much longer with 24 mL being collected before the maximum was reached. The cadmium, mercury, lead and arsenic ions all took 30 mL before their maximum was reached. Selenium failed to release any ions despite the analysis being repeated three times, each analysis using different samples.

It was interesting to observe that arsenic had the highest percentage release despite having the lowest sorption uptake and selenium had the lowest (zero) percentage release despite having one of the highest sorption uptakes.

7.3 Over-coating studies

The over-coating studies conclude that it is possible to coat the PMPS particles with some form of polymer to contain the ions, although the method of stirring and filtering is not a practical method. When overcoating care has to be taken to get the ratio of PMPS particles to polymer balanced so that the ions are encapsulated long enough to be practically contained for the correct length of time but are also able to be released when needed.

7.4 Further work

A details study of the porosimetry of the PMPS particles needs to be undertaken. This will provide information about the surface area and porosity. For this type of research data to be generated the micropores in the particles need to be analyzed in a special machine by being subjected to gas adsorption at very low pressures in a high vacuum system. The gas adsorption technique is usually performed by the addition of a known volume of gas, typically nitrogen or krypton, to the solid material in a sample vessel, the solid is cooled with liquid nitrogen (77.35K). At these cryogenic

temperatures, weak molecular attractive forces will cause the gas molecules to adsorb onto a solid material. Adsorption continues until the amount of gas adsorbed is in equilibrium with the concentration in the gas phase. The amount is close to that needed to cover the surface in a monolayer. The gas is added to the sample in a series of controlled doses, the pressure in the sample vessel is measured after each dosing. There is a direct relationship between the pressure and the volume of gas in the sample vessel. By measuring the reduced pressure due to adsorption, the ideal gas law can then be used to determine the volume of gas adsorbed by the sample. The results are analysed on a computer and the surface area and pore size distribution of the sample can be derived. The surface area, thus measured, includes the entire surface accessible to the gas whether external or internal.

Investigations using nitrogen absorbtion studies, of the porosimetry of the PMPS particles have recently been undertaken outside the bounds of this project. These investigations indicate that the PMPS particles have a surface area of 10 m^2/g, which is a standard surface area for 1-2 micron spherical particles. This also indicates that the pore sizes in the particles are at a molecular level because such pores are not detected using nitrogen absorption. Scanning electron microscope pictures of the PMPS particles containing elements would also help to confirm how the particles sorb ions.

In order to further prove that the PMPS particles have a preference for sorbing soft acids and bases a linkage isomer that can have a configuration of soft acid/base or borderline or hard acid/base depending on its linkage could be sorbed into the PMPS particles in both forms. A common example of a linkage isomer that has these properties is the thiocyanate ion, NCS^-. This ion can bond through the nitrogen atom (-NCS) which classes it as a borderline base or alternatively it can bond through the

sulfur atom (-SCN) changing it to a soft base. Since the compounds are made up of the same atoms, if the HSAB theory is wrong then both compounds will sorb the same quantities. If however the -SCN compound (that has the soft base linkage) sorbs more than the -NCS borderline base this will further confirm the theory. The only problem with using this isomer is the fact that sulfur did not have very high sorption results.

A controllable method of slow release technology needs to be developed so that PMPS particles can be incorporated into viable commercial products. The possibility of spray drying will be the most obvious method of encapsulating ions into the PMPS particles if powdered materials are required. For the production of polymer sheets care needs to be taken to get the thickness of the polymer correct to allow leaching of the PMPS particles. Previous work at Coventry University has already shown that phosphated PMPS particles can be spun into fibres and successfully incorporated into products as a slow releasing medium (Spicer, 2006) therefore it should be possible to incorporate other ions as appropriate. These fibres can then be spun into sheets and manufactured into many different products such as new forms of slow release fertilizers; micro-organism feed stocks and/or anti-bacterial materials. The PMPS should also be examined for practical commercial applications in chromatography used for the separation of metal elemental mixtures.

Studies should be undertaken to discover whether ions that have been sorbed into the PMPS particles are still chemically reactive or inert. If ions were still able to react whilst bound to PMPS particles, i.e. once the initial ions have been released through washing and maximum release had been obtained, the ions that remain bound to the PMPS particles would make easily recyclable catalysts. Selenium is a catalyst in many chemical reactions and is widely used in various industrial and laboratory

syntheses, but is also very toxic to man in excess quantities. If a simple filtration process can recover all of the catalyst easily for recycling this would be good for both the environment and manufacturing costs. As well as being a catalyst selenium is used world-wide in many industries such as the pottery industry where it is used to give a red colour in the manufacture of glass and ceramics and tyre manufacturing to improve abrasion resistance in vulcanized rubbers. Selenium also has exellent photovoltaic and photoconductive properties, making it ideal for use in xeroradiography, photocopiers, photocells, light meters and solar cells (Miessler, 2004, Rayner-Canham, 1999). If the selenium in these products can be bound into PMPS particles, it will prevent it from ever being released into the environment, therefore reducing toxins.

Further investigation could be carried out to see whether the PMPS particles can absorb at low concentration for applications such as water purification or the recovery of gold in effluent. Displacement studies could be carried out to see whether the PMPS particles could successfully be used as an ion-exchanger. It would also be interesting to see whether the PMPS particles could sorb things other than pure ions, for example slow releasing pharmaceuticals.

References

AJAYAGHOSH, A. (2003) Donor-acceptor type low band gap polymers: polysquaraines and related systems. *Chemical Society reviews,* 32**,** 181-191.

AJAYAGHOSH, A. (2005) Chemistry of Squaraine-Derived Materials: Near-IR Dyes, Low Band Gap Systems, and Cation Sensors. *Accounts of Chemical Research,* 38**,** 449-459.

AJAYAGHOSH, A. & ARUNKUMAR, E. (2005) 1H NMR Spectral Evidence for a Specific Host-Guest Complexation Induced Charge Localization in Squaraine Dyes. *Organic Letters***,** 3135-3138.

AJAYAGHOSH, A., ARUNKUMAR, E. & DAUB, J. (2002) A Highly Specific Ca^{2+}-Ion Sensor: Signaling by Exciton Interaction in a Rigid - Flexible - Rigid Bichromophoric "H" Foldamer. *Angewandte Chemie,* 41**,** 1766-1769.

AJAYAGHOSH, A., CHENTHAMARAKSHAN, C. R., DAS, S. & GEORGE, M. V. (1997) Zwitterionic Dye-Based Conducting Polymers. Synthesis and Optical Properties of Pyrrole-Derived Polysquaraines. *Chem. Mater.,* 9**,** 644-646.

AJAYAGHOSH, A. & ELDO, J. (2001) A novel approach toward low optical band gap polysquaraines. *Organic letters,* 3**,** 2595-2598.

AKGOL, S. & DENIZLI, A. (2004) Novel metal-chelate affinity sorbents for reversible use in catalase adsorption. *Journal of Molecular Catalysis B: Enzymatic,* 28**,** 7-14.

ALBION (1994) A Compilation of Vital Research Updates on Human Nutrition. *Albion Research Notes,3,1-4.*

AMETHYST, (2006) http://mineral.galleries.com/minerals/silicate/zeolitres.htm

ARPA, C., ALIM, C., BEKTAS, S., GENC, O. & DENIZLI, A. (2001) Adsorption of heavy metal ions on polyhydroxyethylmethacrylate microbeads carrying Cibacron Blue F3GA. *Colloids and Surfaces a Physicochemical and Engineering Aspects,* 176**,** 225 - 232.

ARUNKUMAR, E., AJAYAGHOSH, A. & DAUB, J. (2005) Selective Calcium Ion Sensing with a Bichromophoric Squaraine Foldamer. *Journal of the American Chemical Society,* 127**,** 3156-3164.

ARUNKUMAR, E., CHITHRA, P. & AJAYAGHOSH, A. (2004) A Controlled Supramolecular Approach toward Cation-Specific Chemosensors: Alkaline Earth Metal Ion-Driven Exciton Signaling in Squaraine Tethered Podands. *Journal of the American Chemical Society,* 126**,** 6590-6598.

ATKINS, P. W. (1998) *Physical Chemistry,* Oxford, Oxford University Press.

BAILEY, S. E., OLIN, T. J., BRICKA, R. M. & ADRIAN, D. D. (1999) A review of potentially low-cost sorbents for heavy metals. *Water Research,* 33**,** 2469-2479.

BALBO BLOCK, M. A. & HECHT, S. (2004) Alternating (Squaraine-Receptor) Sensory Polymers: Modular One-Pot Synthesis and Signal Transduction via Conformationally Controlled Exciton Interaction. *Macromolecules,* 37**,** 4761-4769.

BALBO BLOCK, M. A., KHAN, A. & HECHT, S. (2004) Avenues into the Synthesis of Illusive Poly(m-phenylene-alt-squaraine)s: Polycondensation of m-Phenylenediamines with Squaric Acid Intercepted by Intermediate Semisquaraines of Exceptionally Low Reactivity. *The Journal of Organic Chemistry,* 69**,** 184-187.

BAYRAMOGLU, G., KAYA, B. & ARICA, M. Y. (2002) Procion Brown MX-5BR attached and Lewis metals ion-immobilized poly(hydroxyethyl methacrylate)/chitosan IPNs membranes: Their lysozyme adsorption equilibria and kinetics characterization. *Chemical Engineering Science,* 57**,** 2323-2334.

BELL, R. G. (2001) What are zeolites. *British Zeolite Association.* Nottingham.

BODENANT, B., WEIL, T., BUSINELLI-POURCEL, M., FAGES, F., BARBE, B., PIANET, I. & LAGUERRE, M. (1999) Synthesis and Solution Structure Analysis of a Bispyrenyl Bishydroxamate Calix[4]arene-Based Receptor, a Fluorescent Chemosensor for Cu^{2+} and Ni^{2+} Metal Ions. *The Journal of Organic Chemistry,* 64**,** 7034-7039.

BONNETT, R., MOTEVALLI, M. & SIU, J. (2004) Squaraines based on 2-arylpyrroles. *Tetrahedron,* 60**,** 8913-8918.

BOSS, C. B. & FREDEEN, K. J. (2004) *Concepts, Instrumentation and Techniques in Inductively Coupled Plasma Optical Emission Spectroscopy,* USA, Perkin Elmer Inc.

BRECK, D. W. (1974) *Zeolite Molecular Sieves, Structure, Chemistry and Use,* New York, Wiley-Interscience.

BROCKS, G. & TOL, A. (1996a) Small Band Gap Semiconducting Polymers Made from Dye Molecules: Polysquaraines. *Journal of Physical Chemistry,* 100**,** 1838-1846.

BROCKS, G. & TOL, A. (1996b) A theoretical study of polysquaraines. *Synthetic Metals,* 76**,** 213-216.

BROWNER, C. M. (2000) Notice of Regulatory Determination on Wastes From the Combustion of Fossil Fuels. *U S Environmental Protection Agency, 65, 32213-32237.*

BUCHNER, W., SCHLIEBS, R., WINTER, G. & BUCHEL, K. H. (1989) *Industrial Inorganic Chemistry,* Germany, VCH Publishers.

BUSCHEL, M., AJAYAGHOSH, A., ARUNKUMAR, E. & DAUB, J. (2003) Redox-Switchable Squaraines with Extended Conjugation. *Organic Letters,* 5**,** 2975-2978.

BUYUKTIRYAKI, S., SAY, R., ERSOZ, A., BIRLIK, E. & DENIZLI, A. (2005) Selective preconcentration of thorium in the presence of UO_2^{2+}, Ce^{3+} and La^{3+} using Th(IV)-imprinted polymer. *Talanta,* 67**,** 640-645.

CHEESEMAN, I. M. & BROWN, R. M. (1995) The Microscopy of Curdlan Structure. *Howard Hughes Molecular Biology Summer Research Program Poster,* Austin. Texas, Department of Botany.

CHENTHAMARAKSHAN, C. R. & AJAYAGHOSH, A. (1998a) Enhanced sensitivity and selectivity in lithium ion recognition property of an oligomeric squaraine dye based fluorescent sensor. *Tetrahedron Letters,* 39**,** 1795-1798.

CHENTHAMARAKSHAN, C. R. & AJAYAGHOSH, A. (1998b) Synthesis and Properties of Water-Soluble Squaraine Oligomers Containing Pendant Propanesulfonate Moities. *Chem. Mater.,* 10**,** 1657-1663.

CHENTHAMARAKSHAN, C. R., ELDO, J. & AJAYAGHOSH, A. (1999a) Squaraine Dye Based Molecular Wires Containing Flexible Oxyethylene Chains as Sensors. Enhanced Fluorescence Response on Li^+ Recognition. *Macromolecules,* 32**,** 5846-5851.

CHENTHAMARAKSHAN, C. R., ELDO, J. & AJAYAGHOSH, A. (1999b) Synthesis and Properties of Alternating Acceptor-Donor Copolymers of Squaric Acid with 1 Dodecyl- and 3-Dodecylpyrroles. *Macromolecules,* 32**,** 251-257.

CHESICK, P. (1981) Chromium Squarates:. *Acta Cryst.,* B37**,** 1076-1079.

CHO, H., OH, D. & KIM, K. (2005) A study on removal characteristics of heavy metals from aqueous solution by fly ash. *Journal of Hazardous Materials,* 127**,** 187-195.

CLAFF, C. E. (2003) http://accurapid.com/journal/20org.htm, A Translator's Guide to Organic Chemical Nomenclature. *Science and Technology Translation Journal,* 6, 2, Part XXVII.

CLEAREARTH (2006) www.zandercorporation.com/clearearth.html

COTTON, F. & WILKINSON, G. (1962) *Advanced Inorganic Chemistry,* John Wiley & Sons.

DE LA ROSA, G., GARDEA-TORRESDEY, J. L., PERALTA-VIDEA, J. R., HERRERA, I. & CONTRERAS, C. (2003) Use of silica-immobilized humin for heavy metal removal from aqueous solution under flow conditions. *Bioresource Technology,* 90**,** 11-17.

DELMAU, L. H., SIMON, N., SCHWING-WEILL, M., ARNAUD-NEU, F., DOZOL, J., EYMARD, S., TOURNOIS, B., BOHMER, V., GRUTTNER, C., MUSIGMANNC, C. & TUNAYARC, A. (1998) 'CMPO-substituted' calix[4]arenes, extractants with selectivity among trivalent lanthanides and between trivalent actinides and lanthanides. *Chem. Commun.***,** 16, 1627-1628.

DENIZLI, A., GARIPCAN, B., KARABAKAN, A. & SENOZ, H. (2005) Synthesis and characterization of poly(hydroxyethyl methacrylate-N-methacryloyl-(l)-glutamic acid) copolymer beads for removal of lead ions. *Materials Science and Engineering: C,* 25**,** 448-454.

DENIZLI, A., KIREMITCI, M. & PISKIN, E. (1988) Subcutaneous polymeric matrix system poly(HEMA-BGA) for controlled release of an anticancer drug (5-fluorouracil) : I. Synthesis and structure. *Biomaterials,* 9**,** 257-262.

DENIZLI, A., OZKAN, G. & UCAR, M. (2001) Removal of chlorophenols from aquatic systems with dye-affinity microbeads. *Separation and Purification Technology,* 24**,** 255-262.

DENIZLI, A., SAY, R., PATIR, S. & ARICA, M. Y. (2000a) Adsorption of heavy metal ions onto ethylene diamine-derived and Cibacron Blue F3GA-incorporated microporous poly(2-hydroxyethyl methacrylate) membranes. *Reactive and Functional Polymers,* 43**,** 17-24.

DENIZLI, A., SENEL, S., ALSANCAK, G., TUZMEN, N. & SAY, R. (2003) Mercury removal from synthetic solutions using poly(2-hydroxyethylmethacrylate) gel beads modified with poly(ethyleneimine). *Reactive and Functional Polymers,* 55**,** 121-130.

DENIZLI, A., TANYOLAC, D., SALIH, B., AYDINLAR, E., OZDURAL, A. & PISKIN, E. (1997) Adsorption of heavy-metal ions on Cibacron Blue F3GA-immobilized microporous polyvinylbutyral-based affinity membranes. *Journal of Membrane Science,* 137**,** 1-8.

DENIZLI, A., YAVUZ, H. & ARICA, Y. (2000b) Monosize and non-porous p(HEMA-co-MMA) microparticles designed as dye- and metal-chelate affinity sorbents. *Colloids and Surfaces A: Physicochemical and Engineering Aspects,* 174**,** 307-317.

DESILVA, F. J. (1999) Essentials of Ion Exchange. *WQA Conference.*

ELDO, J. & AJAYAGHOSH, A. (2002) New Low Band Gap Polymers: Control of Optical and Electronic Properties in near Infrared Absorbing pi-Conjugated Polysquaraines. *Chemistry of Materials,* 14**,** 410-418.

ELLIS, A. L. (2001) The Solvent Encapsulation Properties of Bis(N-Hexylpyrrol-2-yl)Squaraine. Unpublished final year undergraduate project, *School of Science and the Environment,* Coventry University.

FELLOWS, A. (2003) Inclusion of Metal or Metal Complexes into Hollow Silica Spheres. Unpublished final year undergraduate project, *School of Science and the Environment.* Coventry University.

FISHER & SCIENTIFIC (2007) Material Safety Data Sheet, Fisher Scientific UK Web Catalogue. 20/9/2007 ed., Fisher.

FLANIGEN, E. M. (2005) Molecular sieve zeolites: an industrial research success story: the discovery and development of zeolites and molecular sieves... Union Carbide Corp. Linde Div. (Research).

GEISSLER, U., LYNCH, D. E., ROHDE, N., HALLENSLEBEN, M. L. & WALTON, D. J. (1997) Poly(oligo(1-methylpyrrole))s and their squaraine-derivatives: an electrochemical and spectroelectrochemical investigation. *Synthetic Metals,* 84**,** 171-172.

GENC, O., ARPA, C., BAYRAMOGLU, G., ARICA, M. Y. & BEKTAS, S. (2002) Selective recovery of mercury by Procion Brown MX 5BR immobilized poly(hydroxyethylmethacrylate/chitosan) composite membranes. *Hydrometallurgy,* 67**,** 53-62.

GENC, O., SOYSAL, L., BAYRAMOGLU, G., ARICA, M. Y. & BEKTAS, S. (2003) Procion Green H-4G immobilized poly(hydroxyethylmethacrylate/chitosan) composite membranes for heavy metal removal. *Journal of Hazardous Materials,* 97**,** 111-125.

GODE, F. & PEHLIVAN, E. (2007) Sorption of Cr(III) onto chelating b-DAEG-sporopollenin and CEP-sporopollenin resins. *Bioresource Technology,* 98**,** 904-911.

GOEL, J., KADIRVELU, K., RAJAGOPAL, C. & KUMAR GARG, V. (2005) Removal of lead(II) by adsorption using treated granular activated carbon: Batch and column studies. *Journal of Hazardous Materials,* 125**,** 211-220.

GOMEZ-SERRANO, V., MACIAS-GARCIA, A., ESPINOSA-MANSILLA, A. & VALENZUELA-CALAHORRO, C. (1998) Adsorption of mercury, cadmium and lead from aqueous solution on heat-treated and sulphurized activated carbon. *Water Research,* 32**,** 1-4.

HARDIN, A. M. & ADMASSU, W. (2005) Kinetics of heavy metal uptake by vegetation immobilized in a polysulfone or polycarbonate polymeric matrix. *Journal of Hazardous Materials,* 126**,** 40-53.

HAVINGA, E. E., HOEVE, W. & WYNBERG, H. (1992) A new class of small band gap organic polymer conductors. *Polymer Bulletin,* 29**,** 119-126.

HAVINGA, E. E., TEN HOEVE, W. & WYNBERG, H. (1993) Alternate donor-acceptor small-band-gap semiconducting polymers; Polysquaraines and polycroconaines. *Synthetic Metals,* 55**,** 299-306.

HAVINGA, E. E., WYNBERG, H., POMP, A. & TEN HOEVE, W. (1995) Water-soluble polysquaraines and polycroconaines. *Synthetic Metals,* 69**,** 581-582.

HEEGER, A. J., MACDIARMID, A. G. & SHIRAKAWA, H. (2000) The discovery and development of electrically conducting polymers. *The Nobel Prize in Chemistry, 2000.* Sweden.

HIGSON, S. P. J. (2004) *Analytical Chemistry,* Oxford, Oxford University Press.

HOFFMAN, G. K. (2000) Uses of fly ash from new mexico coals. *New Mexico Geology,* 22**,** 25-36.

http://www.wonderpeat.com/process_main.html (2008) Processing of Cocopeat

JUSOH, A., SU SHIUNG, L., ALI, N. A. & NOOR, M. J. M. M. (2007) A simulation study of the removal efficiency of granular activated carbon on cadmium and lead. *Desalination,* 206**,** 9-16.

JYOTHISH, K., ARUN, K. T. & RAMAIAH, D. (2004) Synthesis of novel quinaldine-based squaraine dyes: Effect of substituents and role of electronic factors. *Organic Letters,* 6**,** 3965-3968.

KARA, A., UZUN, L., BESIRLI, N. & DENIZLI, A. (2004) Poly(ethylene glycol dimethacrylate-n-vinyl imidazole) beads for heavy metal removal. *Journal of Hazardous Materials,* 106**,** 93-99.

KARAGUNDUZ, A., KAYA, Y., KESKINLER, B. & ONCEL, S. (2006) Influence of surfactant entrapment to dried alginate beads on sorption and removal of Cu2+ ions. *Journal of Hazardous Materials,* 131**,** 79-83.

KAVAKLI, C., OZVATAN, N., TUNCEL, S. A. & SALIH, B. (2002) 1,4,8,11-Tetraazacyclotetradecane bound to poly(p-chloromethylstyrene-ethylene glycol dimethacrylate) microbeads for slective gold uptake. *Analytica Chimica Acta,* 464**,** 313-322.

KENTUCKY (2005) Experiment 7: Determination of sodium by flame atomic-emission spectroscopy. The Department of Chemistry, University of Kentucky.

KESENCI, K., SAY, R. & DENIZLI, A. (2002) Removal of heavy metal ions from water by using poly(ethyleneglycol dimethacrylate-co-acrylamide) beads. *European Polymer Journal,* 38**,** 1443-1448.

KIRCHHOFF, G. & BUNSEN, R. (1860) Chemical Analysis by Observation of Spectra. *Annalen der Physik und der Chemie (Poggendorff),* 110**,** 161-189.

KYODA, M. M., H.; SADAI, Y.; NISHIGUCHI, I. (2006) Synthesis, structures and properties of calix[4]arenes bearing four phosphanate or phosphine oxide groups at the upper arm. *AZojomo Journal of Materials Online,* 2**,** 1-10.

LEYVA RAMOS, R., BERNAL JACOME, L. A., MENDOZA BARRON, J., FUENTES RUBIO, L. & GUERRERO CORONADO, R. M. (2002) Adsorption of zinc(II) from an aqueous solution onto activated carbon. *Journal of Hazardous Materials,* 90**,** 27-38.

LOFTSSON, T. & DUCHÊNE, D. (2007) Cyclodextrins and their pharmaceutical applications. *International Journal of Pharmaceutics,* 329**,** 1-11.

LV, L., LEE, F. Y., ZHOU, J., SU, F. & ZHAO, X. S. (2006) XPS study on microporous titanosilicate ETS-10 upon acid treatment. *Microporous and Mesoporous Materials,* 96**,** 270-275.

LV, L., WANG, K. & ZHAO, X. S. (2007) Effect of operating conditions on the removal of Pb2+ by microporous titanosilicate ETS-10 in a fixed-bed column. *Journal of Colloid and Interface Science,* 305**,** 218-225.

LV, L. S., F.; ZHAO, X. S. (2006) Synthesis and characterization of microporous titanosilicate ETS-10 with different titanium precursors. *J. Porous Mater.,* 13**,** 263-267.

LYNCH, D. E., GEISSLER, U. & BYRIEL, K. A. (2001) An investigation into the electrical conduction properties of poly(oligo(1-methylpyrrol-2-yl)squaraine)s. *Synthetic Metals,* 124**,** 385-391.

LYNCH, D. E., GEISSLER, U., CALOS, N. J., WOOD, B. & KINAEV, N. N. (1998a) Towards processible poly(pyrrol-2-ylsquaraines). *Polymer Bulletin,* 40**,** 373-380.

LYNCH, D. E., GEISSLER, U., KWIATKOWSKI, J. & WHITTAKER, A. K. (1997a) An investigation into the synthesis of polycarbazole squaraine derivatives. *Polymer Bulletin,* 38**,** 493-499.

LYNCH, D. E., GEISSLER, U., PETERSON, I. R., FLOERSHEIMER, M., TERBRACK, R., CHI, L. F., FUCHS, H., CALOS, N. J., WOOD, B.,

KENNARD, C. H. L. & J., L. G. (1997b) The synthesis and non-linear optical properties of (N-alkylpyrrol-2-yl)squaraine derivatives. Part 1. *J. Chem. Soc. Perkin Trans,* 2**,** 827-832.

LYNCH, D. E., NAWAZ, Y. & BOSTROM, T. (2005) Preparation of sub-micrometer silica shells using poly(1-methylpyrrol-2-ylsquaraine). *Langmuir : The ACS Journal of Surfaces and Colloids,* 21**,** 6572-6575.

LYNCH, D. E., PETERSON, I. E., FLOERSHEIMER, M., ESSING, D., CHI, L., FUCHS, H., CALOS, N. J., WOOD, B., KENNARD, C. H. L. & LANGLEY, G. J. (1998b) Synthesis and non-linear optical properties of (N-alkylpyrrol-2-yl)-squaraine derivatives. Part 2. *J. Chem. Soc., Perkin Trans.,* 2**,** 779-784.

MAAHS, G. & HEGENBERG, P. (1966) Synthesis and Derivatives of Squaric Acid. *Angew. Chem. Internat. Edit.,* 5**,** 888-893.

MATTHEWS, S. E., PARZUCHOWSKI, P., GARCIA-CARRERA, A., GRUTTNER, C., DOZOL, J. & BOHMER, V. (2001) Extraction of lanthanides and actinides by a magnetically assisted chemical separation technique based on CMPO-calix[4]arenes. *Chem. Commun.***,** 417-418.

MEENA, A. K., MISHRA, G. K., RAI, P. K., RAJAGOPAL, C. & NAGAR, P. N. (2005) Removal of heavy metal ions from aqueous solutions using carbon aerogel as an adsorbent. *Journal of Hazardous Materials,* 122**,** 161-170.

MEMON, S., TABAKCI, M., MAX ROUNDHILL, D. & YILMAZ, M. (2005) A useful approach toward the synthesis and metal extractions with polymer appended thioalkyl calix[4]arenes. *Polymer,* 46**,** 1553-1560.

MERRIFIELD, J. D., DAVIDS, W. G., MACRAE, J. D. & AMIRBAHMAN, A. (2004) Uptake of mercury by thiol-grafted chitosan gel beads. *Water Research,* 38**,** 3132-3138.

MIESSLER, G. L. & TARR, D. A. (2004) *Inorganic Chemistry,* New Jersey, Pearson Education Inc.

MOHAN, D. & PITTMAN, J. C. U. (2006) Activated carbons and low cost adsorbents for remediation of tri- and hexavalent chromium from water. *Journal of Hazardous Materials,* 137**,** 762-811.

MOON, C. J. & LEE, J.-H. (2005) Use of curdlan and activated carbon composed adsorbents for heavy metal removal. *Process Biochemistry,* 40**,** 1279-1283.

MUKKANTI, A. & PERIASAMY, M. (2005) Methods of synthesis of cyclobutenediones. *ARKAT,* xi**,** 48-77.

NACHTIGALL, F. F., LAZZAROTTO, M. & NOME, F. (2002) Interaction of Calix[4]arene and Aliphatic Amines: A combined NMR, spectrophotometric and conductimetric investigation. *Journal of the Brazilian Chemical Society,* 13**,** 295-299.

NALCO (1998) www.onlinewatertreatment.com/literature/Nalco/docs/Tf-024.pdf, Ion Exchange Processes, Naperville, Illinois,

NAMASIVAYAM, C. & SANGEETHA, D. (2006) Recycling of agricultural solid waste, coir pith: Removal of anions, heavy metals, organics and dyes from water by adsorption onto $ZnCl_2$ activated coir pith carbon. *Journal of Hazardous Materials,* 135**,** 449-452.

NICOL, S. (1991) Life after death for empty shells: Crustacean fisheries create a mountain of waste shells, made of a strong natural polymer, chitin. Now chemists are helping to put this waste to some surprising uses. *New Scientist,* 1755, 36-38.

OLIVEIRA, B. F., SANTANA, M. H. A. & RE, M. I. (2005) Spray-dried chitosan microspheres cross-linked with d, l-glyceraldehyde as a potential drug delivery

system: preparation and characterization. *Brazilian Journal of Chemical Engineering,* 22**,** 353-360.

PAN, B., PAN, B., CHEN, X., ZHANG, W., ZHANG, X., ZHANG, Q., ZHANG, Q. & CHEN, J. (2006) Preparation and preliminary assessment of polymer-supported zirconium phosphate for selective lead removal from contaminated water. *Water Research,* 40**,** 2938-2946.

PARK, J. D., COHEN, S. & LACHER, J. R. (1959) Diketocyclobutenediol. *JACS,* 81**,** 3480.

PARK, J. D., COHEN, S. & LACHER, J. R. (1962) Hydrolysis reactions of halogenated cyclobutene ethers: Synthesis of diketocyclobutenediol. *JACS,* 84**,** 2919-2922.

PAUNOV, V. N., MACKENZIE, G. & STOYANOV, S. D. (2007) Sporopollenin micro-reactors for in-situ preparation, encapsulation and targeted delivery of active components. *J. Mater. Chem.,* 17**,** 609-612.

PEARSON, R. G. (1963) Hard and soft acids and bases. *JACS,* 85**,** 3533-3539.

PEDERSEN, C. J. (1967) Cyclic polyethers and their complexes with metal salts. *JACS,* 89**,** 7017-7019.

PEDERSEN, C. J. (1988) The Discovery of crown ethers (Noble Lecture). *Angewandte Chemie International Edition in English,* 27**,** 1021-1027.

PEKALA, R. W. (1989) Organic aerogels from the polycondensation of resorcinol with formaldehyde. *Journal of Materials Science,* 24**,** 3221-3227.

PITCHER, S. K., SLADE, R. C. T. & WARD, N. I. (2004) Heavy metal removal from motorway stormwater using zeolites. *Science Of The Total Environment,* 334-335**,** 161-166.

PROCTOR & GAMBLE (2001) What is cyclodextrin? *Science In The Box.* Ohio, Proctor & Gamble.

RAYNER-CANHAM, G. (1999) *Descriptive Inorganic Chemistry,* New York, W. H. Freeman and Company.

REALLABWARE.COM (2006) Flame Photometers.

RITTER, P. (1996) *Biochemistry A foundation,* Pacific Grove, Brooks/Cole.

RONCALI, J. (1997) Synthetic principles for bandgap control in linear pi-conjugated systems. *Chemical Reviews,* 97**,** 173-206.

ROYAL, W. R. (2008) http://cape.uwaterloo.ca/che100projects/flyash/env.html, Coal Flyash: A review of the literature and proposed classification system with emphasis on enviromental impacts. University of Waterloo, Canada.

SAGLAM, A., BEKTAS, S., PATIR, S., GENC, O. & DENIZLI, A. (2001) Novel metal complexing ligand: thiazolidine carrying poly(hydroxyethylmethacrylate) microbeads for removal of cadmium(II) and lead(II) ions from aqueous solutions. *Reactive and Functional Polymers,* 47**,** 185-192.

SAHUQUILLO, A., RAURET, G., REHNERT, A. & MUNTAU, H. (2003) Solid sample graphite furnace atomic absorption spectroscopy for supporting arsenic determination in sediments following a sequential extraction procedure. *Analytica Chimica Acta,* 476**,** 15-24.

SAITO, S., RUDKEVICH, D. M. & REBEK, J. (1999) Lower rim functionalized resorcinarenes: Useful modules for supramolecular chemistry. *Organic Letters,* 1**,** 1241-1244.

SATIROGLU, N., YALCINKAYA, Y., DENIZLI, A., ARICA, M. Y., BEKTAS, S. & GENC, O. (2002) Application of NaOH treated polyporus versicolor for

removal of divalent ions of Group IIB elements from synthetic wastewater. *Process Biochemistry,* 38**,** 65-72.

SAY, R., BIRLIK, E., DENIZLI, A. & ERSOZ, A. (2006) Removal of heavy metal ions by dithiocarbamate-anchored polymer/organosmectite composites. *Applied Clay Science,* 31**,** 298-305.

SAY, R., BIRLIK, E., ERSOZ, A., YILMAZ, F., GEDIKBEY, T. & DENIZLI, A. (2003) Preconcentration of copper on ion-selective imprinted polymer microbeads. *Analytica Chimica Acta,* 480**,** 251-258.

SCHMIDT, W. (2006) Properties of Zeolites. Germany, Max-Planck-Institut für Kohlenforschung.

SETHI, S. (2004) Unpublished final year undergraduate project, *School of Science and the Environment.* Coventry University.

SHERWOOD (2006) Whats the lineariser for? Sherwood Scientific Ltd.

SHERWOOD (2007) Model 410 Flame photometer. Sherwood Scientific Ltd.

SINEX, S. A. (2004) EDTA - A Molecule with a complex story, Prince George's Community College, USA in (*Molecule of the Month*) PAUL MAY, B. C. D. University of Bristol. http://www.chm.bris.ac.uk/motm/edta/edta.htm

SKOOG, D. A., HOLLER, F. J. & NIEMAN, T. A. (1998) *Principles of Instrumental Analysis,* Florida, Saunders College Publishing.

SKOOG, D. A., WEST, D. M., HOLLER, F. J. & CROUCH, S. R. (1999) *Fundamentals of Analytical Chemistry,* Florida, ThomsonBrooks/Cole.

SLIWA, W. (2002) Calixarene complexes with transition metal, lanthanide and actinide ions. *Croatica Chemica Acta,* 75**,** 131-153.

SLIWA, W. & DESKA, M. (2002) Cavitands. (Review). *Chemistry of Heterocyclic Compounds,* 38**,** 646-667.

SOLOMONS, G. & FRYHLE, C. (2000) *Organic Chemistry,* New York, John Wiley & Sons Inc.

SPICER, G. (2006) The Development of a Self-Fertilising Geotextile Incorporating Slow Release Phosphate Beads for the Maintenance of Oil Degrading Bacteria in Permeable Pavements. PhD thesis, *Business and Environmental Science.* Coventry University.

SPRYNSKYY, M., BUSZEWSKI, B., TERZYK, A. P. & NAMIESNIK, J. (2006) Study of the selection mechanism of heavy metal (Pb^{2+}, Cu^{2+}, Ni^{2+}, and Cd^{2+}) adsorption on clinoptilolite. *Journal of Colloid and Interface Science,* 304**,** 21-28.

TATARETS, A. L., FEDYUNYAEVA, I. A., TERPETSCHNIG, E. & PATSENKER, L. D. (2005) Synthesis of novel squaraine dyes and their intermediates. *Dyes and Pigments,* 64**,** 125-134.

TAYLOR, L. R., PAPP, R. B. & POLLARD, B. D. (1994) *Instrumental Methods for Determining Elements, Selection and Application,* USA, VCH Publishers.

TECMEC (2005) What is the ICP? Tecmec Ltd., http://www.atomicabsorption.co.uk/whatisicp.html

THOMAS, J. M. (1992) Solid acid catalysts. *Scientific American,* 266**,** 112-118.

TOL, A. J. W. (1994) Using symmetry forbidden interactions to create small band gap polymers: Poly-aminosquaraine and related compounds. *The Journal of Chemical Physics,* 100**,** 8463-8470.

TREIBS, A. & JACOB, K. (1965) Cyclotrimethine dyes derived from squaric acid. *Angewandte Chemie International Edition,* 4**,** 694.

TREIBS, A. & JACOB, K. (1966) Cyclobutenderivate der pyttolreihe. *Leibigs Ann. Chem,* 699**,** 153.

TREIBS, V. A. & FRITZ, G. (1957) Die substitutionsregeln des pyrrols und der mechanismus der pyrrol-austausch-reaktionen. *Leibig's Annalen der Chemie,* 611**,** 162-193.

VALIX, M., CHEUNG, W. H. & MCKAY, G. (2004) Preparation of activated carbon using low temperature carbonisation and physical activation of high ash raw bagasse for acid dye adsorption. *Chemosphere,* 56**,** 493-501.

VAN DIENST, E., BAKKER, W. I. I., ENGBERSEN, J. F. J., VERBOOM, W. & REINHOUDT, D. N. (1993) Calixarenes, chemical chameleons. *Pure and Applied Chemistry,* 65**,** 387-392.

VIJAYAN, V., BEHERA, S. N., RAMAMURTHY, V. S., SANJIV PURI, J. S., SHAHI, J. S. & SINGH, N. (1997) Elemental Composition of fly ash from a coal-fired thermal power plant: A study using PIXE and EDXRF. *X-Ray Spectrometry,* 26**,** 65-68.

VOLESKY, B. (2003) *Sorption and Biosorption,* Montreal, BV-Sorbex, Inc.

WALKER, C. (2007) http://www.uksaf.org/tech/shg.html, SHG - Second Harmonic Generation. *UK Surface Analysis Forum,* University of York.

WALLACE, G. G., DASTOOR, P. C., OFFICER, D. L. & TOO, C. O. (2000) Conjugated polymers: New materials for photovolataics. *Chemical Innovation,* 30**,** 14-22.

WEST, R., NUI, H. Y., POWELL, D. L. & EVANS, M. V. (1960) Symmetrical resonance stabilized anions. *JACS,* 82**,** 6204-6205.

WEST, R., YING NUI, H. & ITO, M. (1963) New aromatic anions. V. The synthesis of diketocyclo butenediol and its conversion to octahydroxycyclobutane. *JACS,* 85**,** 2584-2590.

WILCOCK, R. (2004) Lanthanides. Unpublished final year undergraduate project, *School of Science and the Environment.* Coventry University.

WILLIAMS, D. (1998) Storing up trouble *chembytes e-zine* 1ed., Royal Society of Chemistry

WWW3.JETRO.GO.JP/.../0001069000/1069870_E.HTML (1995) Chitin-Chitosan, Glucosamine, Collagen etc.

YU, L. P., CHEN, M., DALTON, L. R., CAO, X. F., JIANG, J. P. & HELLWARTH, R. W. (1990) Synthesis and characterization of third order nonlinear optical materials. *Materials Research Society Symposium Proc.,* 173**,** 607-612.

ZHANG, Q., HUANG, D. & LIU, Y. (2003) Preparation of Langmuir-Blodget films of phthalocyanines and investigation by atomic force microscope. *Synthetic Metals,* 137**,** 989-990.

ZHAO, G. (2006) http://cheed.nus.edu.sg/~chezxs/Zhao/research.htm. Research Programme. Department of Chemical & Biomolecular Engineering. University of Singapore.

ZHAO, X. S., LU, G. Q. & MILLAR, G. J. (1996) Advances in Mesoporous Molecular Sieve MCM - 41. *Ind. Eng. Chem. Res.,* 35**,** 2075-2090.

ZHAO, X. S., MA, Q. & LU, G. Q. (2004) VOC Removal: Comparison of MCM-41 with Hydrophobic Zeolites and Activated Carbon. *Enery and Fuels,* 12**,** 1051-1054.

ZHAO, X. S., SU, F., YAN, Q., GUO, W., BAO, X. Y., LV, L. & ZHOU, Z. (2006) Templating methods for preparation of porous structures. *J. Mater. Chem.,* 16**,** 637-648.

Appendices

Appendix 1: Calibration data

Li Absorption calibration 24/6/05

Lithium standards ppm	Intensity
blank	2912.3
25	196951.7
50	384529.0
75	559714.0
100	752097.3
Correlation Coefficient 0.9999	
Wavelength 670.781 nm	

(ICP Plasma 400)

B Absorption calibration 24/2/05

Boron standards ppm	Intensity
blank	3817.3
25	39022.3
50	74442.0
75	115061.7
100	155144.0
Correlation Coefficient 0.9994	
Wavelength 249.773 nm	

(ICP Plasma 400)

NaOH Absorption calibration 15/12/04

Sodium standards ppm	Intensity
blank	12196.0
25	42670.0
50	74655.0
75	104624.3
100	135034.3
125	160876.3
Correlation Coefficient 0.9996	
Wavelength 589.592 nm	

(ICP Plasma 400)

B Absorption calibration 6/4/05

Boron standards ppm	Intensity
blank	2501.1
10	12442.0
20	20364.3
30	36281.3
40	36450.7
Correlation Coefficient 0.9745	
Wavelength 249.773 nm	

(ICP Plasma 400) microwave digestion

NaCl Absorption calibration 9/11/05

Sodium standards ppm	Emission
blank	0.0
25	42.7
50	70.3
75	93.3
100	100.3

(Flame Photometer)

Mg Absorption calibration 9/6/05

Magnesium standards ppm	Intensity
blank	106.3
25	1480.7
50	2770.7
75	4158.7
100	5425.7
Correlation Coefficient 0.9999	
Wavelength	

(ICP Plasma 400)

Al Absorption calibration 18/4/05

Aluminium standards ppm	Intensity
blank	290.3
25	1482.0
50	2662.3
75	3830.0
100	4916.7
Correlation Coefficient 0.9998	
Wavelength 226.910 nm	

(ICP Plasma 400)

P Absorption calibration 12/5/06

Ruthenium standards ppm	Intensity
blank	133.0
25	27558.6
50	56357.2
75	88783.8
100	120892.0
Correlation Coefficient 0.999326	
Wavelength 213.617nm	

(Optima 5300 DV)

K Absorption calibration 24/3/06

Ruthenium standards ppm	Intensity
blank	-405.6
25	1894.1
50	3910.5
75	6448.4
100	8626.0
Correlation Coefficient 0.998622	
Wavelength 404.721 nm	

(Optima 5300 DV)

Ca Absorption calibration 9/6/05

Calcium standards ppm	Intensity
blank	1169.7
25	13200.0
50	25785.3
75	37754.3
100	53163.7
Correlation Coefficient 0.9988	
Wavelength 315.887 nm	

(ICP Plasma 400)

Ti Absorption calibration 28/4/06

Ruthenium standards ppm	Intensity
blank	582.9
25	3670855.3
50	7040351.5
75	10339147.6
100	13480181.0
Correlation Coefficient 0.999581	
Wavelength 337.279 nm	

(Optima 5300 DV)

V Absorption calibration 11/3/05

Vanadium standards ppm	Intensity
blank	92.0
25	1536.7
50	2718.7
75	4141.0
100	5686.7
Correlation Coefficient 0.9991	
Wavelength 214.009 nm	

(ICP Plasma 400)

Cr Absorption calibration 3/305

Chromium standards ppm	Intensity
blank	150.7
25	8813.7
50	12681.7
75	22494.0
100	31831.3
Correlation Coefficient 0.9918	
Wavelength 205.552 nm	

(ICP Plasma 400)

Mn Absorption calibration 24/1/05

Manganese standards ppm	Intensity
blank	105.3
25	3212.0
50	6405.7
75	9767.0
100	13236.7
Correlation Coefficient 0.9997	
Wavelength 403.1 nm	

(ICP Plasma 400)

Mn Leach Test Calibration 11/11/05

Manganese standards ppm	Intensity
blank	
25	
50	
75	
100	
Correlation Coefficient 1.0000	
Wavelength 403.1 nm	

(ICP Optima 5300 DV)

Mn Absorption calibration 3/3/06

Manganese standards ppm	Intensity
blank	10179.9
25	7809829.1
50	14801501.6
75	21022917.6
100	26258474.7
Correlation Coefficient 0.9997117	
Wavelength 259.372 nm	

(ICP Optima 5300 DV)

Fe Absorption calibration 9/12/04

Iron standards ppm	Intensity
blank	485.3
25	24051.7
50	46449.7
75	77645.3
100	90908.3
125	112983.0
Correlation Coefficient 0.9961	
Wavelength 233.280 nm	

(ICP Plasma 400)

Fe Absorption calibration 6/4/05

Iron standards ppm	Intensity
blank	427.3
25	3184.3
50	6344.7
75	9821.7
100	11197.3
Correlation Coefficient 0.9929	
Wavelength 233.280 nm	

(ICP Plasma 400) microwave digestion

Co Absorption calibration 17/3/05

Cobolt standards ppm	Intensity
blank	405.0
25	17382.3
50	33571.7
75	50824.0
100	64956.0
Correlation Coefficient 0.9995	
Wavelength 228.616 nm	

(ICP Plasma 400)

Ni Absorption calibration 17/3/05

Nickel standards ppm	Intensity
blank	276.7
25	5883.7
50	10622.7
75	16842.7
100	21242.7
Correlation Coefficient 0.9989	
Wavelength 216.556 nm	

(ICP Plasma 400)

Cu Absorption calibration 10/1/05

Copper standards ppm	Intensity
blank	130.7
25	4945.7
50	9068.7
75	13227.7
100	19259.7
Correlation Coefficient 0.9974	
Wavelength 213.598 nm	

(ICP Plasma 400)

Cu Leach Test Calibration 9/5/05

Copper standards ppm	Intensity
blank	62.3
25	1401.3
50	2662.0
75	4139.3
100	5519.3
Correlation Coefficient 0.9997	
Wavelength 213.598	

(ICP Plasma 400)

Cu Leach Test Calibration 17/5/05

Copper standards ppm	Intensity
blank	186.3
25	7617.0
50	14538.3
75	20497.7
100	27204.7
Correlation Coefficient 0.9993	
Wavelength 213.598 nm	

(ICP Plasma 400)

Zn Absorption calibration 21/12/04

Zinc standards ppm	Intensity
blank	40.7
25	3057.3
50	5627.0
150	18407.7
Correlation Coefficient 0.9995	
Wavelength 213.856 nm	

(ICP Plasma 400)

As Absorption calibration 12/1/06

Arsenic standards ppm	Intensity
blank	669.0
25	44721.5
50	87840.7
75	132087.9
100	171862.1
Correlation Coefficient 0.999804	
Wavelength 188.979 nm	

(ICP Optima 5300 DV)

As Leach Test calibration 12/1/06

Arsenic standards ppm	Intensity
blank	359.2
2	3716.4
4	7325.1
8	15099.7
12	22885.2
Correlation Coefficient 0.999906	
Wavelength 188.979	

(ICP Optima 5300 DV)

Se Absorption calibration 1/3/05

Selenium standards ppm	Intensity
blank	46.3
25	1442.0
50	2784.3
75	4168.3
100	5412.3
Correlation Coefficient 0.9998	
Wavelength 196.026 nm	

(ICP Plasma 400)

Se Absorption calibration 6/4/05

Selenium standards ppm	Intensity
blank	97.0
50	1671.7
100	3648.7
150	5463.3
200	7326.7
Correlation Coefficient 0.9995	
Wavelength 196.026 nm	

(ICP Plasma 400) microwave digestion

Se Leach Test calibration 18/11/05

Selenium standards ppm	Absorbance
blank	0
25	0.180
50	0.343
75	0.484
100	0.599
Wavelength 196.0 nm	

(AAS Unicam 939)

Se Leach Test calibration 21/11/05

Selenium standards ppm	Intensity
blank	29.7
25	49901.4
50	93245.3
75	134161.4
100	174414.8
Correlation Coefficient 0.999008	
Wavelength 196.026 nm	

(ICP Optima 5300 DV)

Se Leach Test calibration 23/11/05

Selenium standards ppm	Intensity
blank	11.3
2	3650.7
4	7309.7
6	10544.4
Correlation Coefficient 0.999578	
Wavelength 196.026 nm	

(ICP Optima 5300 DV)

Sr Absorption calibration 17/5/05

Strontium standards ppm	Intensity
blank	182.7
50	949.3
75	1339.3
100	1785.0
Correlation Coefficient 0.9994	
Wavelength 215.284 nm	

(ICP Plasma 400)

Y Absorption calibration 16/3/06

Yttrium standards ppm	Intensity
blank	19990.6
25	14093526.9
50	27002056.5
75	38024555.2
Correlation Coefficient 0.998526	
Wavelength 371.029 nm	

(Optima 5300 DV)

Mo Absorption calibration 3/2/05

Molybdenum standards ppm	Intensity
blank	97.3
25	1467.7
50	2852.3
75	4366.3
100	5566.7
Correlation Coefficient 0.9995	
Wavelength 201.511 nm	

(ICP Plasma 400)

Ru Absorption calibration 16/3/06

Ruthenium standards ppm	Intensity
blank	-130.3
25	827051.8
50	1627993.9
75	2445807.9
100	3195745.4
Correlation Coefficient 0.999863	
Wavelength 240.272 nm	

(Optima 5300 DV)

Pd Absorption calibration 12/5/06

Palladium standards ppm	Intensity
blank	-50.3
25	771876.4
50	1564727.6
75	2334530.4
100	3128604.8
Correlation Coefficient 0.999988	
Wavelength 340.458 nm	

(Optima 5300 DV)

Ag Absorption calibration 8/2/05

Silver standards ppm	Intensity
blank	106.3
25	174.0
50	252.3
75	328.3
100	388.7
Correlation Coefficient 0.9991	
Wavelength 211.383 nm	

(ICP Plasma 400)

Ag Absorption calibration 1/6/05

Silver standards ppm	Intensity
blank	432.3
25	223412.7
50	445752.0
100	886674.0
Correlation Coefficient 1.0000	
Wavelength 211.383 nm	

(ICP Plasma 400)

Cd Absorption calibration 9/6/05

Cadmium standards ppm	Intensity
blank	275.3
25	36831.7
50	74264.0
75	110144.7
100	147135.7
Correlation Coefficient 1.0000	
Wavelength 214.438 nm	

(ICP Plasma 400)

In Absorption calibration 20/4/06

Ruthenium standards ppm	Intensity
blank	1394.1
25	311153.1
50	633665.1
75	934448.8
100	1254072.6
Correlation Coefficient 0.999957	
Wavelength 325.609 nm	

(Optima 5300 DV)

Sn Absorption calibration 9/6/05

Tin standards ppm	Intensity
blank	234.3
25	593.7
50	939.0
75	1327.0
100	1696.7
Correlation Coefficient 0.9998	
Wavelength	

(ICP Plasma 400)

Sb Absorption calibration 25/1/06

Arsenic standards ppm	Intensity
blank	61.9
25	106113.2
50	211013.8
75	316152.0
100	420610.5
Correlation Coefficient 0.999996	
Wavelength 206.836 nm	

(Optima 5300 DV)

Cs Absorption calibration 9/2/06

Caesium standards ppm	Intensity
blank	3732.5
1	769.9
2	6313.5
3	9669.7
25	878.76
Correlation Coefficient 0.999569	
Wavelength 455.531 nm	

(Optima 5300 DV)

Cs Leach Test calibration 10/3/05

Caesium standards ppm	Intensity
blank	1006.1
25	92534.2
50	187963.3
75	273948.7
100	359878.6
Correlation Coefficient 0.999728	
Wavelength 455.531 nm	

(ICP Optima 5300 DV)

Ba Absorption calibration 3/3/06

Barium standards ppm	Intensity
blank	4504.5
25	3446045.6
50	6408926.8
75	9202432.5
100	11731939.3
Correlation Coefficient 0.998285	
Wavelength 233.527 nm	

(Optima 5300 DV)

La Absorption calibration 17/5/05

Lanthanum standards ppm	Intensity
blank	1042.0
50	45535.0
75	63929.7
100	88656.3
Correlation Coefficient 0.9992	
Wavelength 333.749 nm	

(ICP Plasma 400)

Ce Absorption calibration 10/3/06

Cerium standards ppm	Intensity
blank	1161.0
25	1683789.2
50	3351934.6
75	5044532.9
100	6661115.1
Correlation Coefficient 0.999973	
Wavelength 413.764 nm	

(Optima 5300 DV)

Yb Absorption calibration 20/4/06

Ruthenium standards ppm	Intensity
blank	
25	
50	
75	
100	
Correlation Coefficient 0.999409	
Wavelength 369.419 nm	

(Optima 5300 DV)

Hf Absorption calibration 10/3/06

Hafnium standards ppm	Intensity
blank	89.3
25	601038.8
50	1194715.7
75	1772719.9
100	2333275.6
Correlation Coefficient 0.999901	
Wavelength 277.336 nm	

(Optima 5300 DV)

W Absorption calibration 10/6/05

Tungsten standards ppm	Intensity
blank	297.0
25	520.0
50	703.7
75	933.0
100	1124.7
Correlation Coefficient 0.9995	
Wavelength 239.709 nm	

(ICP Plasma 400)

Pt Absorption calibration 24/3/06

Ruthenium standards ppm	Intensity
blank	-156.0
25	219469.3
50	433239.6
75	640991.5
100	862878.8
Correlation Coefficient 0.999951	
Wavelength 265.945nm	

(Optima 5300 DV)

Au Absorption calibration 27/1/05

Gold standards ppm	Intensity
blank	86.7
25	819.7
50	1667.0
75	2429.7
100	3350.7
Correlation Coefficient 0.9993	
Wavelength 191.893 nm	

(ICP Plasma 400)

Hg Absorption calibration 27/1/05

Mercury standards ppm	Intensity
blank	536.7
10	1313.7
20	1974.0
Correlation Coefficient 0.9989	
Wavelength	

(ICP Plasma 400)

Pb Absorption calibration 9/2/06

Lead standards ppm	Intensity
blank	-9.3
25	115946.6
50	224232.4
75	339746.5
100	445893.2
Correlation Coefficient 0.999898	
Wavelength 220.353 nm	

(Optima 5300 DV)

Bi Absorption calibration 24/3/06

Ruthenium standards ppm	Intensity
blank	-403.5
25	644463.0
50	1261481.0
75	1885892.4
100	2464135.8
Correlation Coefficient 0.999834	
Wavelength 223.061nm	

(Optima 5300 DV)

Appendix 2 Calculation of results into mg/g and mmol/g

The results from analytical equipment are given in ppm, which is equivalent to mg/L. To calculate the actual ion content in the sample the equation below was used:

Actual mg/L of ions = mg/L x volume used (mL) / mass of sample used (mg)

For example 100 mg sample of Se/PMPS acid digested and diluted to 100 mL was found to contain 285 mg/L (ICP-OES).

Actual content of Se = 286.04 mg/L x 100 mL / 100.2 mg

= 285.47 mg/L

This gives the amount of selenium ions contained in 100 mg of PMPS particles dissolved in one litre of solution. Multiplying the figures by 1000 would calculate the amound of selenium ions w/w into mg/g.

Therefore 1 gram of Se/PMPS contains 285.47 mg/g of selenium ions.

To convert this figure into mmol/g dividing by selenium A.W. (78.96) gives

285.47 / 78.96 = 3.62 mmol of Se/g of PMPS particles

Appendix 3 Calculation of ratio of ions for each PMPS repeat unit

The molecular mass of each repeat unit of PMPS was calculated to have Mr 159.

100 mg (PMPS sample) / Mr 159 = 6.3×10^{-4} moles

6.3×10^{-4} moles x 6.022×10^{23} = 3.8×10^{20} molecules of PMPS repeat unit

100 mL of water = 5.55 moles

5.55 x 6.022×10^{23} = 3.35×10^{24} molecules of water

1 ppm of water = 3.35×10^{18} molecules

1 ppm of Li = 9.5 x 3.35×10^{18} = 3.18×10^{19}

ratio of Li:PMPS = $3.18 \times 10^{19} / 3.8 \times 10^{20}$

So each PMPS repeat unit contains 0.08 ions of Lithium

Appendix 4 Table of all sorption data imported from Minitab